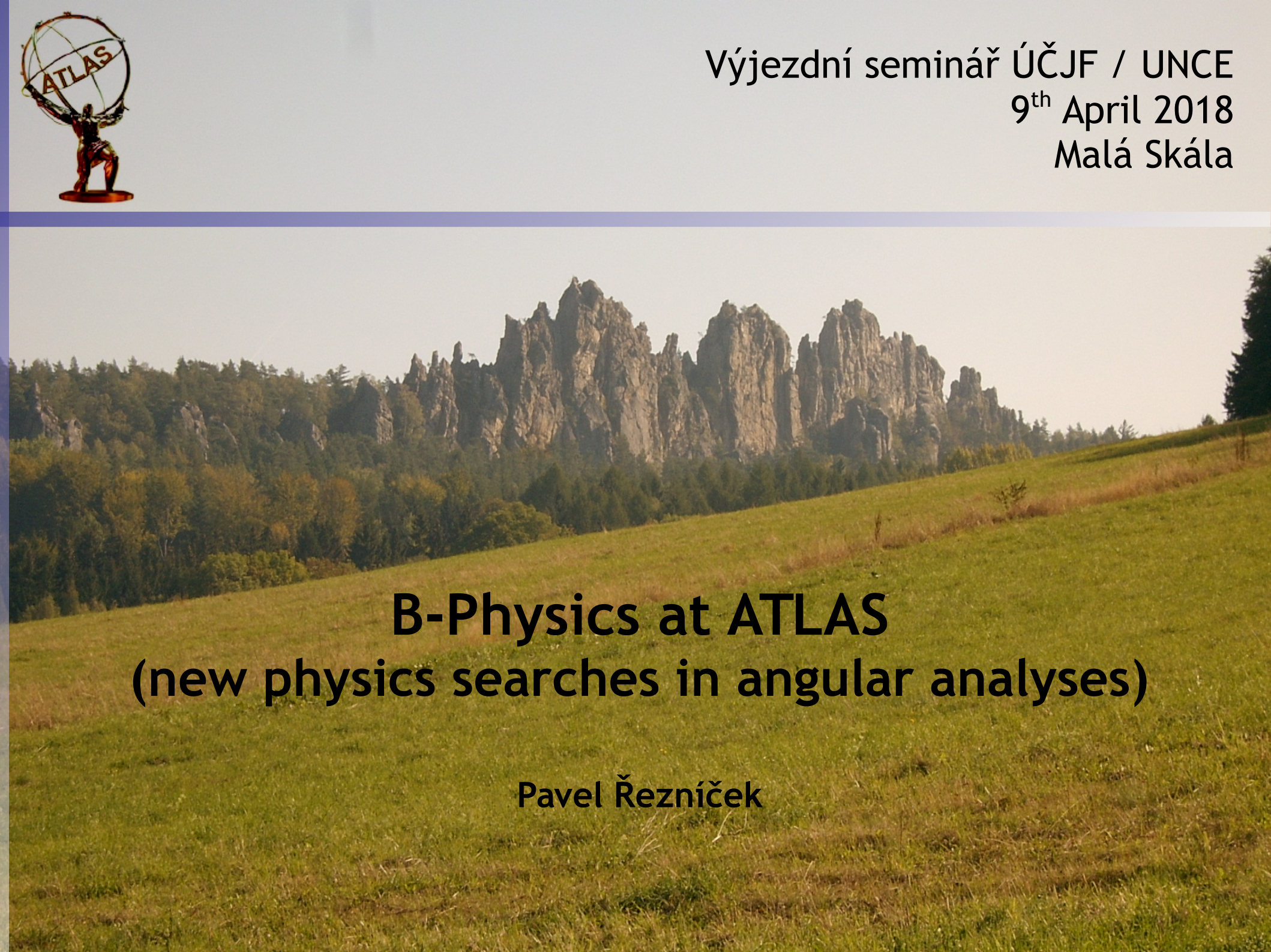

Výjezdní seminář ÚČJF / UNCE
9th April 2018
Malá Skála

B-Physics at ATLAS
(new physics searches in angular analyses)

Pavel Řezníček

New Physics Searches in B-Physics

- Search for new particles indirectly, through their contributions in decays of known particles

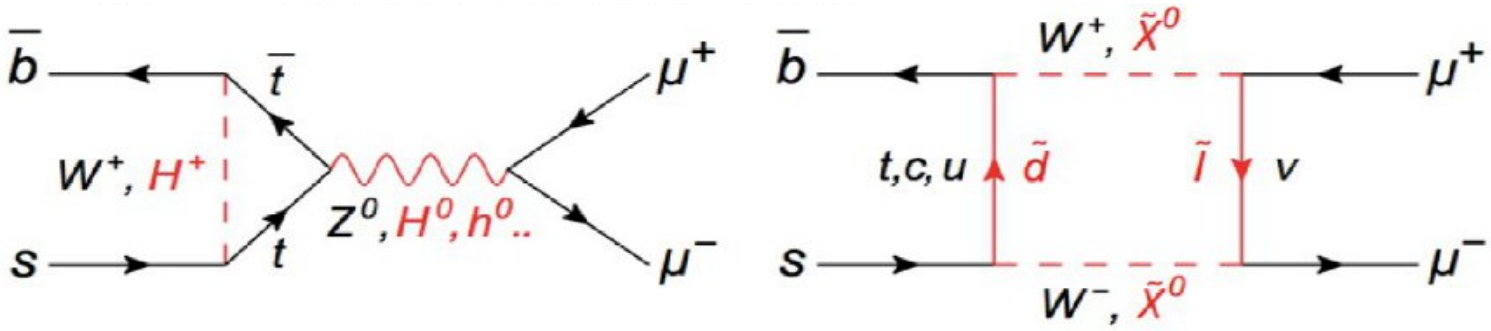

$B_s \rightarrow \mu\mu$

  - Can change known decays branching ratio or differential decay cross-section
  - B-physics decays through flavour changing neutral currents (FCNC) especially sensitive due to several suppression mechanisms in the Standard Model

New Physics Searches in B-Physics

- Search for new particles indirectly, through their contributions in decays of known particles

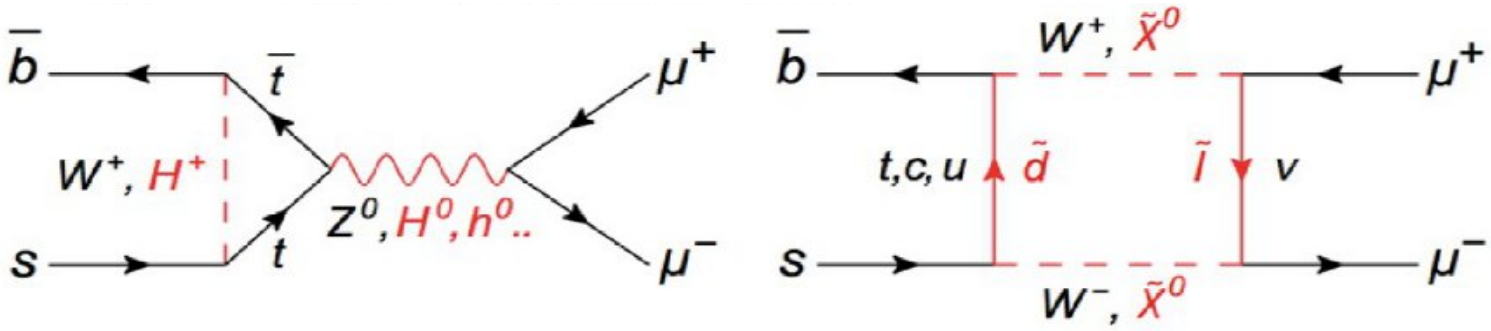

$B_s \rightarrow \mu\mu$

  - Can change known decays branching ratio or differential decay cross-section
  - B-physics decays through flavour changing neutral currents (FCNC) especially sensitive due to several suppression mechanisms in the Standard Model:
    - Proceed via loops, no tree diagrams

New Physics Searches in B-Physics

- Search for new particles indirectly, through their contributions in decays of known particles

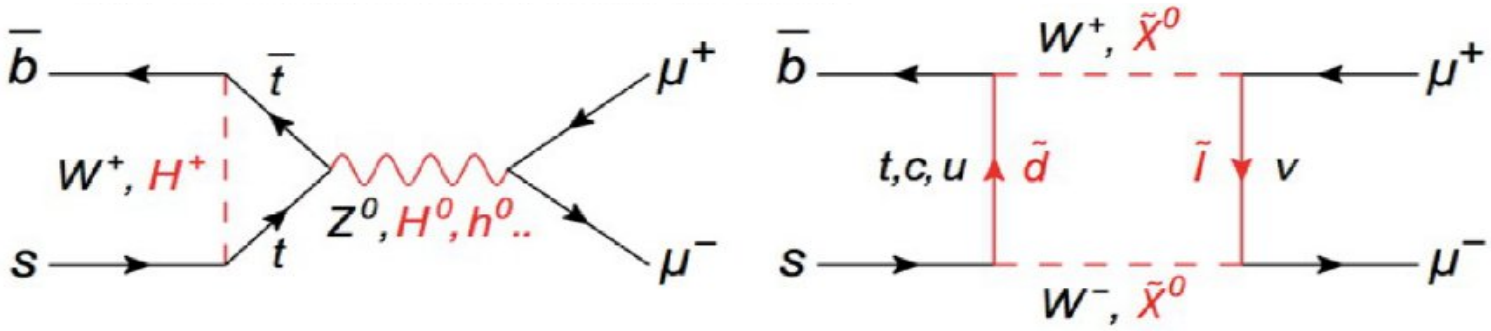

$B_s \rightarrow \mu\mu$

  - Can change known decays branching ratio or differential decay cross-section
  - B-physics decays through flavour changing neutral currents (FCNC) especially sensitive due to several suppression mechanisms in the Standard Model:
    - Proceed via loops, no tree diagrams
    - Presence of small CKM elements ($|V_{ts}| \sim 0.04$, $|V_{td}| \sim 0.01$)

New Physics Searches in B-Physics

- Search for new particles indirectly, through their contributions in decays of known particles

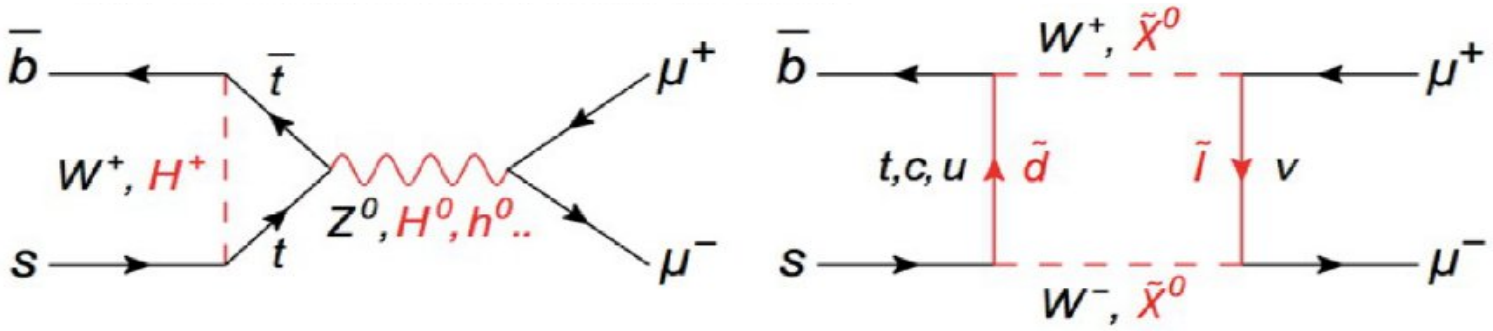

$B_s \rightarrow \mu\mu$

  - Can change known decays branching ratio or differential decay cross-section
  - B-physics decays through flavour changing neutral currents (FCNC) especially sensitive due to several suppression mechanisms in the Standard Model:
    - Proceed via loops, no tree diagrams
    - Presence of small CKM elements ($|V_{ts}| \sim 0.04$, $|V_{td}| \sim 0.01$)
    - GIM suppression in loops with charm or down-type quarks: $(m_s^2 - m_d^2) / M_W^2$

New Physics Searches in B-Physics

- Search for new particles indirectly, through their contributions in decays of known particles

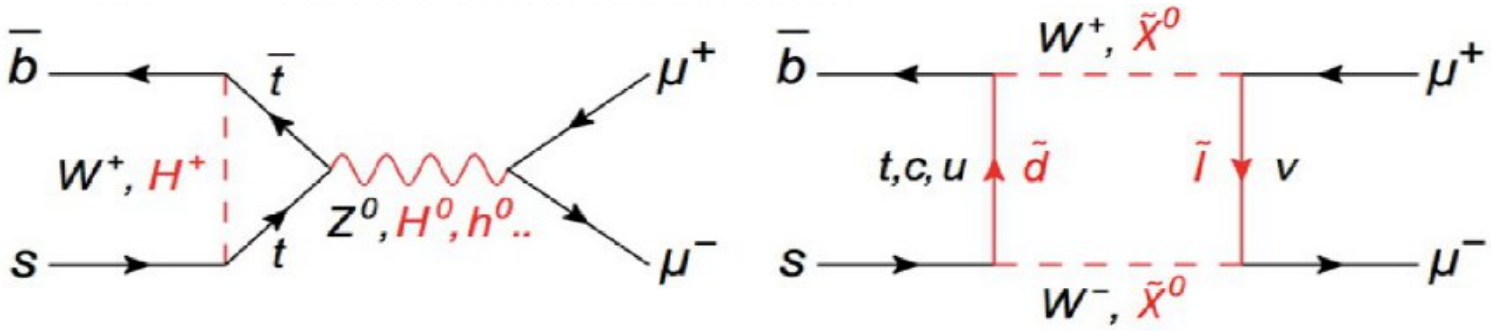

$B_s \rightarrow \mu\mu$

  - Can change known decays branching ratio or differential decay cross-section
  - B-physics decays through flavour changing neutral currents (FCNC) especially sensitive due to several suppression mechanisms in the Standard Model:
    - Proceed via loops, no tree diagrams
    - Presence of small CKM elements ($|V_{ts}| \sim 0.04$, $|V_{td}| \sim 0.01$)
    - GIM suppression in loops with charm or down-type quarks: $(m_s^2 - m_d^2) / M_W^2$
    - Helicity suppression in radiative or leptonic decays: helicity flip ~ $m_{b,s} / M_W$

New Physics Searches in B-Physics

- Search for new particles indirectly, through their contributions in decays of known particles

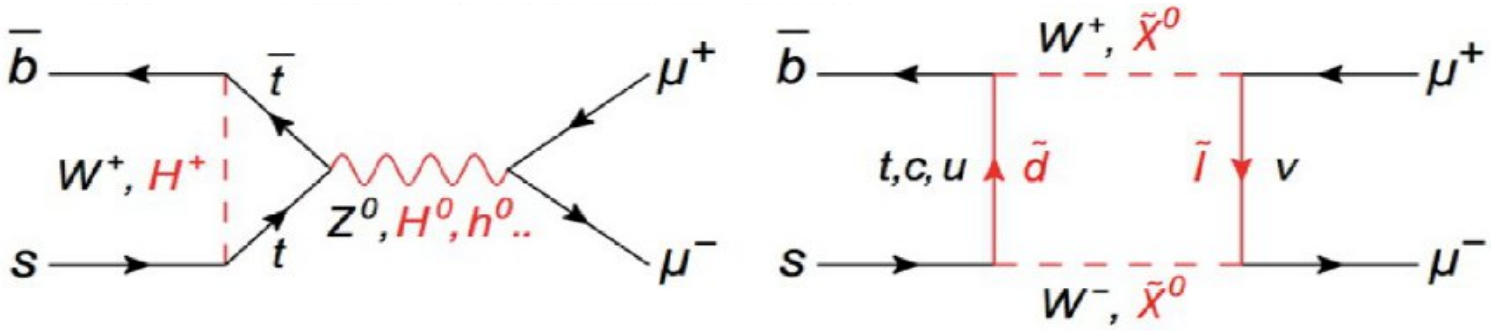

$B_s \rightarrow \mu\mu$

  - Can change known decays branching ratio or differential decay cross-section
  - B-physics decays through flavour changing neutral currents (FCNC) especially sensitive due to several suppression mechanisms in the Standard Model:
    - Proceed via loops, no tree diagrams
    - Presence of small CKM elements ($|V_{ts}| \sim 0.04$, $|V_{td}| \sim 0.01$)
    - GIM suppression in loops with charm or down-type quarks: $(m_s^2 - m_d^2) / M_W^2$
    - Helicity suppression in radiative or leptonic decays: helicity flip ~ $m_{b,s} / M_W$
  - While New Physics can include tree diagrams, no GIM supression, no helicity suppression, ...

New Physics Searches in B-Physics

- Search for new particles indirectly, through their contributions in decays of known particles

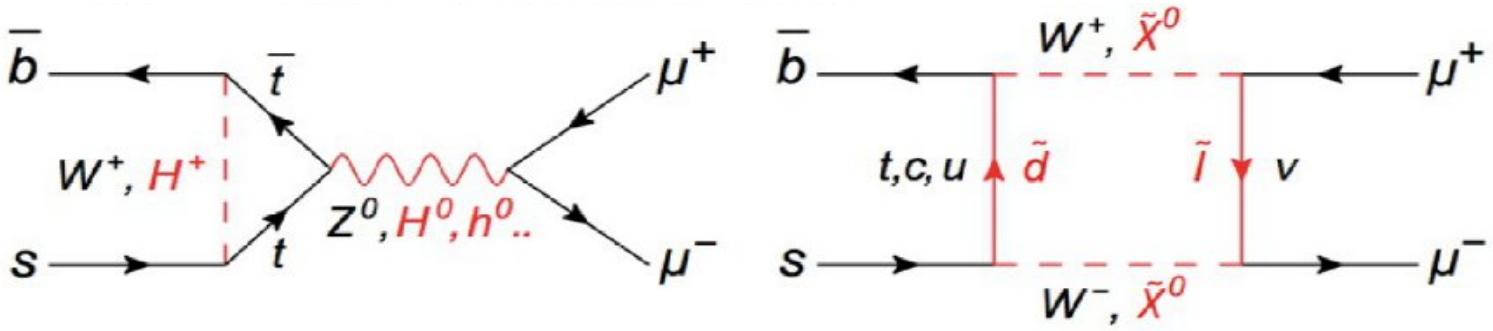

$B_s \rightarrow \mu\mu$

  - Can change known decays branching ratio or differential decay cross-section
  - B-physics decays through flavour changing neutral currents (FCNC) especially sensitive due to several suppression mechanisms in the Standard Model:
  - While New Physics can include tree diagrams, no GIM supression, no helicity suppression, …

- FCNC in leptonic rare decays ($B \rightarrow ll$): BR measurement
- FCNC in semileptonic rare decays ($B \rightarrow K^*ll$): decay angles analysis
- FCNC in radiative decays ($B \rightarrow K^*\gamma$): decay angles analysis
- FCNC in B-meson mixing ($B_s \rightarrow \overline{B}_s$): time-dependent decay angles analysis

New Physics Searches in B-Physics

- Search for new particles indirectly, through their contributions in decays of known particles

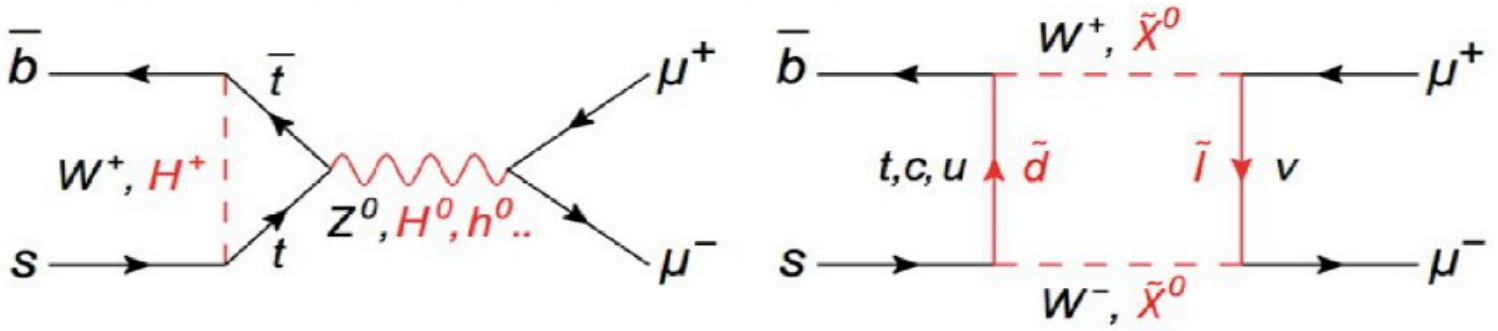

$B_s \rightarrow \mu\mu$

  - Can change known decays branching ratio or differential decay cross-section
  - B-physics decays through flavour changing neutral currents (FCNC) especially sensitive due to several suppression mechanisms in the Standard Model:
  - While New Physics can include tree diagrams, no GIM supression, no helicity suppression, …

- FCNC in leptonic rare decays ($B \rightarrow ll$): BR measurement
- FCNC in semileptonic rare decays ($B \rightarrow K^*ll$): decay angles analysis
- FCNC in radiative decays ($B \rightarrow K^*\gamma$): decay angles analysis
- FCNC in B-meson mixing ($B_s \rightarrow \overline{B}_s$): time-dependent decay angles analysis

Leptonic decays: $B_{(s)} \rightarrow \mu^+\mu^-$

- Very rare decay BR ~ 3×10^{-9}
- Simple signature: $\mu^+\mu^-$ from same displaced point,
  but rare processes can create background: rare B-decays, mis-id hadrons
  => MVA analysis needed
- First observation in 2012 by LHCb

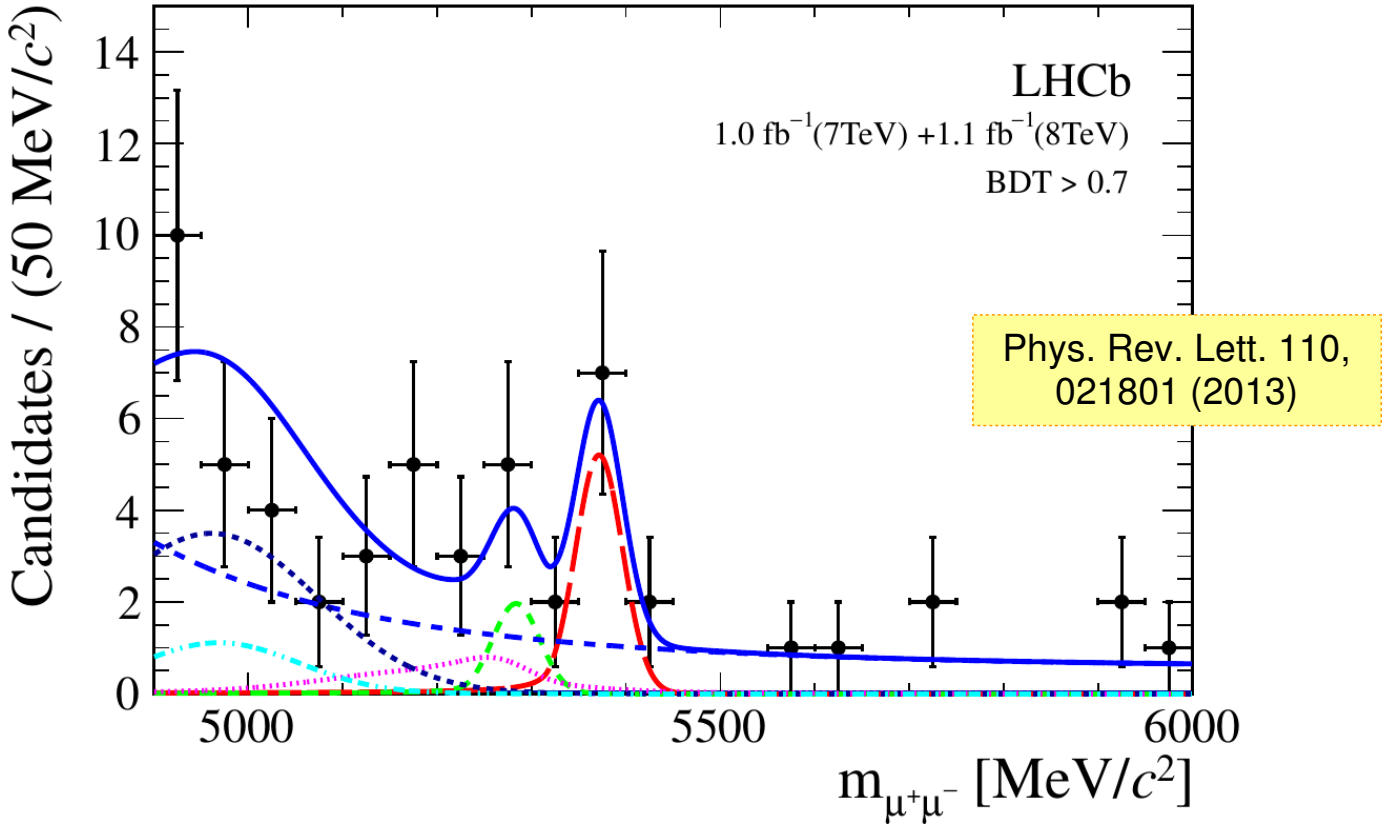

Phys. Rev. Lett. 110, 021801 (2013)

Leptonic decays: $B_{(s)} \to \mu^+\mu^-$

- Very rare decay BR ~ 3×10^{-9}
- Simple signature: $\mu^+\mu^-$ from same displaced point,
  but rare processes can create background: rare B-decays, mis-id hadrons
  => MVA analysis needed
- Current status: compatible with Standard Model (SM) prediction

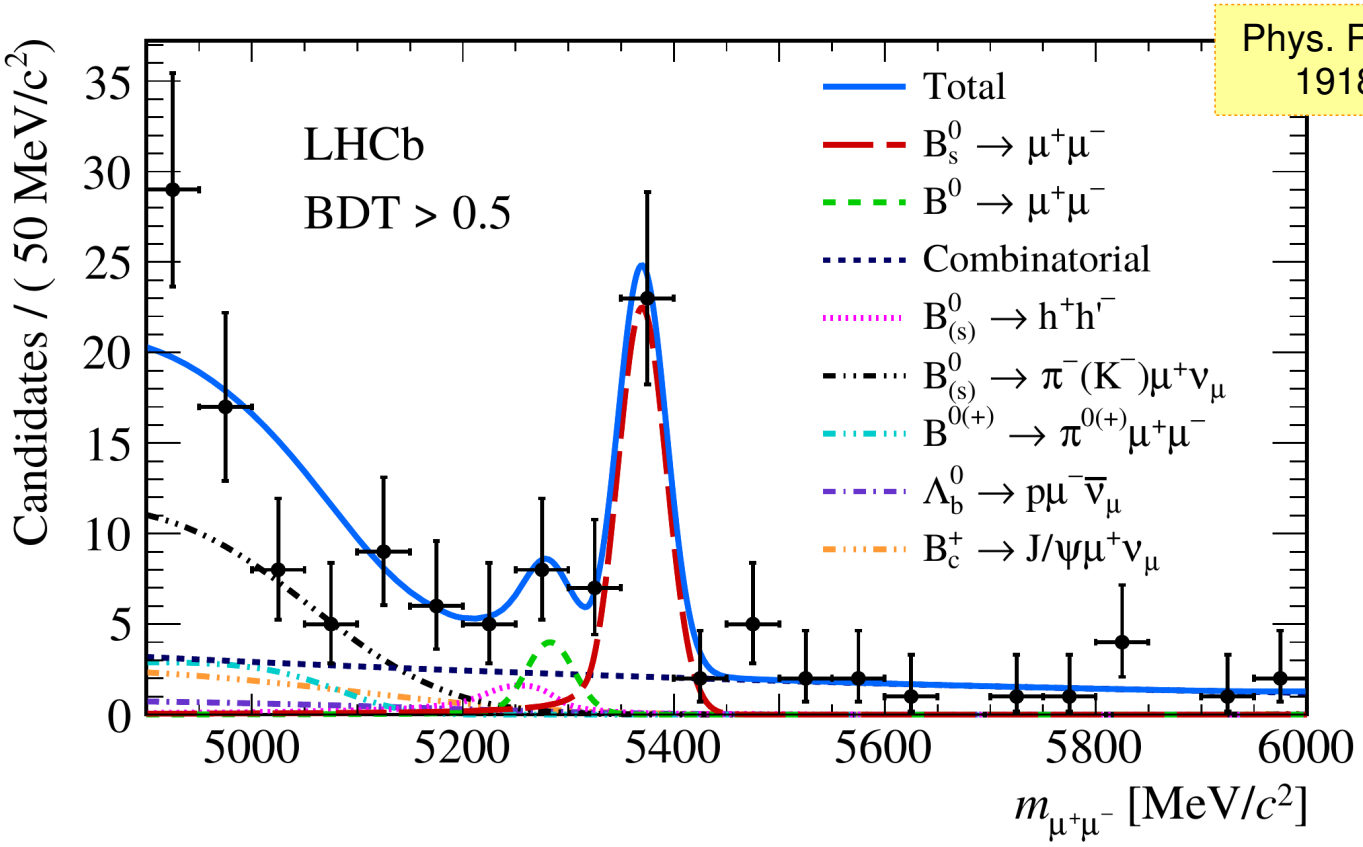

Phys. Rev. Lett. 118, 191801 (2017)

$B_s \to \mu\mu$ at 7.8σ

$B \to \mu\mu$ at 1.6σ

Semileptonic decays: $B \to K^{*0}l^+l^-$

- Rare decay BR ~ 1×10^{-6}

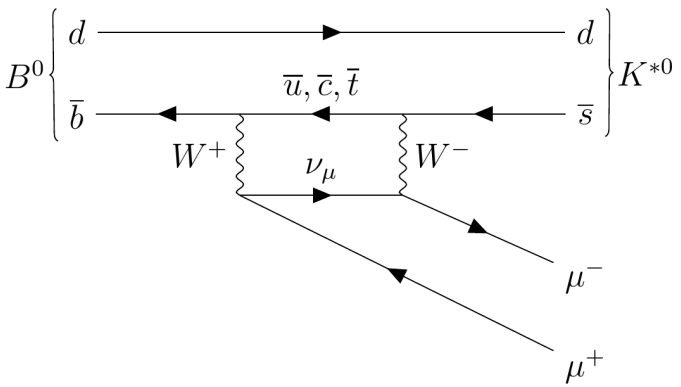

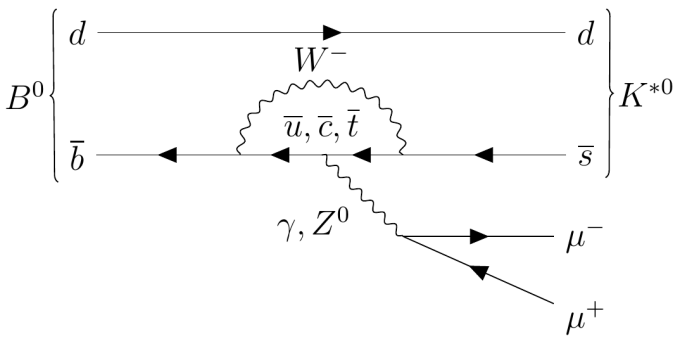

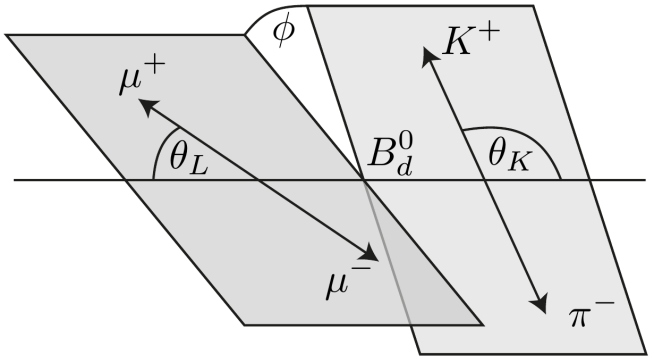

$$s = q^2 = [m(\mu^+\mu^-)]^2$$

- BR measurement
- BR ratio of $B \to K^{*0}\mu^+\mu^-$ / $B \to K^{*0}e^+e^-$
- Analysis of angular distributions between decay products as a function of the di-lepton invariant mass
  - 8 physics parameters describing the 3D distribution

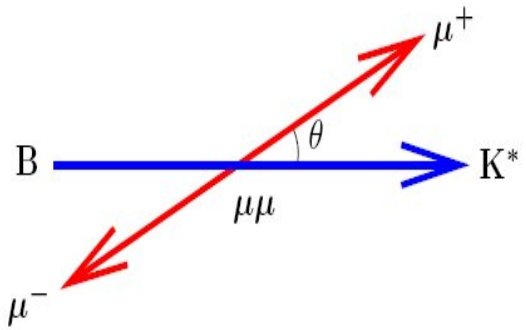

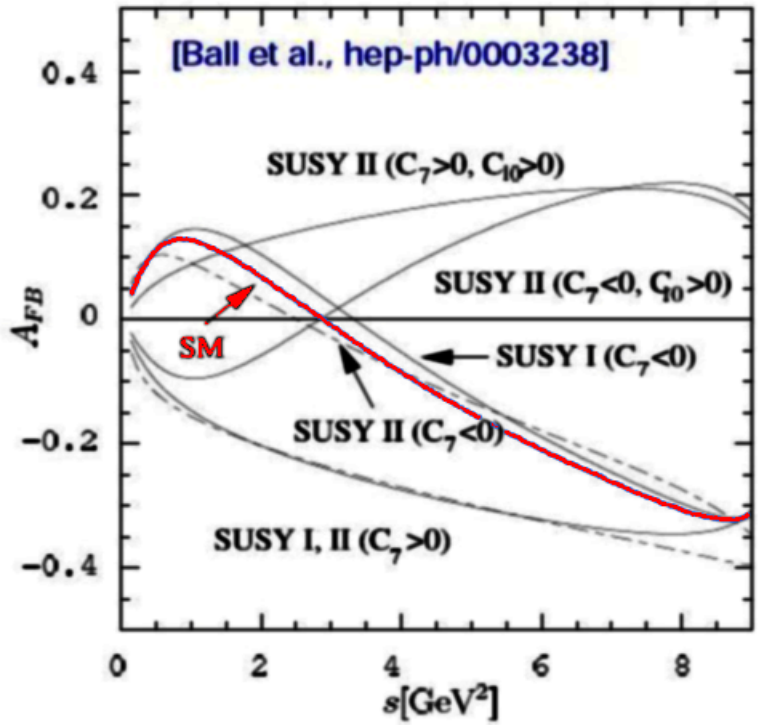

B-Meson Mixing: in $B_s \to J/\psi\phi$

- Interference of mixing and direct decay => CP violation

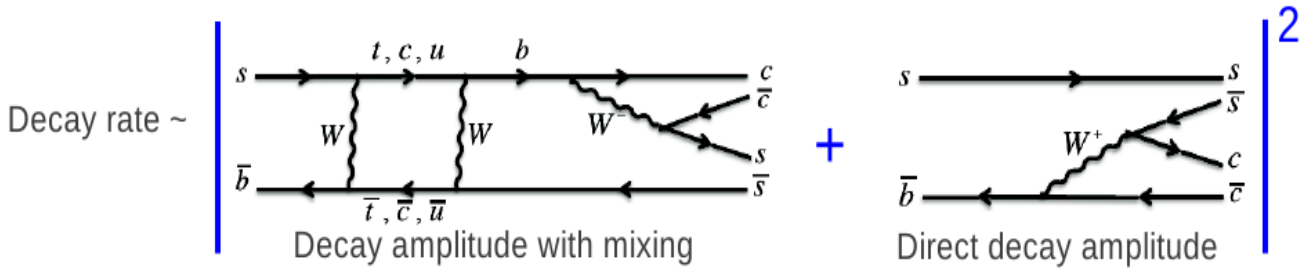

B_s mixing:
- Mass difference $\Delta m = m_H - m_L$
- Mixing phase ϕ_s
- Decay width difference $\Delta\Gamma_s = \Gamma_L - \Gamma_H$

$$|B_s^H\rangle = p|B_s^0\rangle - q|\bar{B}_s^0\rangle$$
$$|B_s^L\rangle = p|B_s^0\rangle + q|\bar{B}_s^0\rangle$$

- Time evolution of decay angles very sensitive to New Physics, described by 9 physics parameters:

Γ_s, $\Delta\Gamma_s$	decay with and decay width difference
ϕ_s ($\approx 2\beta_s$)	CP violating phase
$\lvert A_0\rvert^2$, $\lvert A_{\lvert\rvert}\rvert^2$	CP state amplitudes
$\delta_{\lvert\rvert}$, $\delta_\perp$	Strong phases
$\lvert A_S\rvert^2$, δ_S	S-wave parameters

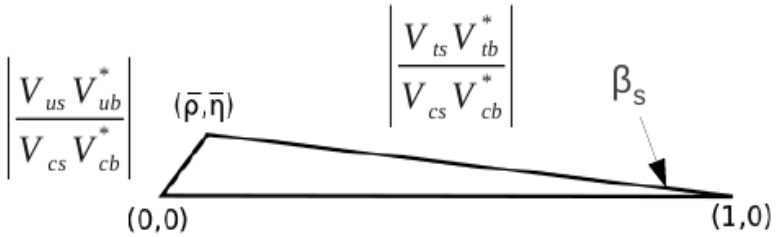

ϕ_s small in SM, clear to see potential excess from NP

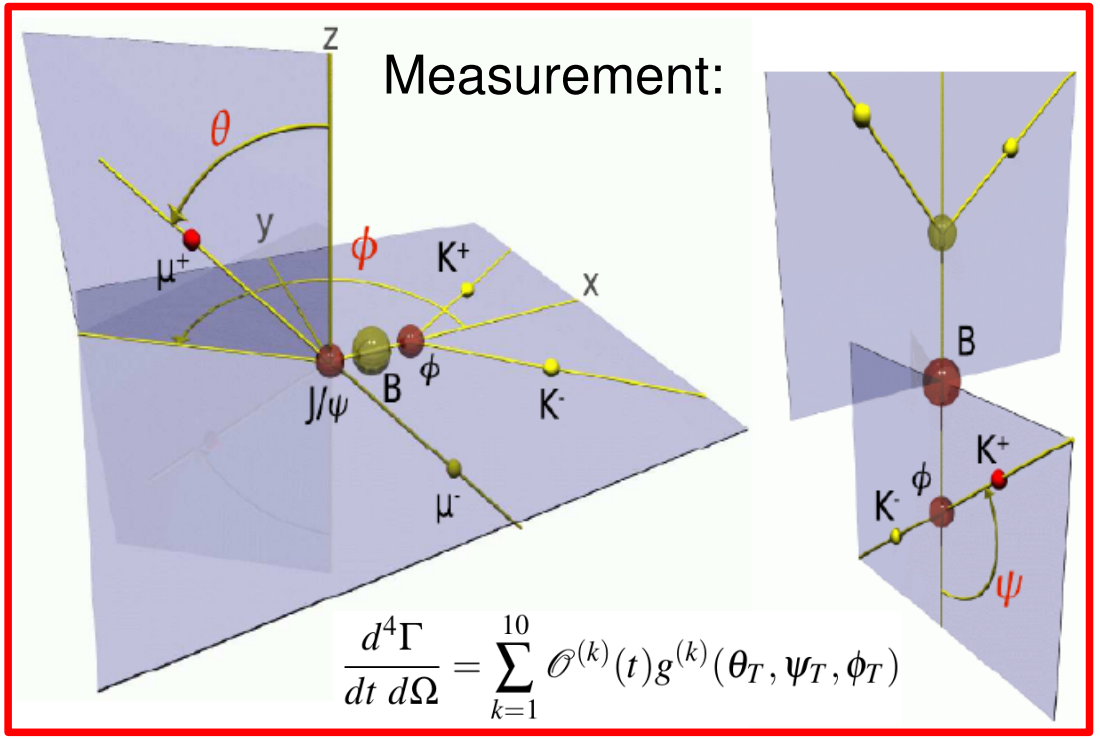

B-Physics at ATLAS

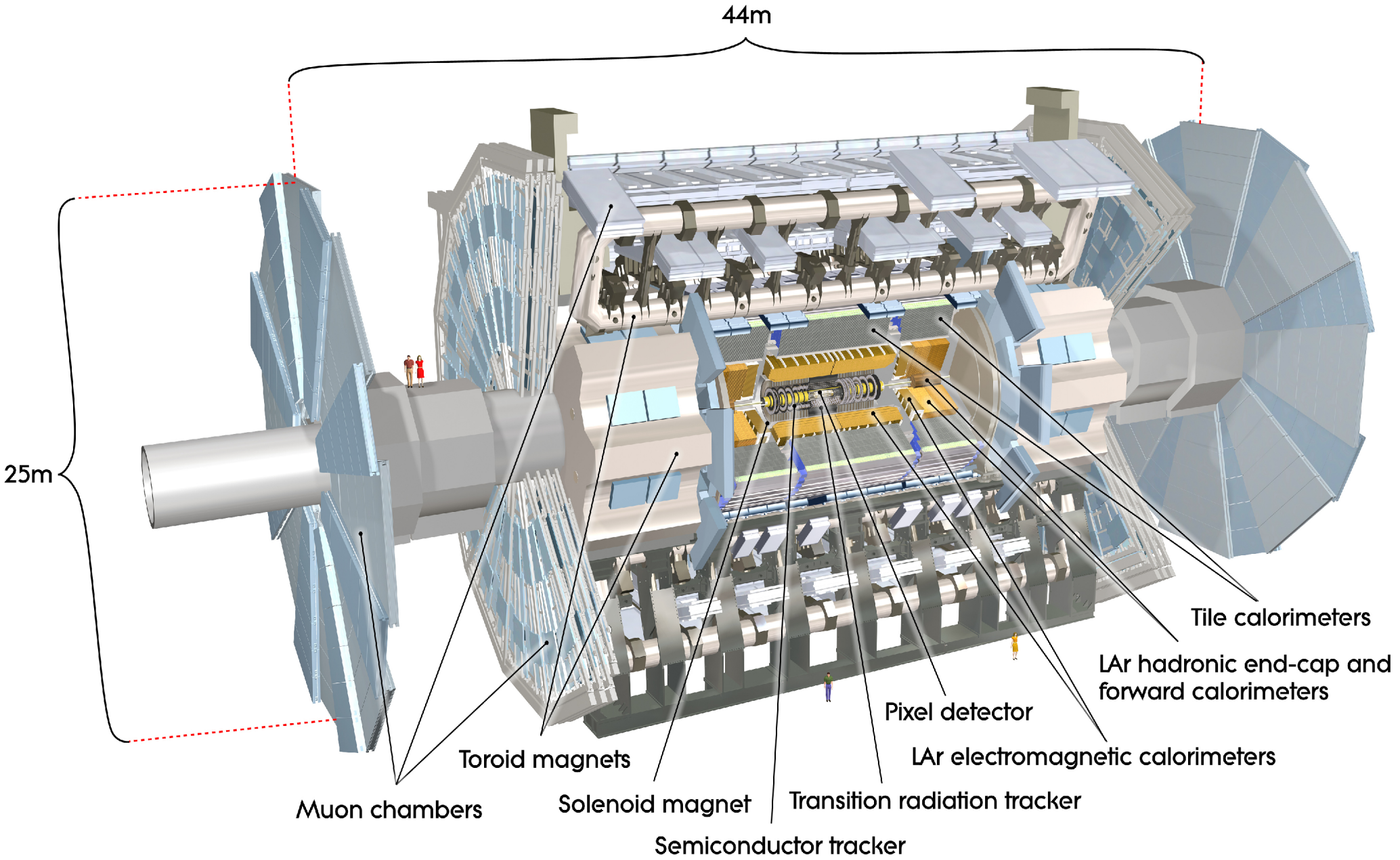

B-Physics at ATLAS

- To fully exploit the large $b\bar{b}$ production x-section at LHC, need to be able to collect low-p_T (relatively) b-hadrons

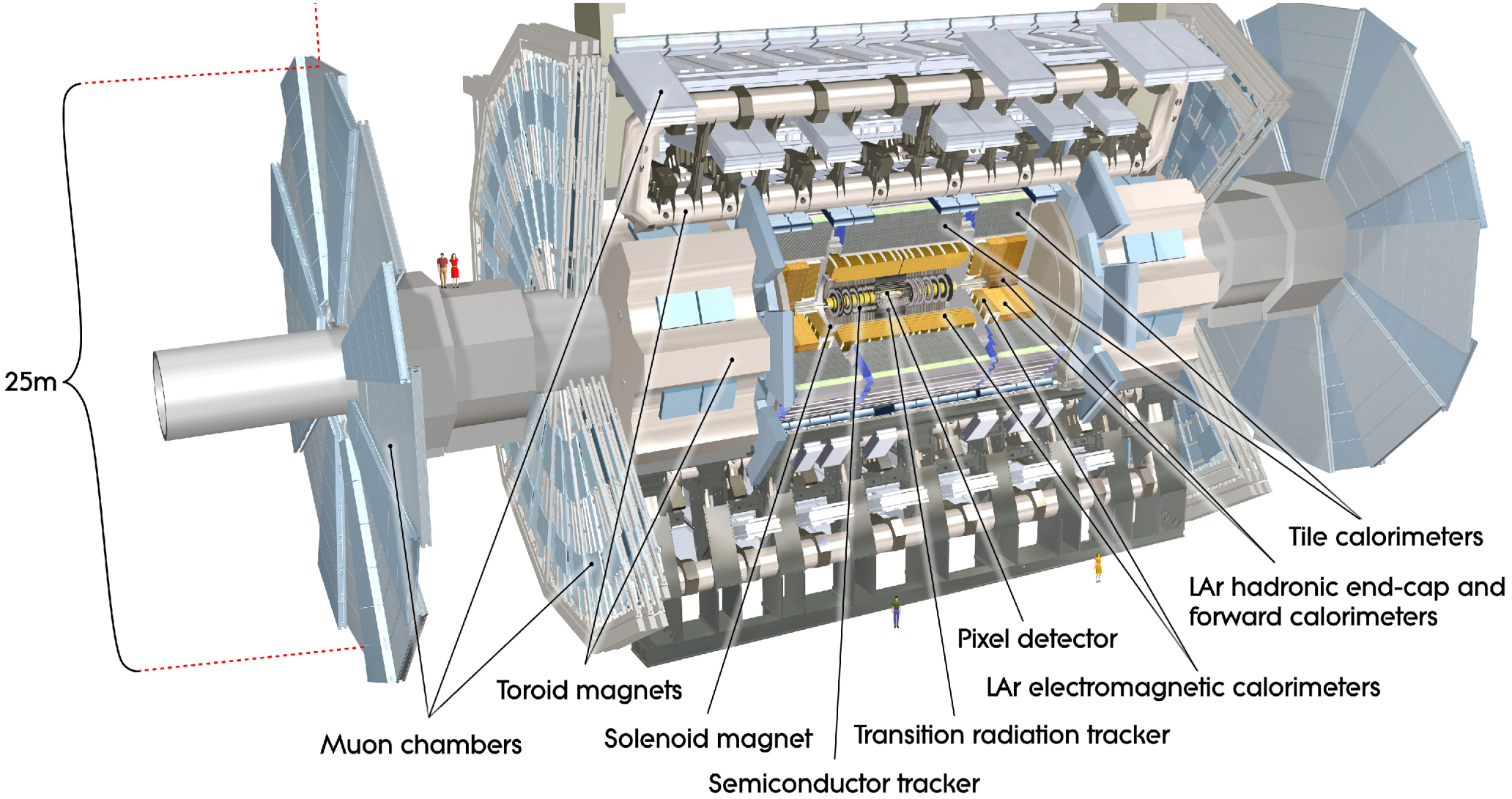

B-Physics at ATLAS

- To fully exploit the large $b\bar{b}$ production x-section at LHC, need to be able to collect low-p_T (relatively) b-hadrons
  - Challenge for reconstruction: focus on fully-reconstructable decays in the Inner Detector (no neutrinos, gamma, …)

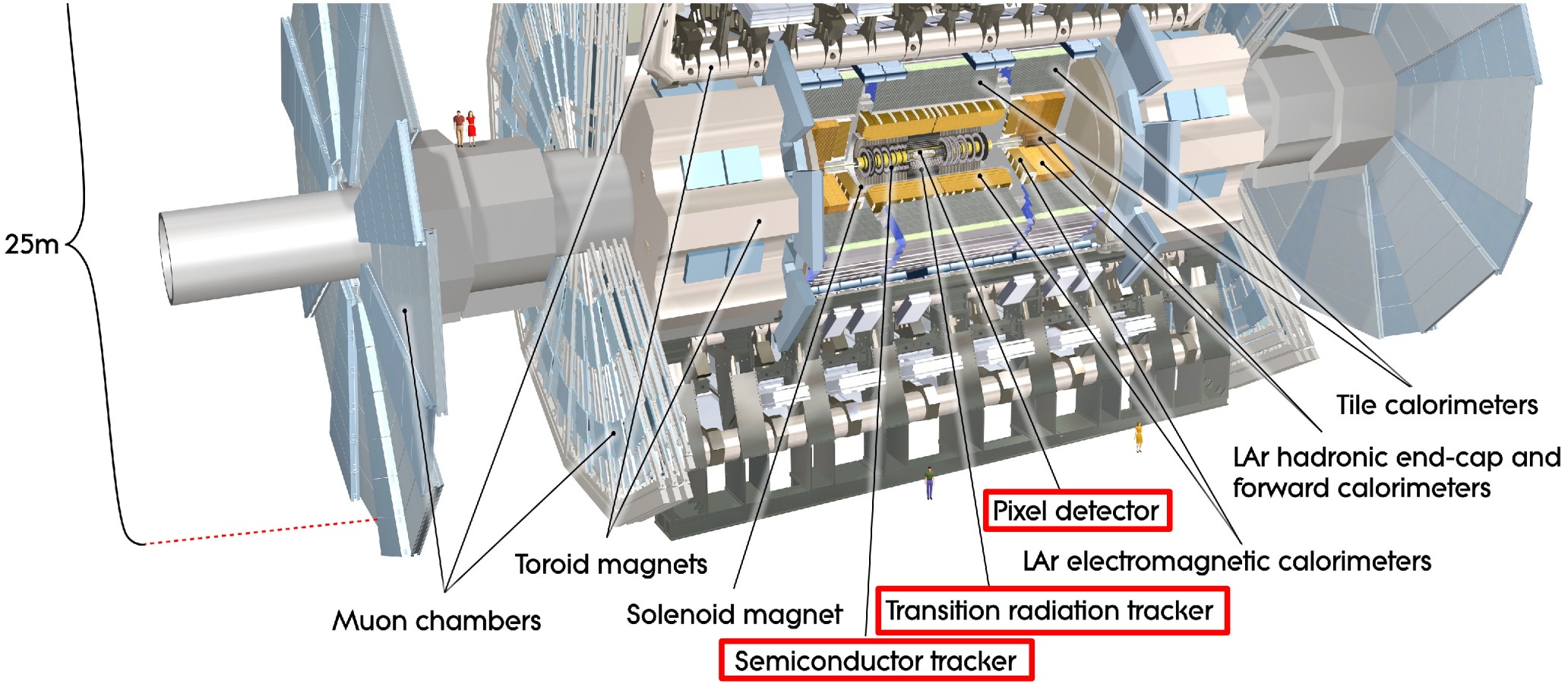

B-Physics at ATLAS

- To fully exploit the large bb production x-section at LHC, need to be able to collect low-p_T (relatively) b-hadrons
  - Challenge for reconstruction: focus on fully-reconstructable decays in the Inner Detector (no neutrinos, gamma, …)
  - Challenge for trigger: only muons are clean enough at low-p_T

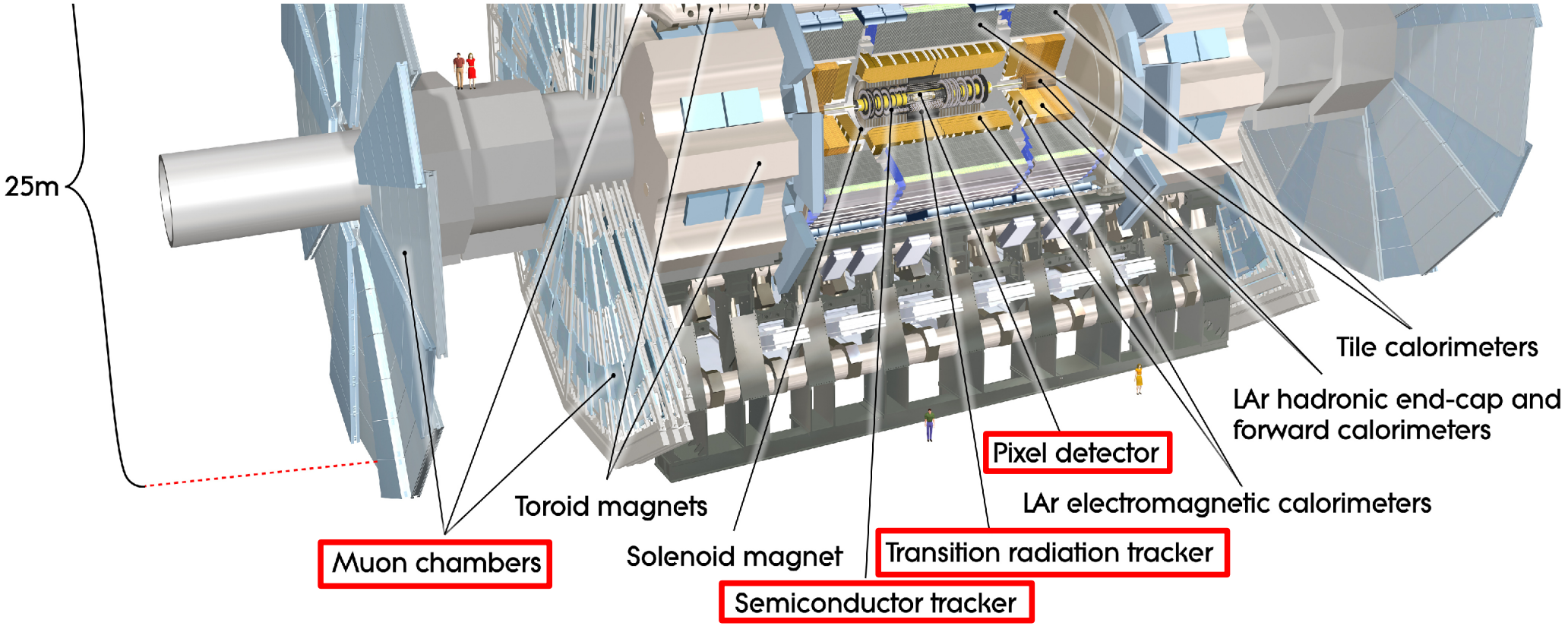

B-Physics Analysis Chain

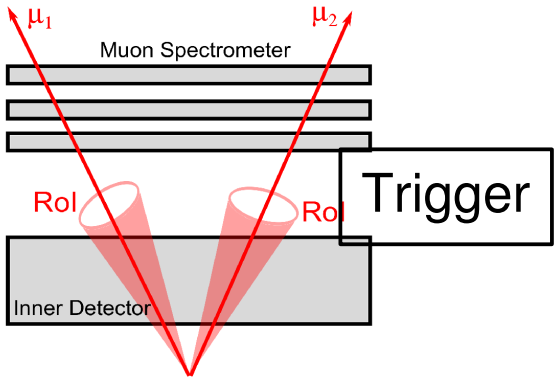

- Cannot store all B-events, fast pre-selection based on simple signatures of the studied decay channel
- Typical analysis chain ($B^0 \rightarrow J/\psi(\mu^+\mu^-)\ K^{*0}(K\pi)$ case):

Reconstructed tracks, muons, jets etc. provided by ATLAS reconstruction

vertexing

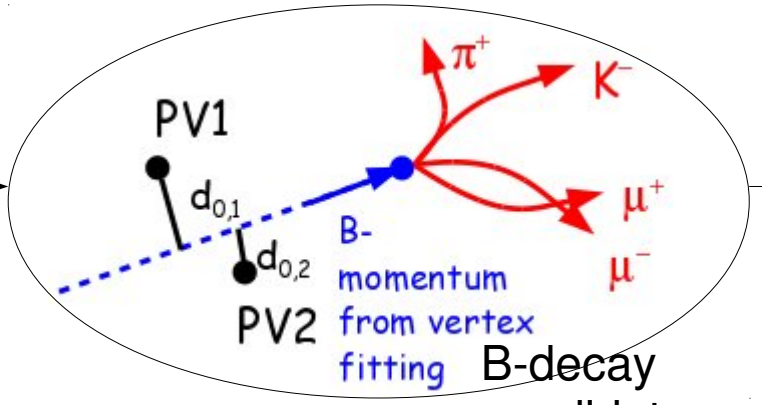

B-decay candidates

Selection (cuts, MVA, BDT) to achieve optimal S/B ratio

Results, systematic uncertainties, ...

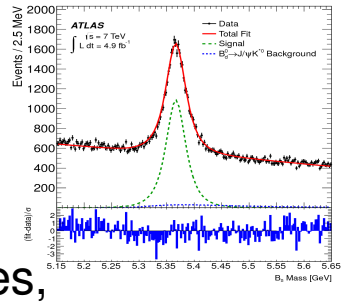

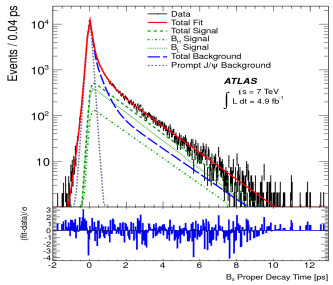

Detector efficiency and acceptance corrections (MC and/or Data based)

Statistical analysis (fits etc.)

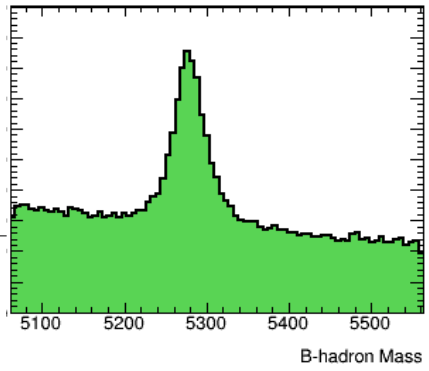

B-Physics at ATLAS

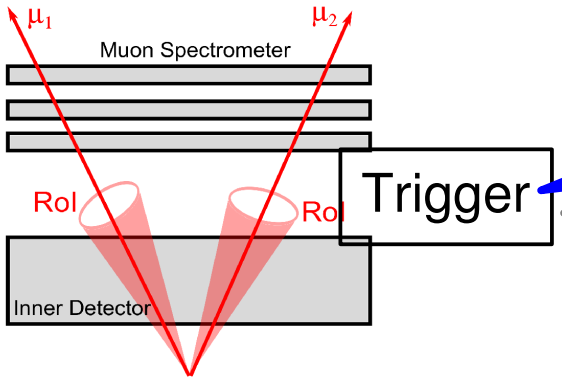

Trigger

- Ca… …on based on simple sig…

Search for $\mu^+\mu^-$ at first level (HW) then try to find K^{*0} from B^0 too

- Typical analysis chain ($B^0 \rightarrow J/\psi(\mu^+\mu^-)\, K^{*0}(K\pi)$ case):

Reconstructed tracks, muons, jets etc. provided by ATLAS reconstruction

vertexing

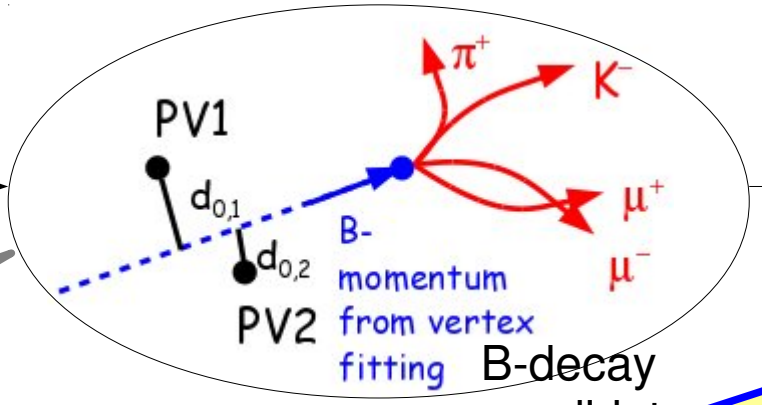

B-decay

Selection (cuts, MVA, BDT) to achieve optimal S/B ratio

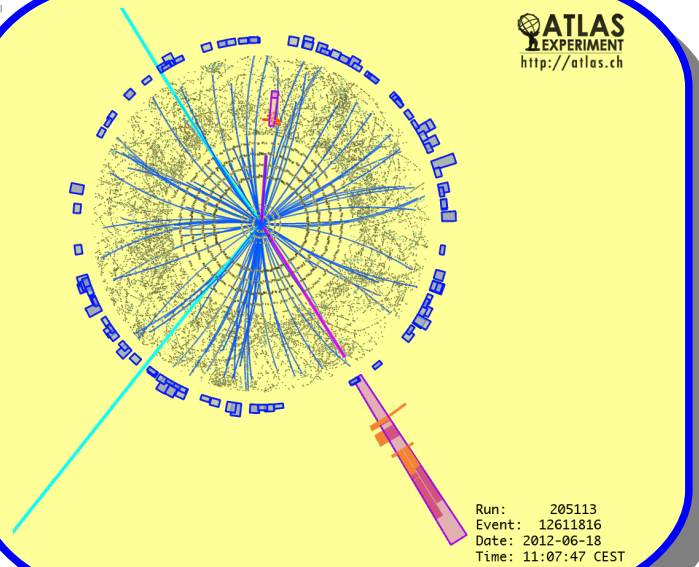

De… an… co… an…

- **Invariant masses of track combinations**
- **B-hadron decay vertex quality and position**
- **Momentum, pointing to primary vertex, ...**
- **B-hadron flavour identification**
- **Isolation**

Statistical analysis (fits etc.)

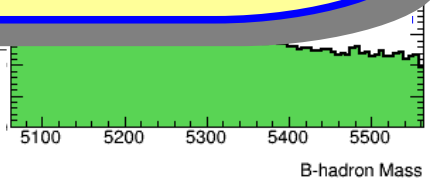

B-Physics at ATLAS

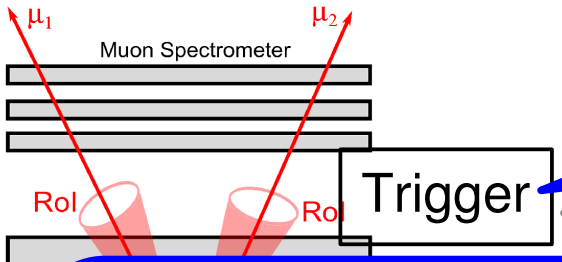

- Ca… …on based on simple sig…

Search for $\mu^+\mu^-$ at first level (HW) then try to find K^{*0} from B^0 too

Trigger

Typical analysis chain ($B^0 \rightarrow J/\psi(\mu^+\mu^-)\, K^{*0}(K\pi)$ case):

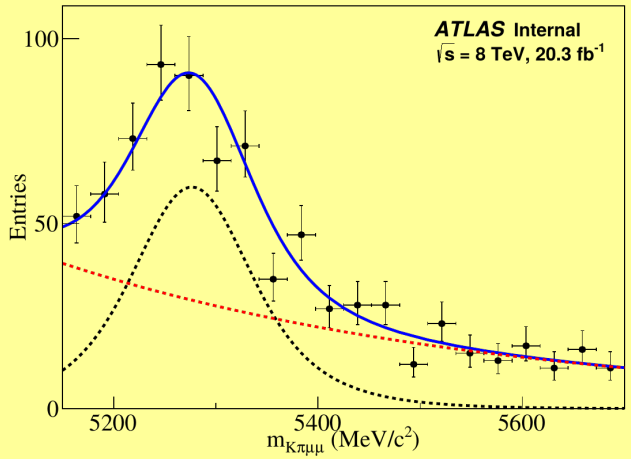

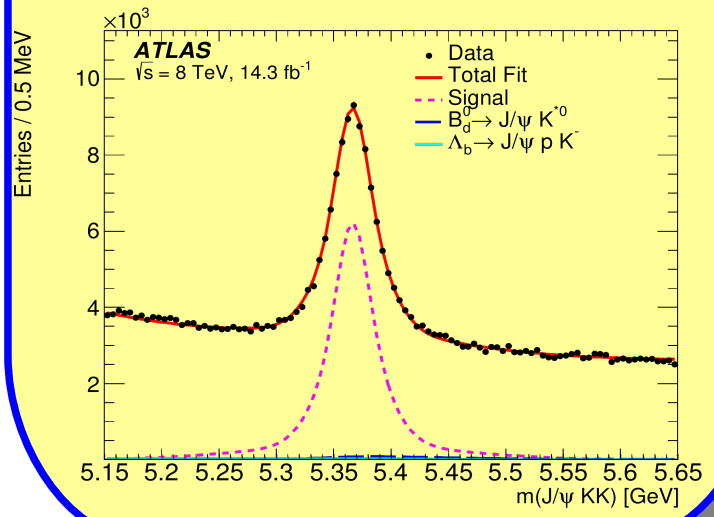

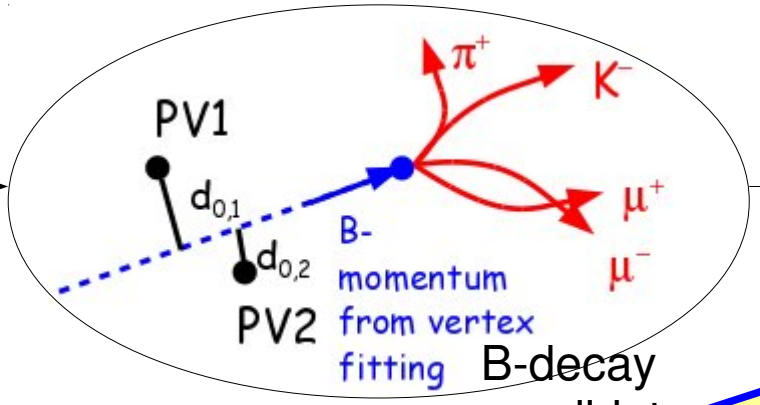

B-decay

Selection (cuts, MVA, BDT) to achieve optimal S/B ratio

- **Invariant masses of track combinations**
- **B-hadron decay vertex quality and position**
- **Momentum, pointing to primary vertex, ...**
- **B-hadron flavour identification**
- **Isolation**

De…

Statistical analysis (fits etc.)

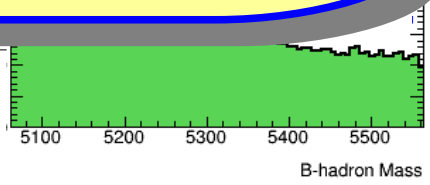

B-Physics Analysis Chain

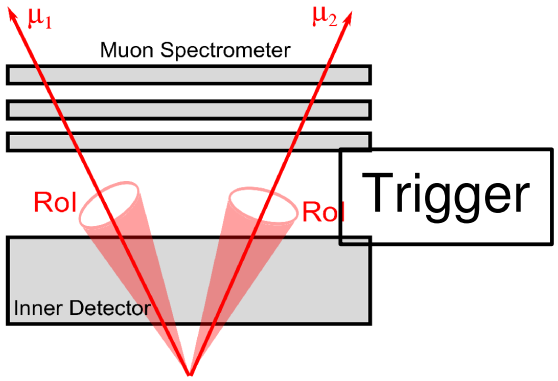

Trigger

Reconstructed tracks, muons, jets etc. provided by ATLAS reconstruction

- **MC simulation determines detector sculpting of angular distributions:**

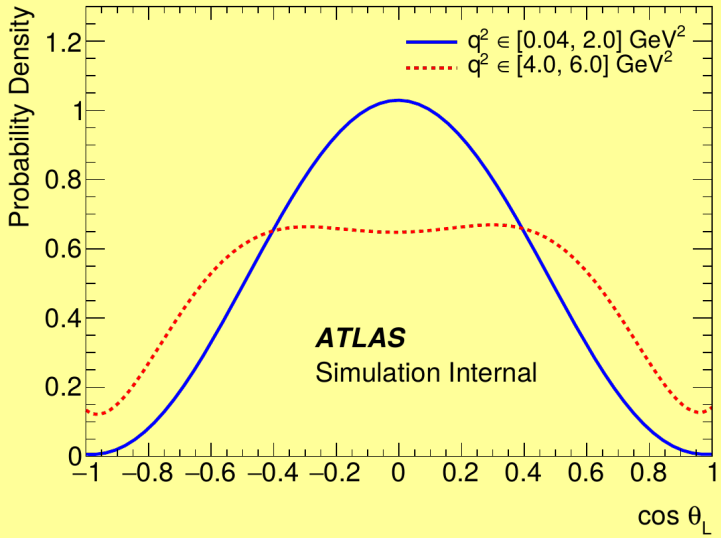

candidates

Results, systematic uncertainties, ...

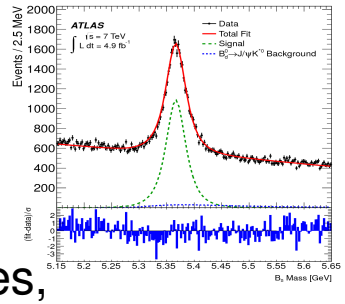

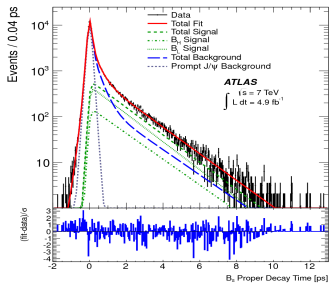

Detector efficiency and acceptance corrections (MC and/or Data based)

- **4(5) dimensional unbinned maximum likelihood fit**

$$\mathcal{L} = \frac{e^{-N}}{n!} \prod_{i=1}^{n} \sum_{j} n_j P_{ij}(m_{K\pi\mu\mu}, \cos\theta_K, \cos\theta_L, \phi; \widehat{p}, \widehat{\theta})$$

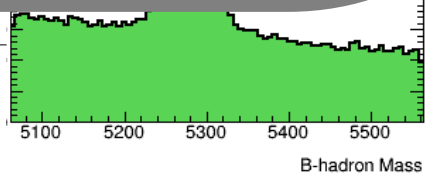

Statistical analysis (fits etc.)

B → K*μμ Analysis

- Decay described in helicity basis amplitudes, measuring coefficients before the terms

$$\frac{1}{\mathrm{d}\Gamma/\mathrm{d}q^2}\frac{\mathrm{d}^4\Gamma}{\mathrm{d}\cos\theta_L\mathrm{d}\cos\theta_K\mathrm{d}\phi\mathrm{d}q^2} = \frac{9}{32\pi}\left[\frac{3(1-F_L)}{4}\sin^2\theta_K + F_L\cos^2\theta_K + \frac{1-F_L}{4}\sin^2\theta_K\cos 2\theta_L\right.$$
$$-F_L\cos^2\theta_K\cos 2\theta_L + S_3\sin^2\theta_K\sin^2\theta_L\cos 2\phi$$
$$+S_4\sin 2\theta_K\sin 2\theta_L\cos\phi + S_5\sin 2\theta_K\sin\theta_L\cos\phi$$
$$+S_6\sin^2\theta_K\cos\theta_L + S_7\sin 2\theta_K\sin\theta_L\sin\phi$$
$$\left.+S_8\sin 2\theta_K\sin 2\theta_L\sin\phi + S_9\sin^2\theta_K\sin^2\theta_L\sin 2\phi\right]$$

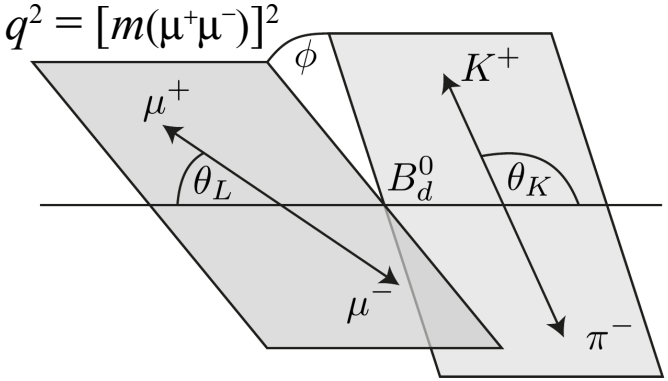

- S_i have large hadronic uncertainties from form-factors
  → cancel at leading order under transformations
- $F_L(q^2)$, $S_i(q^2)$, $P_i(q^2)$ measurement in bins of q^2
  (low statistics => rough binning)
- No K/π identification at ATLAS
  => can't determine B/$\overline{\mathrm{B}}$ flavour in some cases
  => MC: in ~10% events wrong flavour
  => dilution in S5, S8, S6 and S9

$$P_1 = \frac{2S_3}{1-F_L}$$
$$P_2 = \frac{2}{3}\frac{A_{\mathrm{FB}}}{1-F_L}$$
$$P_3 = -\frac{S_9}{1-F_L}$$
$$P'_{i=4,5,6,8} = \frac{S_{j=4,5,7,8}}{\sqrt{F_L(1-F_L)}}$$

Folding

- Not enough statistics for full 3D angular fit → fold distributions, but lost sensitivity to S_6 and S_9 (and thus also $A_{FB} = \frac{3}{4} S_6$)

$$F_L, S_3, S_4, P_4' : \begin{cases} \phi \to -\phi & \text{for } \phi < 0 \\ \phi \to \pi - \phi & \text{for } \theta_L > \frac{\pi}{2} \\ \theta_L \to \pi - \theta_L & \text{for } \theta_L > \frac{\pi}{2} \end{cases}$$

$\cos\theta_L \in [0,1], \cos\theta_K \in [-1,1]$ and $\phi \in [0,\pi]$

$$\frac{1}{d\Gamma/dq^2}\frac{d^4\Gamma}{d\cos\theta_\ell d\cos\theta_K d\phi dq^2} = \frac{9}{8\pi}\left[\frac{3(1-F_L)}{4}\sin^2\theta_K + F_L\cos^2\theta_K + \frac{1-F_L}{4}\sin^2\theta_K\cos 2\theta_\ell - F_L\cos^2\theta_K\cos 2\theta_\ell + S_3\sin^2\theta_K\sin^2\theta_\ell\cos 2\phi + S_4\sin 2\theta_K\sin 2\theta_\ell\cos\phi\right]$$

$$F_L, S_3, S_5, P_5' : \begin{cases} \phi \to -\phi & \text{for } \phi < 0 \\ \theta_L \to \pi - \theta_L & \text{for } \theta_L > \frac{\pi}{2} \end{cases}$$

$\cos\theta_L \in [0,1], \cos\theta_K \in [-1,1]$ and $\phi \in [0,\pi]$

$$\frac{1}{d\Gamma/dq^2}\frac{d^4\Gamma}{d\cos\theta_\ell d\cos\theta_K d\phi dq^2} = \frac{9}{8\pi}\left[\frac{3(1-F_L)}{4}\sin^2\theta_K + F_L\cos^2\theta_K + \frac{1-F_L}{4}\sin^2\theta_K\cos 2\theta_\ell - F_L\cos^2\theta_K\cos 2\theta_\ell + S_3\sin^2\theta_K\sin^2\theta_\ell\cos 2\phi + S_5\sin 2\theta_K\sin\theta_\ell\cos\phi\right]$$

$$F_L, S_3, S_7, P_6' : \begin{cases} \phi \to \pi - \phi & \text{for } \phi > \frac{\pi}{2} \\ \phi \to -\pi - \phi & \text{for } \phi < -\frac{\pi}{2} \\ \theta_L \to \pi - \theta_L & \text{for } \theta_L > \frac{\pi}{2} \end{cases}$$

$\cos\theta_L \in [0,1], \cos\theta_K \in [-1,1]$ and $\phi \in [-\pi/2,\pi/2]$

$$\frac{1}{d\Gamma/dq^2}\frac{d^4\Gamma}{d\cos\theta_\ell d\cos\theta_K d\phi dq^2} = \frac{9}{8\pi}\left[\frac{3(1-F_L)}{4}\sin^2\theta_K + F_L\cos^2\theta_K + \frac{1-F_L}{4}\sin^2\theta_K\cos 2\theta_\ell - F_L\cos^2\theta_K\cos 2\theta_\ell + S_3\sin^2\theta_K\sin^2\theta_\ell\cos 2\phi + S_7\sin 2\theta_K\sin\theta_\ell\sin\phi\right]$$

$$F_L, S_3, S_8, P_8' : \begin{cases} \phi \to \pi - \phi & \text{for } \phi > \frac{\pi}{2} \\ \phi \to -\pi - \phi & \text{for } \phi < -\frac{\pi}{2} \\ \theta_L \to \pi - \theta_L & \text{for } \theta_L > \frac{\pi}{2} \\ \theta_K \to \pi - \theta_K & \text{for } \theta_L > \frac{\pi}{2} \end{cases}$$

$\cos\theta_L \in [0,1], \cos\theta_K \in [-1,1]$ and $\phi \in [-\pi/2,\pi/2]$

$$\frac{1}{d\Gamma/dq^2}\frac{d^4\Gamma}{d\cos\theta_\ell d\cos\theta_K d\phi dq^2} = \frac{9}{8\pi}\left[\frac{3(1-F_L)}{4}\sin^2\theta_K + F_L\cos^2\theta_K + \frac{1-F_L}{4}\sin^2\theta_K\cos 2\theta_\ell - F_L\cos^2\theta_K\cos 2\theta_\ell + S_3\sin^2\theta_K\sin^2\theta_\ell\cos 2\phi + S_8\sin 2\theta_K\sin 2\theta_\ell\sin\phi\right]$$

Results

- Results ~compatible with Standard Model predictions and compatible with other experiments
- Largest deviation of 2.7 sigma in P_5' w.r.t DHWM model, follow LHCb observation

ATLAS-CONF-2017-023

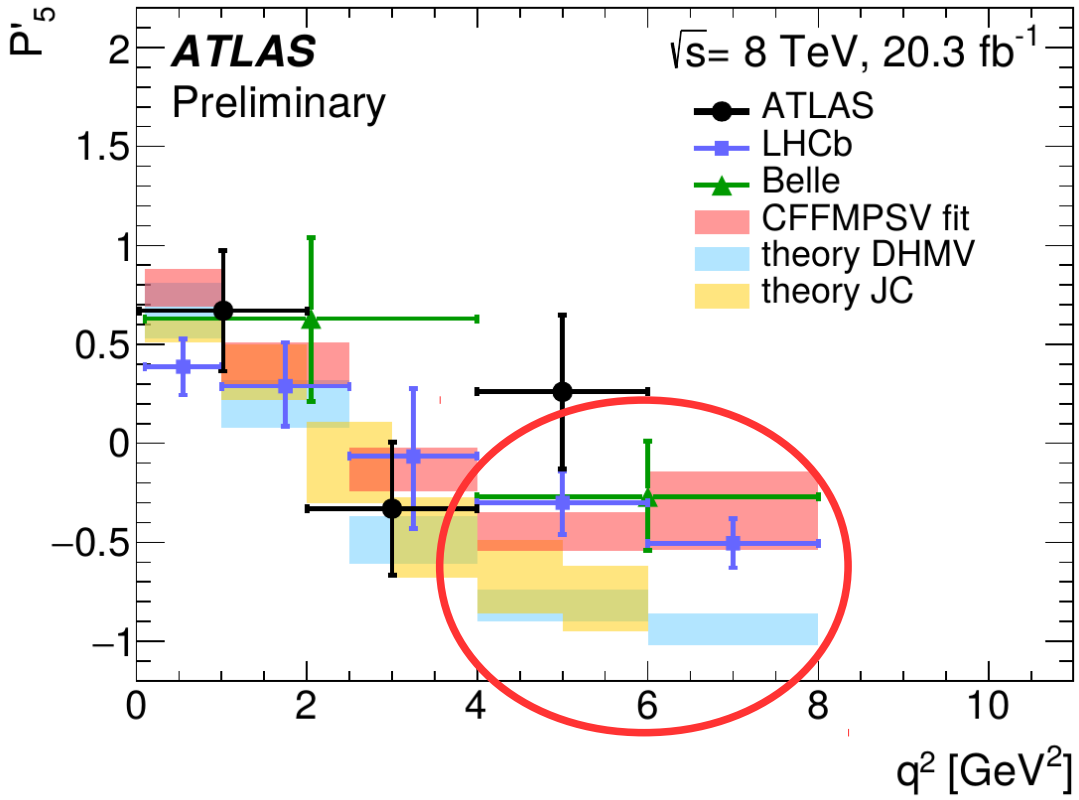

JHEP 02 (2016) 104

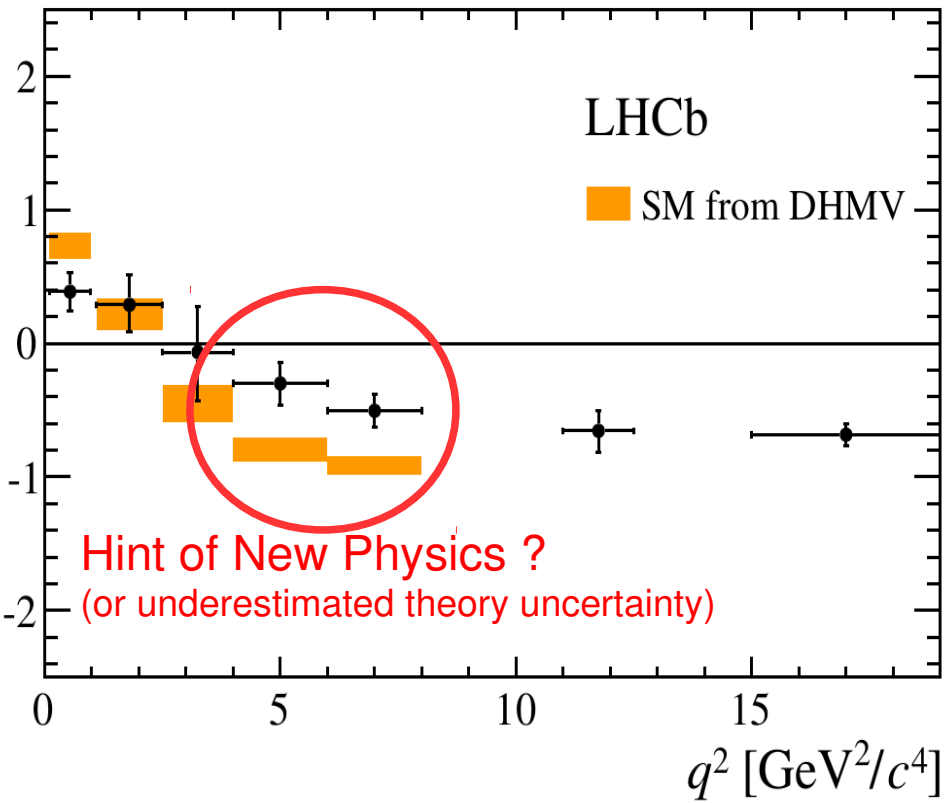

$B_s \to J/\psi\phi$ Analysis

- **Signal time-angular PDF:**
  (convolved with detector resolution)

$$\frac{d^4\Gamma}{dt\, d\Omega} = \sum_{k=1}^{10} O^{(k)}(t) g^{(k)}(\theta_T, \psi_T, \phi_T)$$

2 PDFs for B_s and $\overline{B}_s$(alternative ± signs): PDF(B_s), PDF($\overline{B}_s$)
Tagged fit: Prob(B_s-tag)*PDF(B_s) + (1-Prob(B_s-tag))*PDF($\overline{B}_s$)
Untagged fit: Prob(B_s-tag) = 0.5

Symmetries: $\{\phi_s, \Delta\Gamma_s, \delta_\perp, \delta_\parallel\} \to \{\pi - \phi_s, -\Delta\Gamma_s, \pi - \delta_\perp, 2\pi - \delta_\parallel\}$

~~$\{\phi_s, \Delta\Gamma_s, \delta_\perp, \delta_\parallel, \delta_S\} \to \{\phi_s, \Delta\Gamma_s, \pi - \delta_\perp, -\delta_\parallel, -\delta_S\}$~~ (untagged fit only)

	k	$\mathcal{O}^{(k)}(t)$	$g^{(k)}(\theta_T, \psi_T, \phi_T)$
CP +1	1	$\frac{1}{2}\lvert A_0(0)\rvert^2 \left[(1+\cos\phi_s)\, e^{-\Gamma_L^{(s)} t} + (1-\cos\phi_s)\, e^{-\Gamma_H^{(s)} t} \pm 2e^{-\Gamma_s t}\sin(\Delta m_s t)\sin\phi_s\right]$	$2\cos^2\psi_T(1-\sin^2\theta_T\cos^2\phi_T)$
CP +1	2	$\frac{1}{2}\lvert A_\parallel(0)\rvert^2 \left[(1+\cos\phi_s)\, e^{-\Gamma_L^{(s)} t} + (1-\cos\phi_s)\, e^{-\Gamma_H^{(s)} t} \pm 2e^{-\Gamma_s t}\sin(\Delta m_s t)\sin\phi_s\right]$	$\sin^2\psi_T(1-\sin^2\theta_T\sin^2\phi_T)$
CP -1	3	$\frac{1}{2}\lvert A_\perp(0)\rvert^2 \left[(1-\cos\phi_s)\, e^{-\Gamma_L^{(s)} t} + (1+\cos\phi_s)\, e^{-\Gamma_H^{(s)} t} \mp 2e^{-\Gamma_s t}\sin(\Delta m_s t)\sin\phi_s\right]$	$\sin^2\psi_T\sin^2\theta_T$
Inter-ference terms	4	$\frac{1}{2}\lvert A_0(0)\rvert\lvert A_\parallel(0)\rvert\cos\delta_\parallel \left[(1+\cos\phi_s)\, e^{-\Gamma_L^{(s)} t} + (1-\cos\phi_s)\, e^{-\Gamma_H^{(s)} t} \pm 2e^{-\Gamma_s t}\sin(\Delta m_s t)\sin\phi_s\right]$	$\frac{1}{\sqrt{2}}\sin 2\psi_T\sin^2\theta_T\sin 2\phi_T$
	5	$\lvert A_\parallel(0)\rvert\lvert A_\perp(0)\rvert[\frac{1}{2}(e^{-\Gamma_L^{(s)} t} - e^{-\Gamma_H^{(s)} t})\cos(\delta_\perp-\delta_\parallel)\sin\phi_s \pm e^{-\Gamma_s t}(\sin(\delta_\perp-\delta_\parallel)\cos(\Delta m_s t) - \cos(\delta_\perp-\delta_\parallel)\cos\phi_s\sin(\Delta m_s t))]$	$-\sin^2\psi_T\sin 2\theta_T\sin\phi_T$
	6	$\lvert A_0(0)\rvert\lvert A_\perp(0)\rvert[\frac{1}{2}(e^{-\Gamma_L^{(s)} t} - e^{-\Gamma_H^{(s)} t})\cos\delta_\perp\sin\phi_s \pm e^{-\Gamma_s t}(\sin\delta_\perp\cos(\Delta m_s t) - \cos\delta_\perp\cos\phi_s\sin(\Delta m_s t))]$	$\frac{1}{\sqrt{2}}\sin 2\psi_T\sin 2\theta_T\cos\phi_T$
S-wave terms	7	$\frac{1}{2}\lvert A_S(0)\rvert^2 \left[(1-\cos\phi_s)\, e^{-\Gamma_L^{(s)} t} + (1+\cos\phi_s)\, e^{-\Gamma_H^{(s)} t} \mp 2e^{-\Gamma_s t}\sin(\Delta m_s t)\sin\phi_s\right]$	$\frac{2}{3}\left(1-\sin^2\theta_T\cos^2\phi_T\right)$
	8	$\lvert A_S(0)\rvert\lvert A_\parallel(0)\rvert[\frac{1}{2}(e^{-\Gamma_L^{(s)} t} - e^{-\Gamma_H^{(s)} t})\sin(\delta_\parallel-\delta_S)\sin\phi_s \pm e^{-\Gamma_s t}(\cos(\delta_\parallel-\delta_S)\cos(\Delta m_s t) - \sin(\delta_\parallel-\delta_S)\cos\phi_s\sin(\Delta m_s t))]$	$\frac{1}{3}\sqrt{6}\sin\psi_T\sin^2\theta_T\sin 2\phi_T$
	9	$\frac{1}{2}\lvert A_S(0)\rvert\lvert A_\perp(0)\rvert\sin(\delta_\perp-\delta_S) \left[(1-\cos\phi_s)\, e^{-\Gamma_L^{(s)} t} + (1+\cos\phi_s)\, e^{-\Gamma_H^{(s)} t} \mp 2e^{-\Gamma_s t}\sin(\Delta m_s t)\sin\phi_s\right]$	$\frac{1}{3}\sqrt{6}\sin\psi_T\sin 2\theta_T\cos\phi_T$
	10	$\lvert A_0(0)\rvert\lvert A_S(0)\rvert[\frac{1}{2}(e^{-\Gamma_H^{(s)} t} - e^{-\Gamma_L^{(s)} t})\sin\delta_S\sin\phi_s \pm e^{-\Gamma_s t}(\cos\delta_S\cos(\Delta m_s t) + \sin\delta_S\cos\phi_s\sin(\Delta m_s t))]$	$\frac{4}{3}\sqrt{3}\cos\psi_T\left(1-\sin^2\theta_T\cos^2\phi_T\right)$

B_s Flavour Tagging

- Knowledge of $B_s/\overline{B}_s$ flavour at production significantly increases signal PDF sensitivity to ϕ_s
- Three taggers: muon, electron, b-tagged jet
- Key variable: charge of p_T-weighted tracks in a cone (ΔR) around the opposite side primary object (μ, e, b-jet), used to build per-candidates B_s tag probability

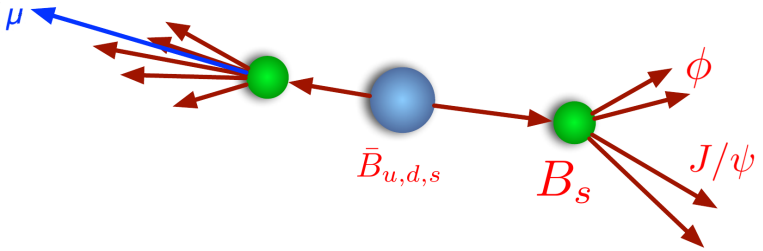

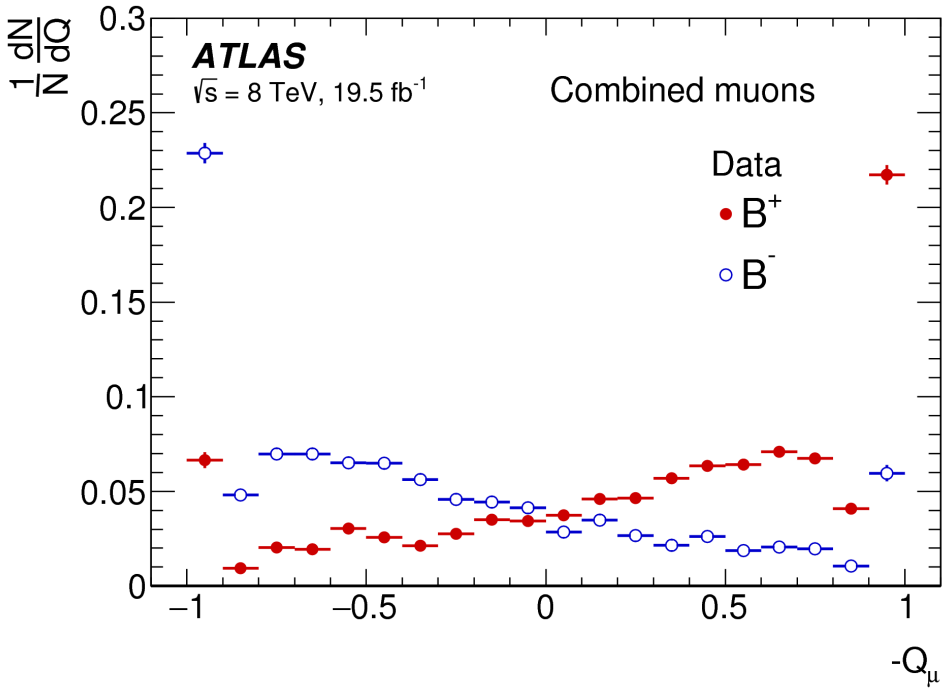

$$Q_\mu = \frac{\sum_i^{N\ \text{tracks}} q_i \cdot (p_{Ti})^\kappa}{\sum_i^{N\ \text{tracks}} (p_{Ti})^\kappa}$$

- Calibration on self-tagged $B^\pm \to J/\psi K^\pm$ channel:

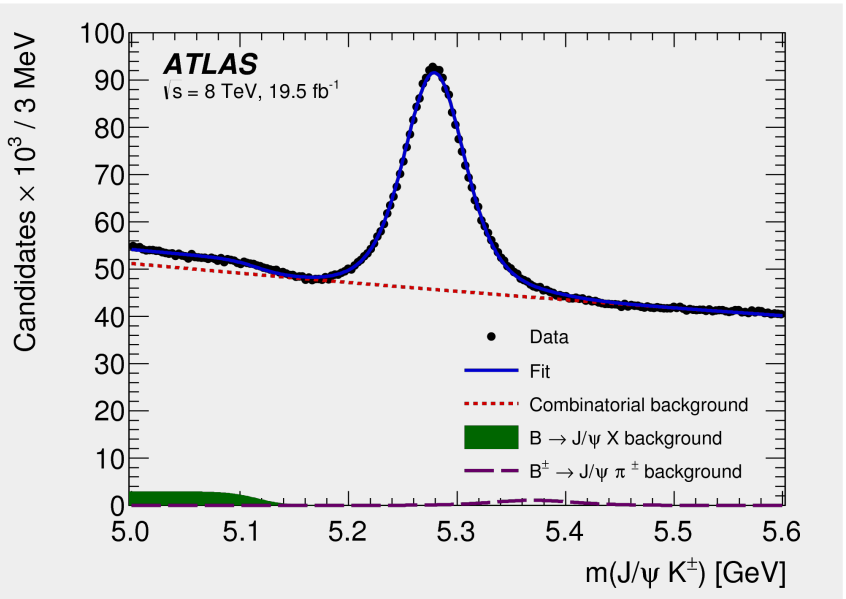

Results

- Full Run-1 dataset
- Consistency with Standard Model prediction
- Experimental precision vs. theory precision in ϕ_s ~ 50x, vs. SM ϕ_s value ~ 2.4x

Par	Run1 combined Value	Stat	Syst
ϕ_s[rad]	−0.090	0.078	0.041
$\Delta\Gamma_s$[ps^{-1}]	0.085	0.011	0.007
Γ_s[ps^{-1}]	0.675	0.003	0.003
$\lvert A_{\parallel}(0)\rvert^2$	0.227	0.004	0.006
$\lvert A_0(0)\rvert^2$	0.522	0.003	0.007
$\lvert A_S\rvert^2$	0.072	0.007	0.018
$\delta_\perp$ [rad]	4.15	0.32	0.16
$\delta_{\parallel}$ [rad]	3.15	0.10	0.05
$\delta_\perp - \delta_S$ [rad]	−0.08	0.03	0.01

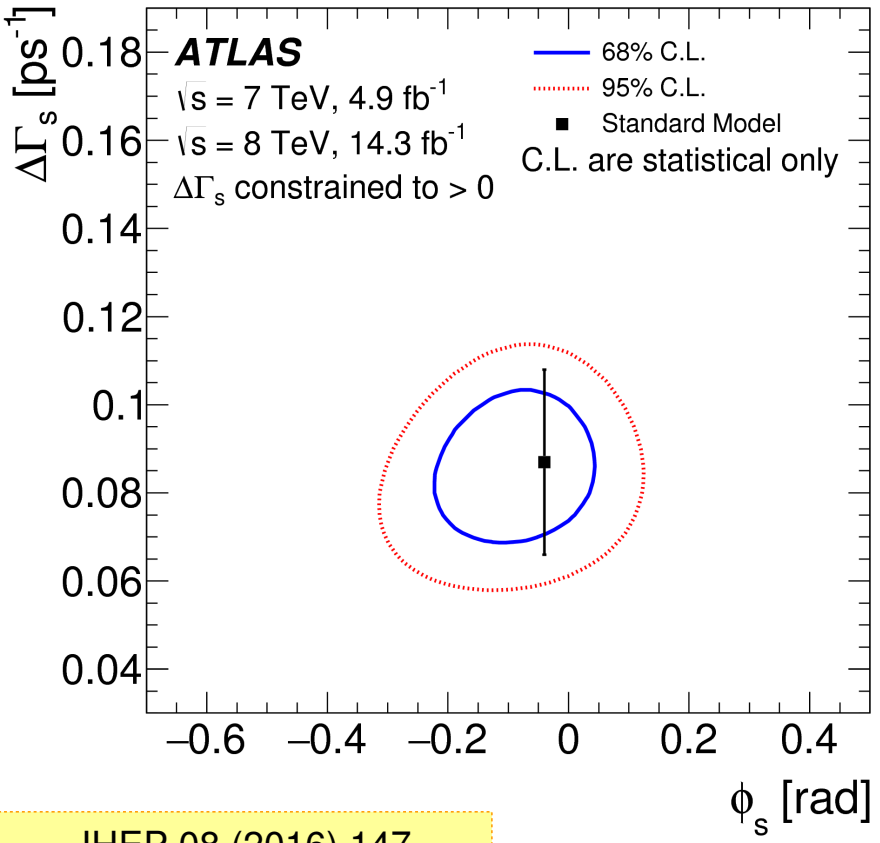

JHEP 08 (2016) 147

Results

- Full Run-1 dataset
- Consistency with Standard Model prediction
- Experimental precision vs. theory precision in ϕ_s ~ 17x, vs. SM ϕ_s value ~ 0.84x

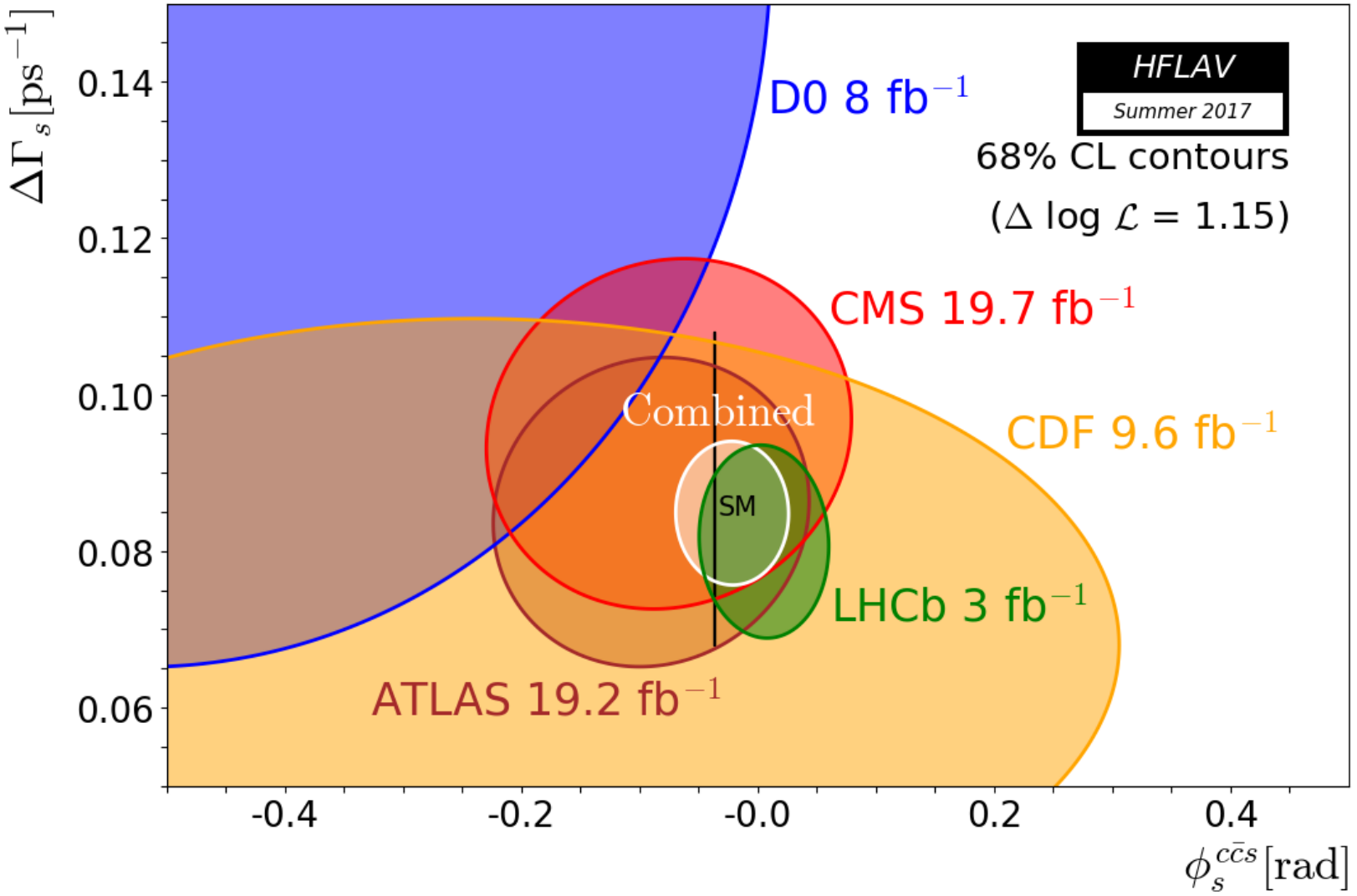

Measurements in Run-2 and Beyond

LHC / HL-LHC Plan

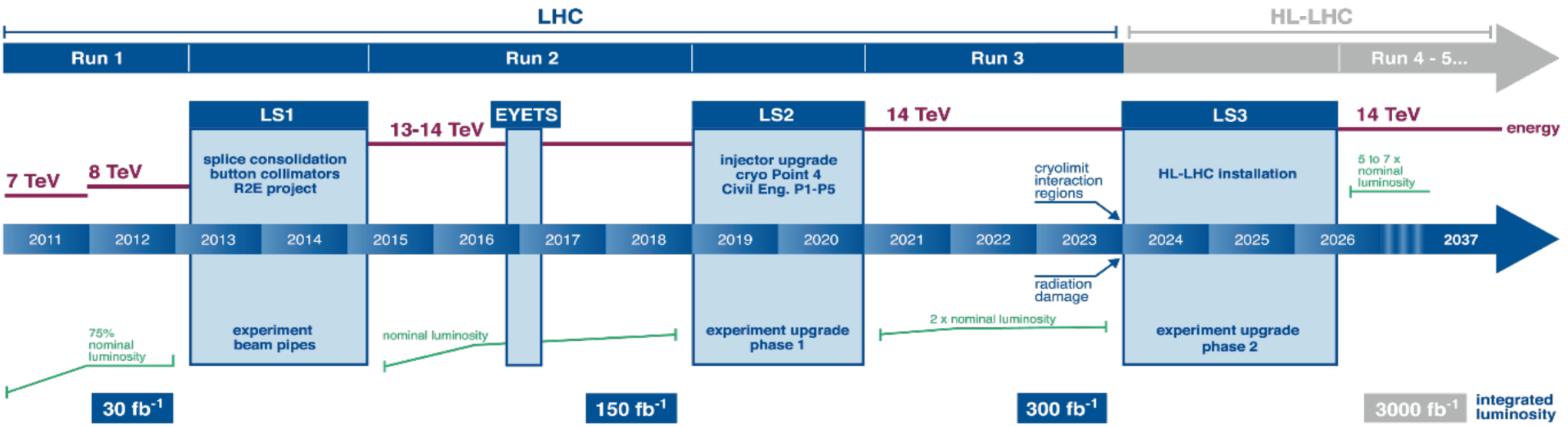

- New pixel layer (IBL, 32-38 mm) + small radius Be beam pipe
- Topological L1 trigger

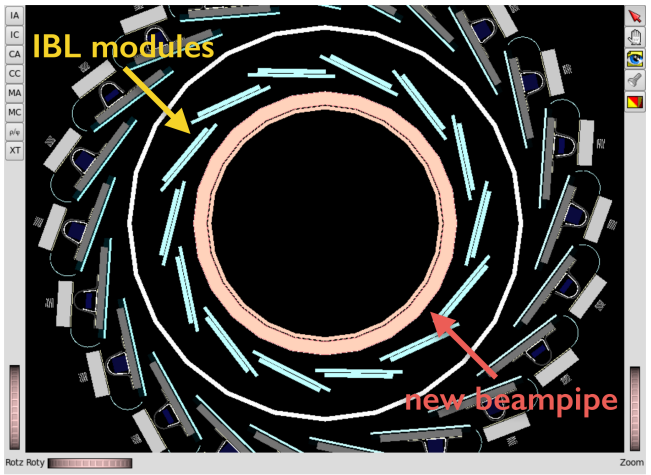

- New small muon wheel
- Fast tracking trigger (FTK) at LVL 1.5; available in Run-2

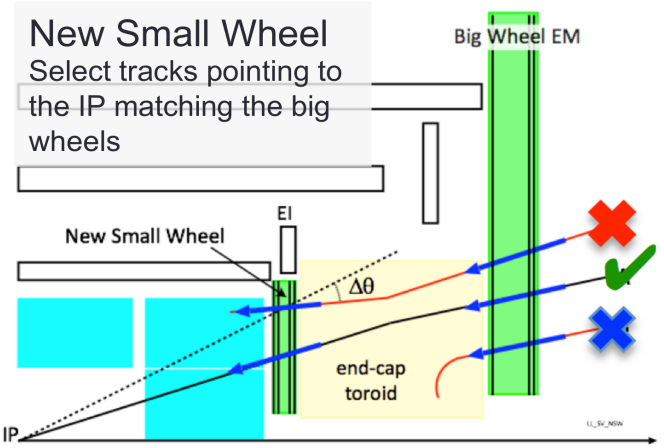

- Completely new Si based tracker (ITK)

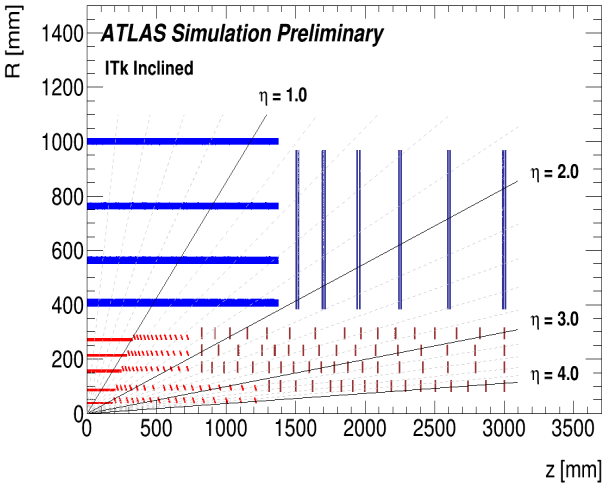

Measurements in Run-2 and Beyond

LHC / HL-LHC Plan

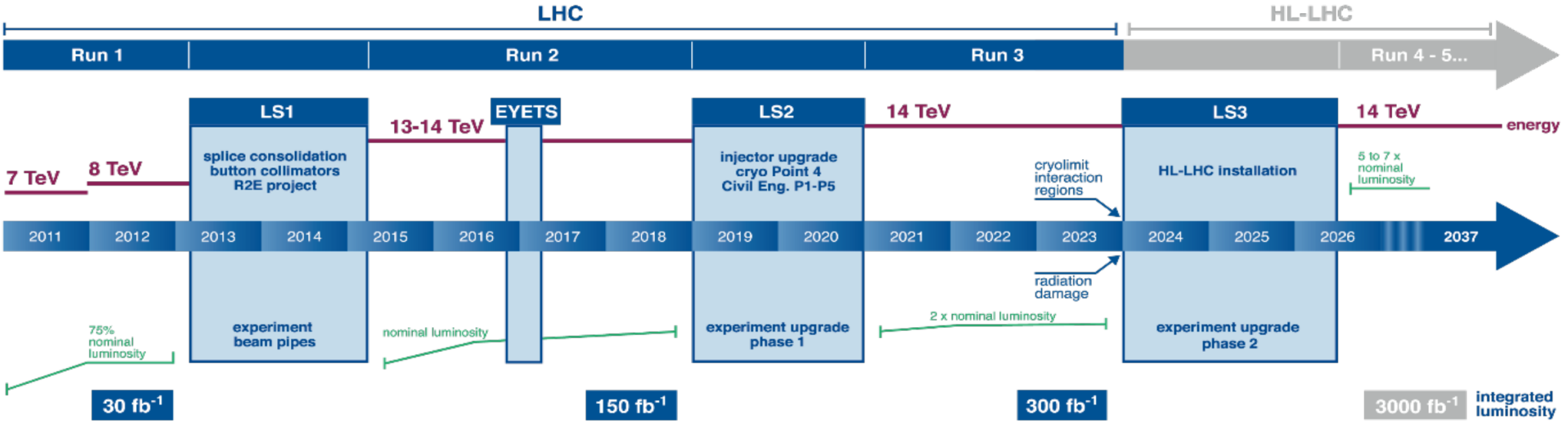

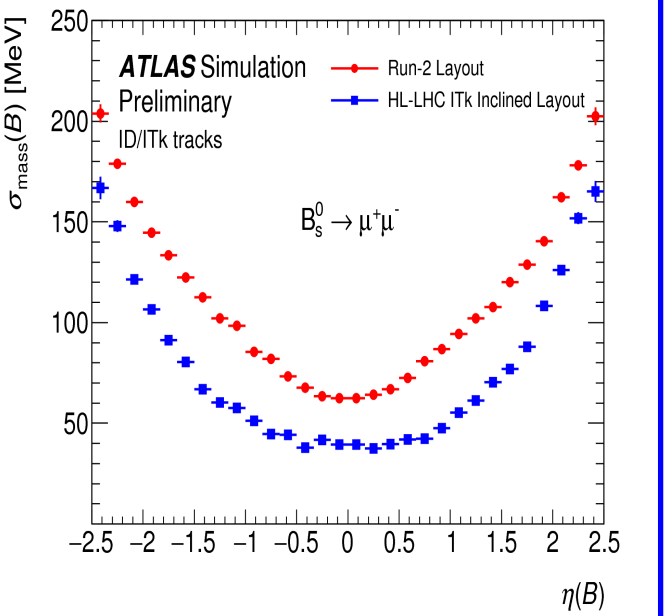

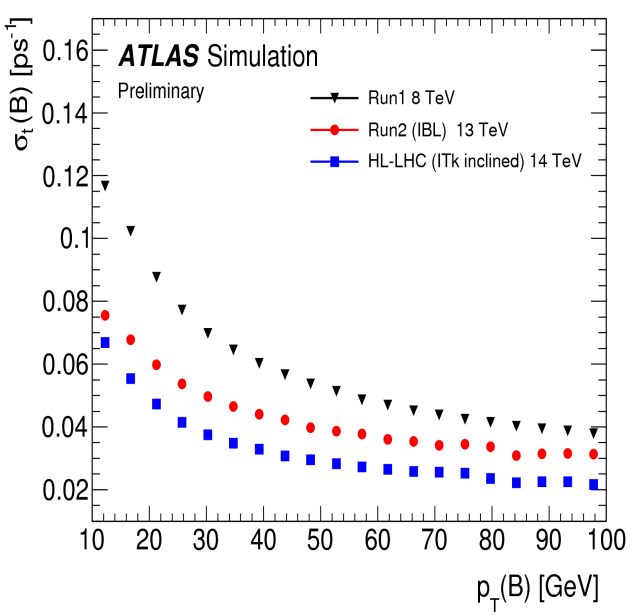

- Completely new Si based tracker (ITK)

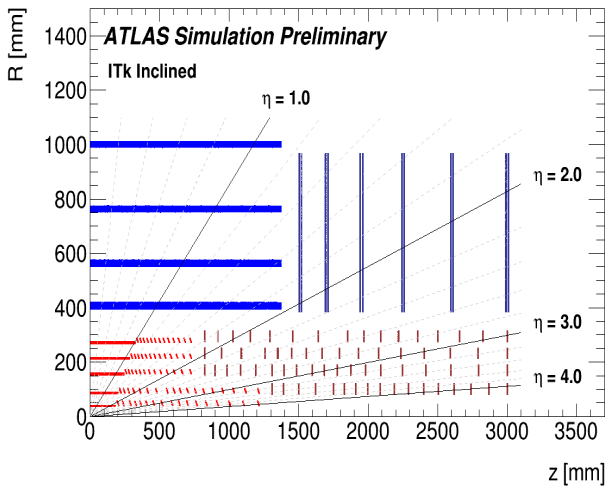

Conclusions

- Experimental reach in B-decays exciting
  - Very rare decays becoming observable
  - Enough statistics for angular analyses of rare decays
  - Experimental errors getting closer to theory uncertainties
- ATLAS prospects: increase statistics in Run-2 and beyond and:
  - Benefit from better decay time (≥ Run-2) and mass (at HL-LHC) resolution
  - Better triggers to cope with high instantaneous luminosity (topology at L1, fast track triggers, partial event building, ...)
  - Fit & Systematics improvement: modeling and fitting small components, finer binning, ...
  - Possibly analyze other decay channels to cross-check observed tensions:

JHEP 02 (2016) 104
Angular analysis of
$B^0 \to K^*\mu\mu$

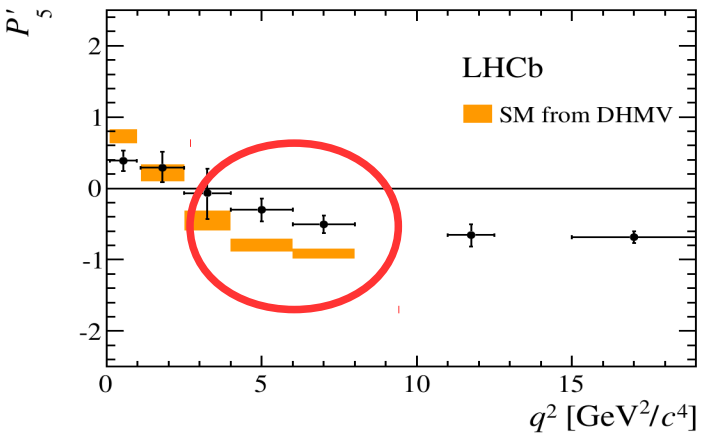

JHEP 09 (2015) 179
Differential decay rate
$B_s \to \phi\mu\mu$

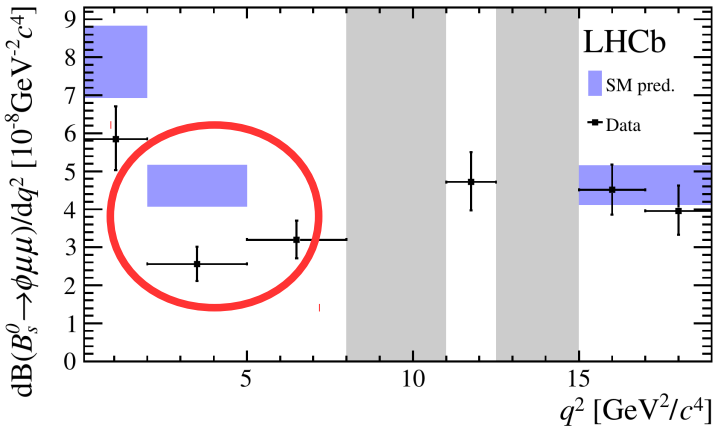

arXiv:1705.05802
Relative production of
$B^0 \to K^*\mu\mu$ / $B^0 \to K^*ee$

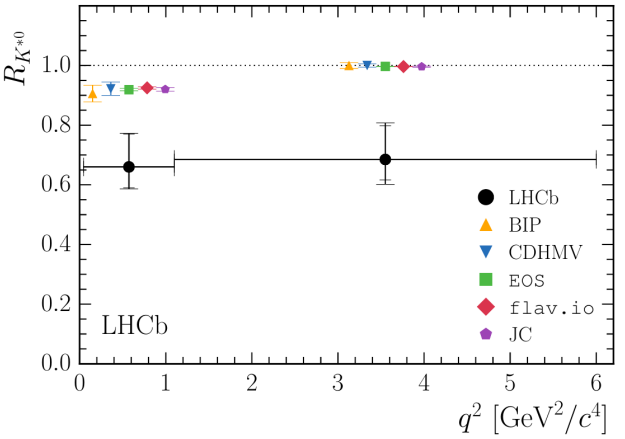

Backup

Leptonic decays: $B_{(s)} \to \mu^+\mu^-$

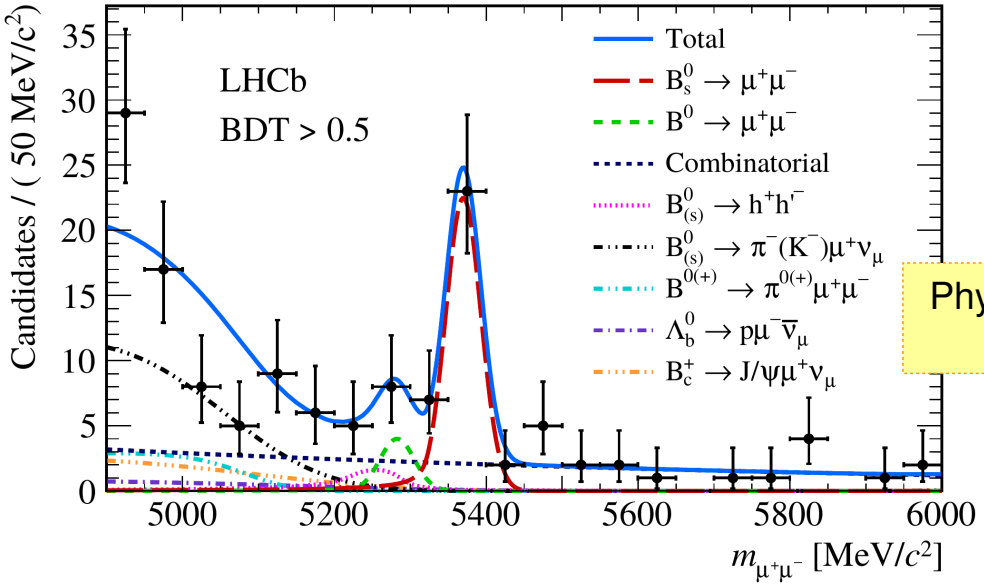

Phys. Rev. Lett. 118, 191801 (2017)

LHCb, ATLAS, CMS

Phys.Rev.Lett. 111 (2013) 101804

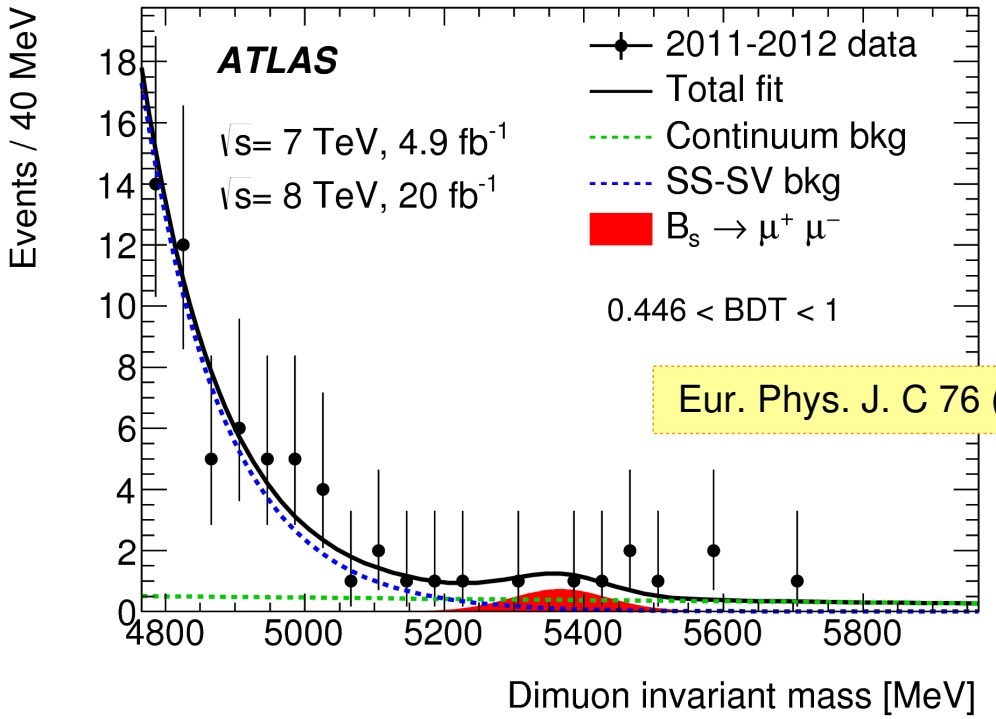

Eur. Phys. J. C 76 (2016) 513

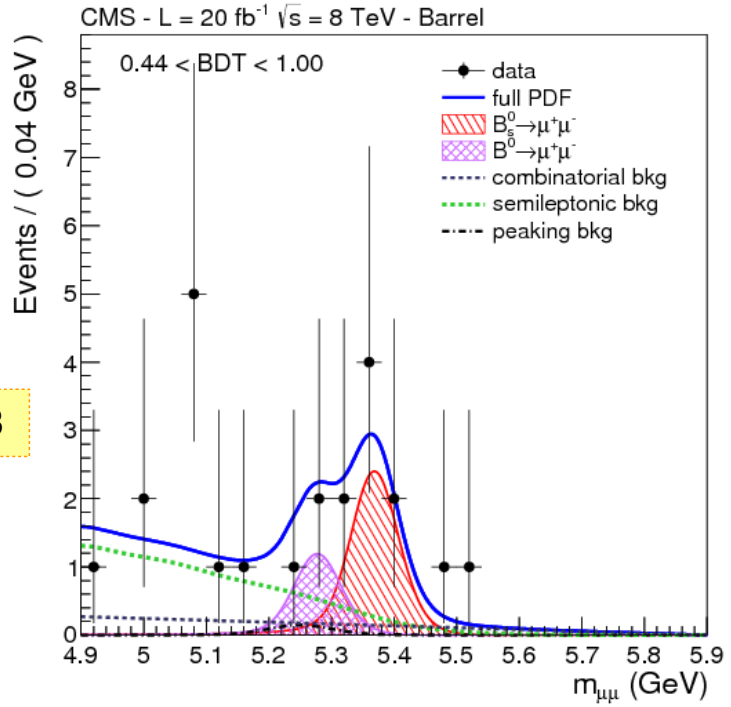

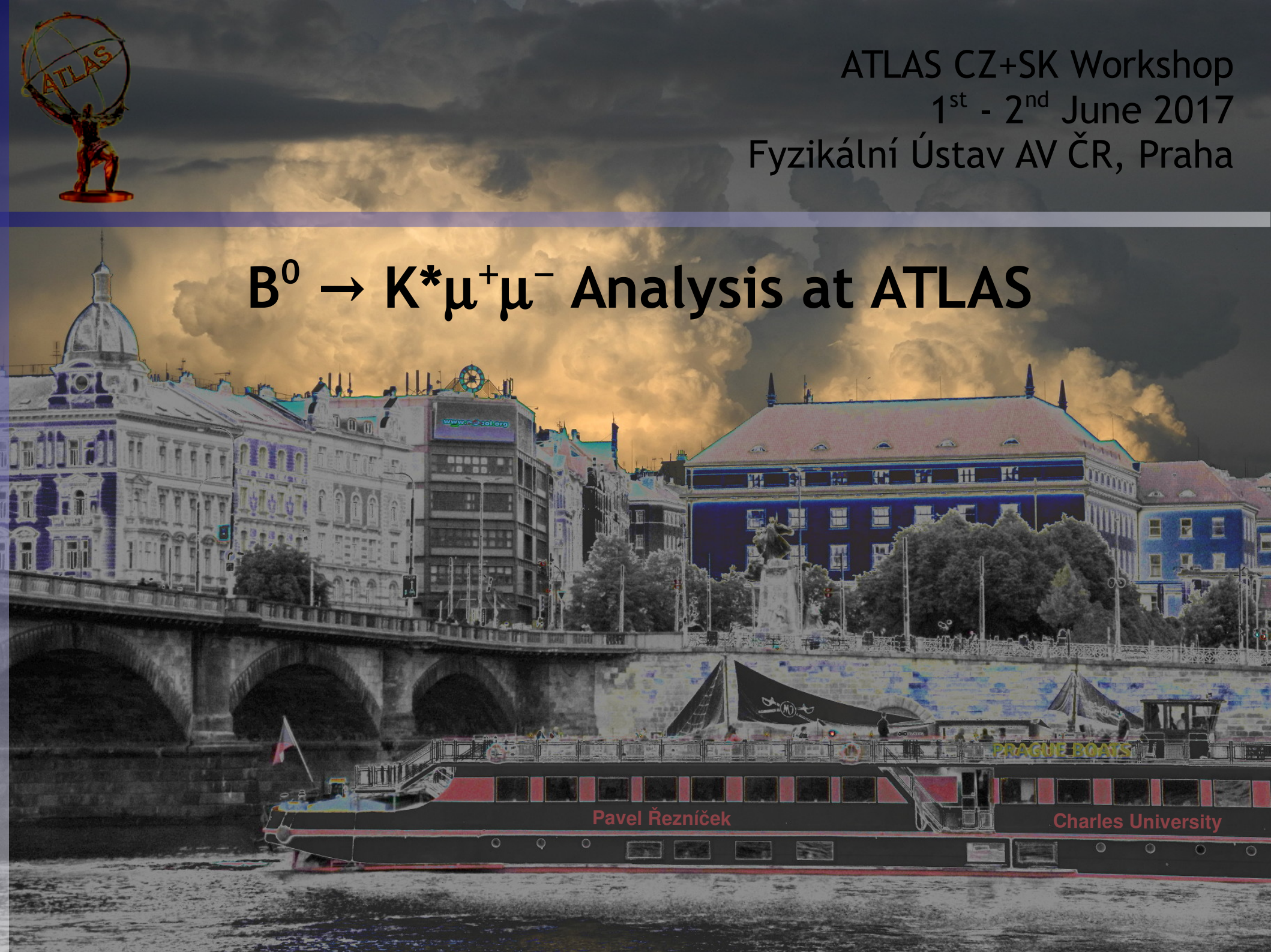
ATLAS CZ+SK Workshop
1st - 2nd June 2017
Fyzikální Ústav AV ČR, Praha
B⁰ → K*μ⁺μ⁻ Analysis at ATLAS
PRAGUE BOATS
Pavel Řezníček
Charles University

The ATLAS Experiment

General purpose detector

Calorimeter System

EM and Hadronic energy
- LAr EM barrel and EC
- LAr Had. EC
- Tile Calorimeter (Fe-Scin.) hadronic barrel

Muon Specrometer

Toroid Magnets
Precision μ tracking:
- MDT (Monitored Drift Tubes)
- CSC (Cathode Strip Chambers)

Trigger:
- RPC (Resistive Plate Chamber)
- TGC (Thin Gas Chamber)

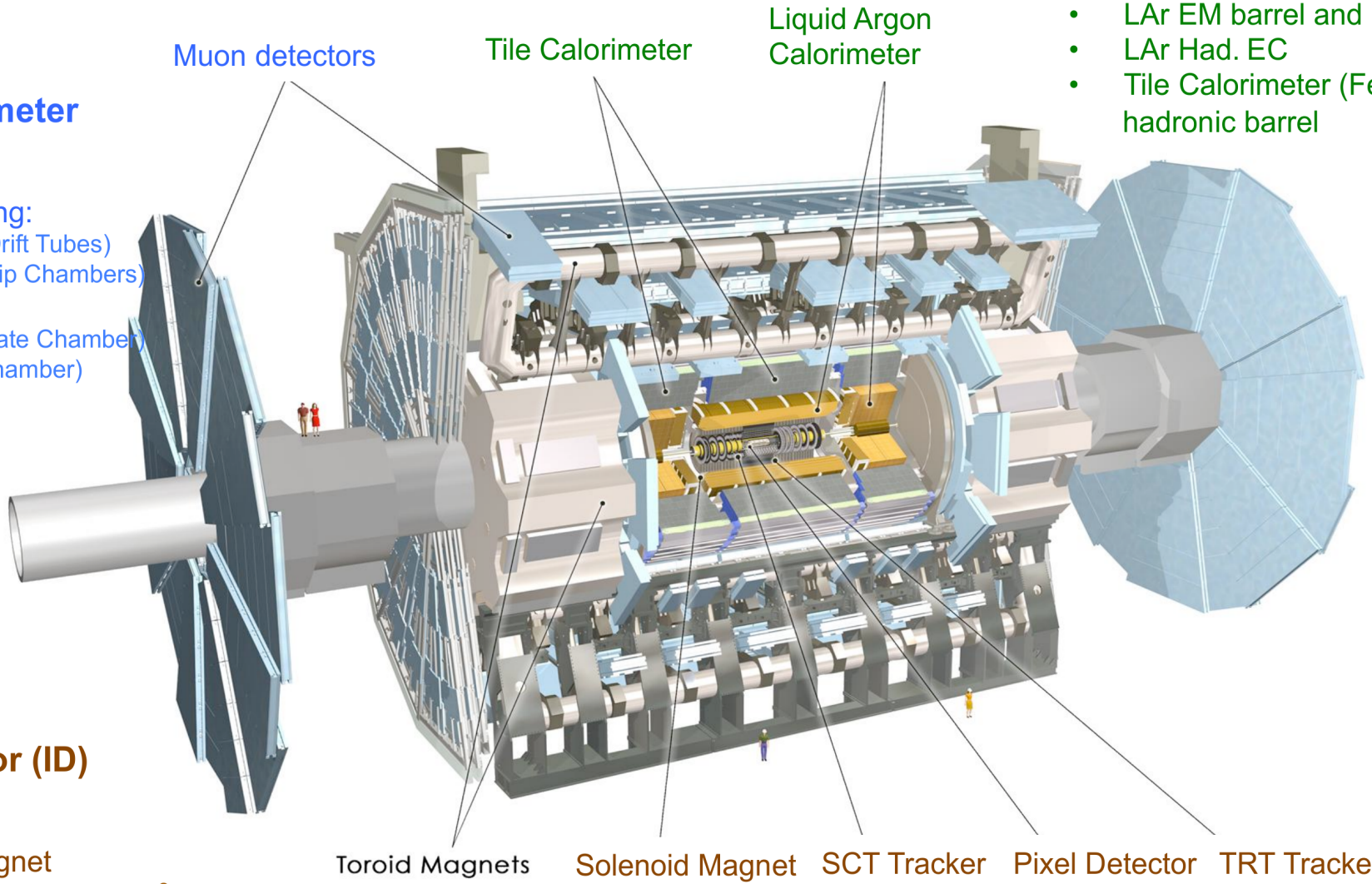

Inner Detector (ID)

Tracking
2T Solenoid Magnet
- Silicon Pixels, 50x400 μm^2
- Silicon Strips (SCT), 80 μm stereo
- Transition Ratiation Tracker (TRT) 36 points/track

B-Physics at the ATLAS Experiment

- Triggering $|\eta| < 2.4$
- Precision Tracking $|\eta| < 2.7$

ATLAS B-physics programme: **precision measurements** (rare decays, b-hadron decay properties, CPV), **HF production** (b-hadrons, quarkonia, associated quarkonia production) and **spectroscopy** (new states&decays)

- Mostly in exclusive decays with single/di-/multi-muon final states, which allows to trigger low-p_T objects

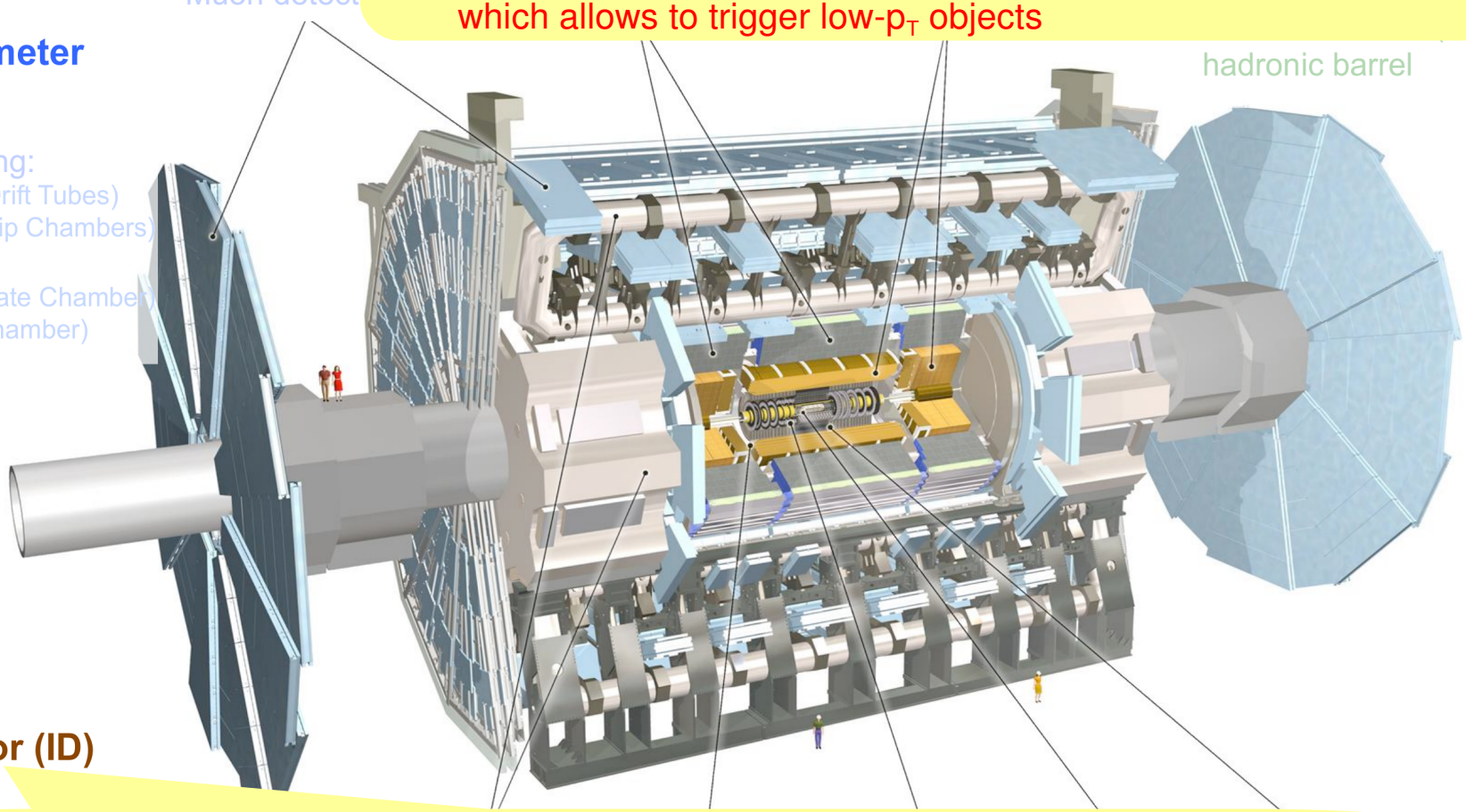

Muon Specrometer

Toroid Magnets

Precision μ tracking:

- MDT (Monitored Drift Tubes)
- CSC (Cathode Strip Chambers)

Trigger:

- RPC (Resistive Plate Chamber)
- TGC (Thin Gas Chamber)

Inner Detector (ID)

- $p_T > 0.4$ GeV, $|\eta| < 2.5$
- New for Run2: Insertable B-Layer (IBL) an additional inner-most pixel layer ($r = 33$mm) and lower x/X_0 beam pipe

- Resolution in $m_{\mu+\mu-}$: around 50 MeV for J/ψ and 150 MeV for Υ(nS)
- Resolution in b-hadron proper decay time in Run-1 data around 100 fs (~30% improvement with IBL in Run-2)

Motivation for $B^0 \to K^* \mu^+ \mu^-$ Analysis

- In Standard Model do not occur at tree level,
  but only via Feynman diagrams with loops => small branching ratio (BR)

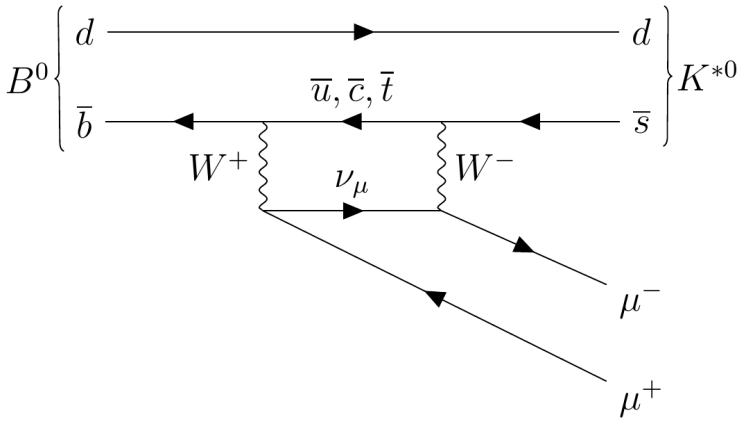

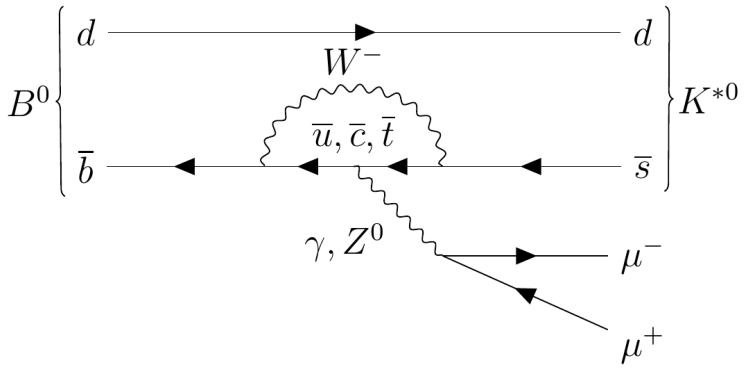

New particles in the loops can significantly change the decay properties

- $B \to K^* \mu^+ \mu^-$: BR ~ 10^{-6}, New Physics can significantly change the differential decay rate

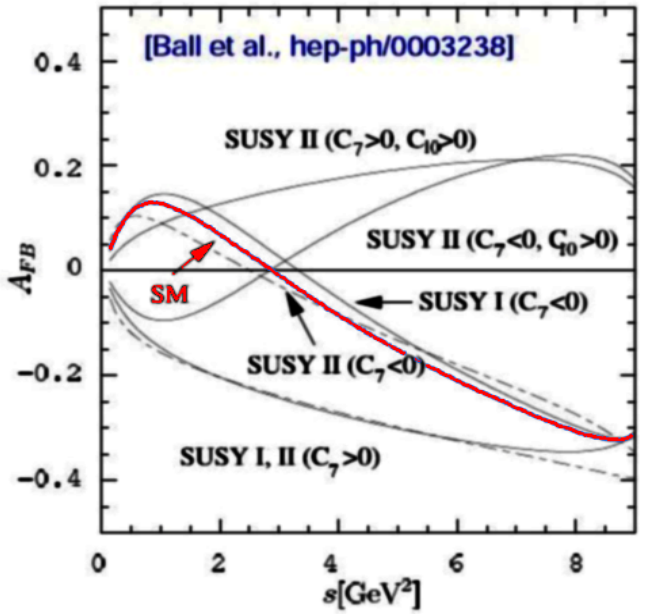

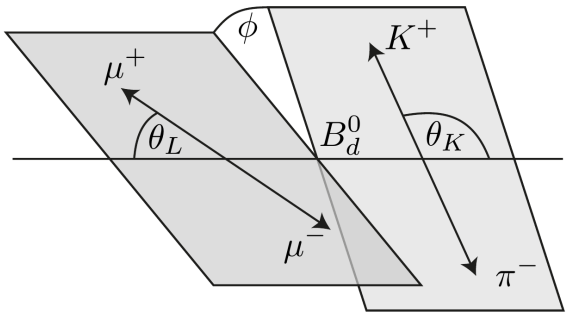

$$s = q^2 = [m(\mu^+\mu^-)]^2$$

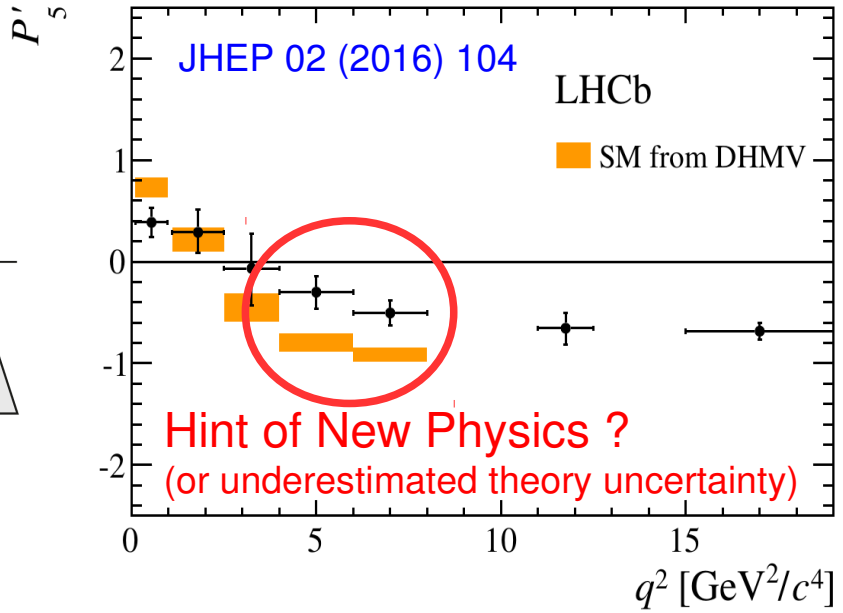

Decay Angles Description

- Decay described in helicity basis amplitudes, measuring coefficients before the terms

$$\frac{1}{\mathrm{d}\Gamma/\mathrm{d}q^2}\frac{\mathrm{d}^4\Gamma}{\mathrm{d}\cos\theta_L\mathrm{d}\cos\theta_K\mathrm{d}\phi\mathrm{d}q^2} = \frac{9}{32\pi}\left[\frac{3(1-F_L)}{4}\sin^2\theta_K + F_L\cos^2\theta_K + \frac{1-F_L}{4}\sin^2\theta_K\cos 2\theta_L\right.$$
$$-F_L\cos^2\theta_K\cos 2\theta_L + S_3\sin^2\theta_K\sin^2\theta_L\cos 2\phi$$
$$+S_4\sin 2\theta_K\sin 2\theta_L\cos\phi + S_5\sin 2\theta_K\sin\theta_L\cos\phi$$
$$+S_6\sin^2\theta_K\cos\theta_L + S_7\sin 2\theta_K\sin\theta_L\sin\phi$$
$$\left.+S_8\sin 2\theta_K\sin 2\theta_L\sin\phi + S_9\sin^2\theta_K\sin^2\theta_L\sin 2\phi\right]$$

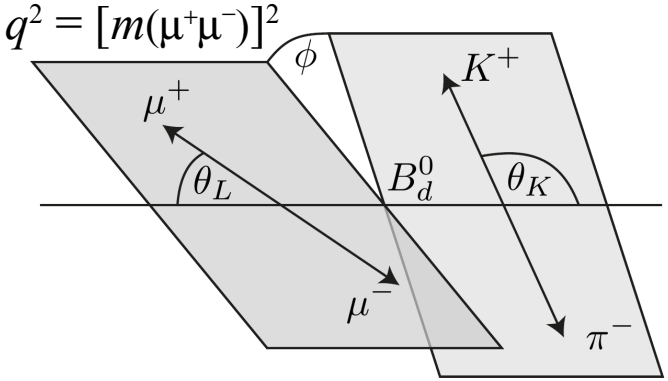

- S_i have large hadronic uncertainties from form-factors
  → cancel at leading order under transformations

$$P_1 = \frac{2S_3}{1-F_L}$$
$$P_2 = \frac{2}{3}\frac{A_{\mathrm{FB}}}{1-F_L}$$
$$P_3 = -\frac{S_9}{1-F_L}$$
$$P'_{i=4,5,6,8} = \frac{S_{j=4,5,7,8}}{\sqrt{F_L(1-F_L)}}$$

- $F_{\mathrm{L}}(q^2)$, $S_i(q^2)$, $\mathrm{P}_i(q^2)$ measurement in bins of q^2
  (low statistics => rough binning)

Folding

- Not enough statistics for full 3D angular fit → fold distributions, but lost sensitivity to S_6 and S_9 (and thus also $A_{FB} = \frac{3}{4} S_6$)

$$F_L, S_3, S_4, P_4' : \begin{cases} \phi \to -\phi & \text{for } \phi < 0 \\ \phi \to \pi - \phi & \text{for } \theta_L > \frac{\pi}{2} \\ \theta_L \to \pi - \theta_L & \text{for } \theta_L > \frac{\pi}{2} \end{cases}$$

$\cos\theta_L \in [0,1], \cos\theta_K \in [-1,1]$ and $\phi \in [0,\pi]$

$$\frac{1}{d\Gamma/dq^2}\frac{d^4\Gamma}{d\cos\theta_\ell d\cos\theta_K d\phi dq^2} = \frac{9}{8\pi}\left[\frac{3(1-F_L)}{4}\sin^2\theta_K + F_L\cos^2\theta_K + \frac{1-F_L}{4}\sin^2\theta_K\cos 2\theta_\ell - F_L\cos^2\theta_K\cos 2\theta_\ell + S_3\sin^2\theta_K\sin^2\theta_\ell\cos 2\phi + S_4\sin 2\theta_K\sin 2\theta_\ell\cos\phi\right]$$

$$F_L, S_3, S_5, P_5' : \begin{cases} \phi \to -\phi & \text{for } \phi < 0 \\ \theta_L \to \pi - \theta_L & \text{for } \theta_L > \frac{\pi}{2} \end{cases}$$

$\cos\theta_L \in [0,1], \cos\theta_K \in [-1,1]$ and $\phi \in [0,\pi]$

$$\frac{1}{d\Gamma/dq^2}\frac{d^4\Gamma}{d\cos\theta_\ell d\cos\theta_K d\phi dq^2} = \frac{9}{8\pi}\left[\frac{3(1-F_L)}{4}\sin^2\theta_K + F_L\cos^2\theta_K + \frac{1-F_L}{4}\sin^2\theta_K\cos 2\theta_\ell - F_L\cos^2\theta_K\cos 2\theta_\ell + S_3\sin^2\theta_K\sin^2\theta_\ell\cos 2\phi + S_5\sin 2\theta_K\sin\theta_\ell\cos\phi\right]$$

$$F_L, S_3, S_7, P_6' : \begin{cases} \phi \to \pi - \phi & \text{for } \phi > \frac{\pi}{2} \\ \phi \to -\pi - \phi & \text{for } \phi < -\frac{\pi}{2} \\ \theta_L \to \pi - \theta_L & \text{for } \theta_L > \frac{\pi}{2} \end{cases}$$

$\cos\theta_L \in [0,1], \cos\theta_K \in [-1,1]$ and $\phi \in [-\pi/2,\pi/2]$

$$\frac{1}{d\Gamma/dq^2}\frac{d^4\Gamma}{d\cos\theta_\ell d\cos\theta_K d\phi dq^2} = \frac{9}{8\pi}\left[\frac{3(1-F_L)}{4}\sin^2\theta_K + F_L\cos^2\theta_K + \frac{1-F_L}{4}\sin^2\theta_K\cos 2\theta_\ell - F_L\cos^2\theta_K\cos 2\theta_\ell + S_3\sin^2\theta_K\sin^2\theta_\ell\cos 2\phi + S_7\sin 2\theta_K\sin\theta_\ell\sin\phi\right]$$

$$F_L, S_3, S_8, P_8' : \begin{cases} \phi \to \pi - \phi & \text{for } \phi > \frac{\pi}{2} \\ \phi \to -\pi - \phi & \text{for } \phi < -\frac{\pi}{2} \\ \theta_L \to \pi - \theta_L & \text{for } \theta_L > \frac{\pi}{2} \\ \theta_K \to \pi - \theta_K & \text{for } \theta_L > \frac{\pi}{2} \end{cases}$$

$\cos\theta_L \in [0,1], \cos\theta_K \in [-1,1]$ and $\phi \in [-\pi/2,\pi/2]$

$$\frac{1}{d\Gamma/dq^2}\frac{d^4\Gamma}{d\cos\theta_\ell d\cos\theta_K d\phi dq^2} = \frac{9}{8\pi}\left[\frac{3(1-F_L)}{4}\sin^2\theta_K + F_L\cos^2\theta_K + \frac{1-F_L}{4}\sin^2\theta_K\cos 2\theta_\ell - F_L\cos^2\theta_K\cos 2\theta_\ell + S_3\sin^2\theta_K\sin^2\theta_\ell\cos 2\phi + S_8\sin 2\theta_K\sin 2\theta_\ell\sin\phi\right]$$

ATLAS Analysis

- Data sample: Full 2012 data: 20.3 fb^{-1} @ 8 TeV
- Limited range to 0.04 GeV^2 < $q^2 = [m(\mu^+\mu^-)]^2$ < 6 GeV^2
  - Avoid complications from $c\bar{c}$-resonances
  - Most demanding after the LHCb measurement…
  - Excluded $\phi \to \mu^+\mu^-$ region [0.98, 1.1] GeV^2

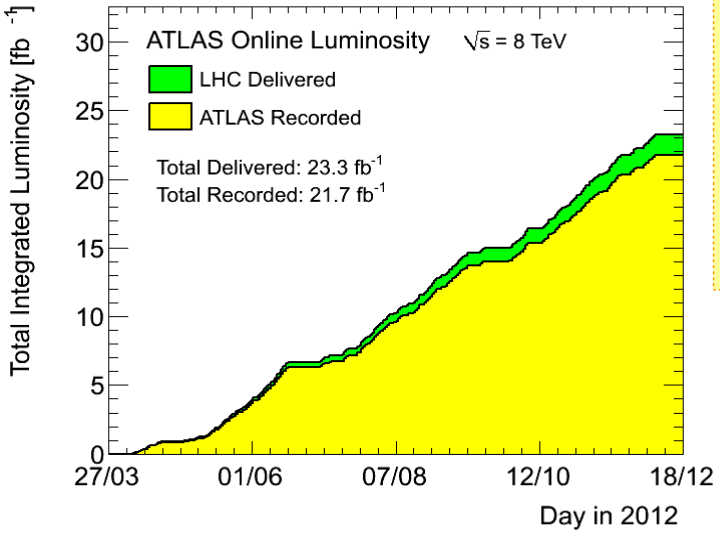

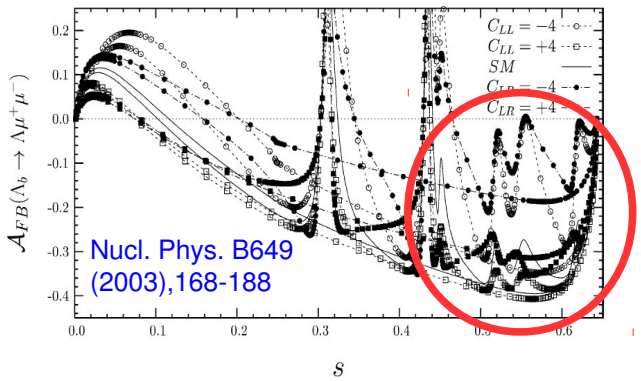

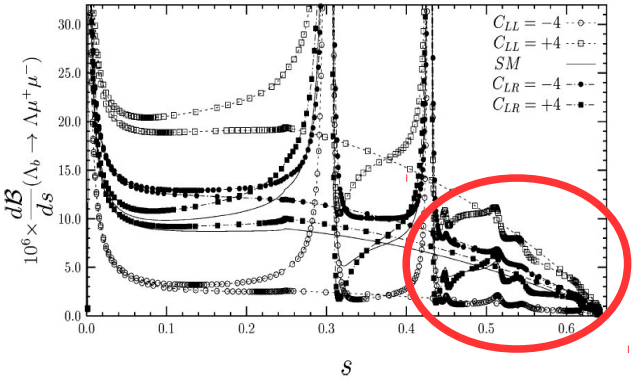

- Trigger: combination of 19 single/di/tri-muon triggers
  - But dominated by di-muon trigger requesting
    - $p_{T\mu1(\mu2)}$ > 4(6) GeV at L1
    - and with $B^0 \to K^*(K\pi)\mu^+\mu^-$ reco. at HLT
- Analysis teams: QMUL, Prague CU, JINR Dubna, Innsbruck

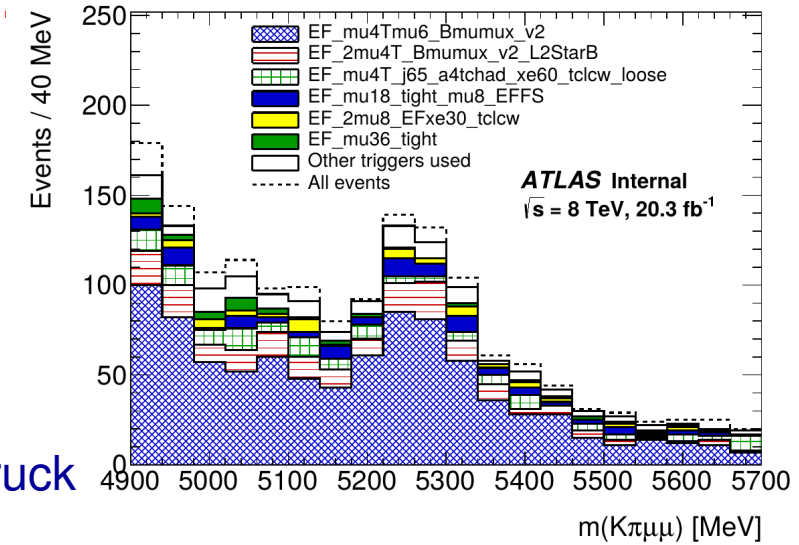

$B^0 \to K^* \mu^+ \mu^-$ Candidates Selection

- Reconstruction of the decay $B^0 \to K^*(K\pi)\mu^+\mu^-$ using Inner Detector tracks
  - Requesting all four tracks originate in same vertex
  - Using tracks parameters at the vertex
- Cut-based optimization on 7 TeV data & MC:
  - Tracks $|\eta| < 2.5$
  - $p_T(\mu) > 3.5$ GeV
  - $p_T(\pi,K) > 0.5$ GeV
  - $p_T(K^*) > 3$ GeV
  - 846 MeV < m(K*) < 946 MeV (B-W width(Γ) of K* = 50 MeV)
  - 5150 MeV < $m(K\pi\mu\mu)$ < 5700 MeV
  - B-hadron lifetime significance $\tau/\sigma_\tau > 12.75$
  - B-momentum pointing angle from B-vertex to PV: $\cos(\theta) > 0.999$
  - Secondary 4-track vertex fit quality χ^2/NDF < 2
  - Radiative tail cut: $|(m(B)-m_{PDG}(B)) - (m(\mu\mu)-m_{PDG}(J/\psi)| < 130$ MeV
  - Resolution of multiple candidates in an event → **next slide**

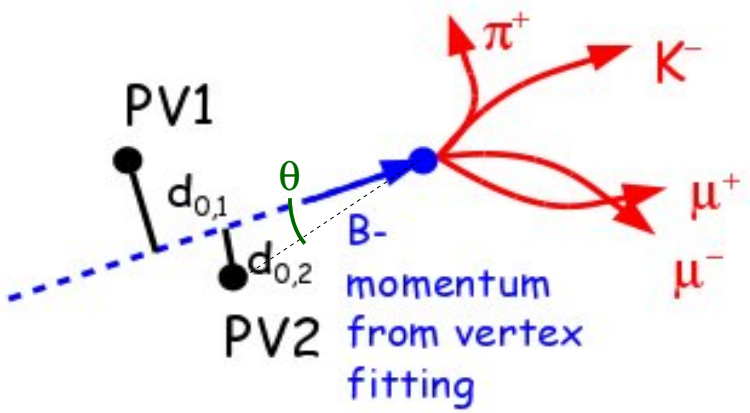

$B^0 \to K^* \mu^+ \mu^-$ Candidates Selection: Ambiguities

- 15% of events have more than single $B^0 \to K^*(K\pi)\mu^+\mu^-$ candidates

- 4% out of the 15% corresponds to B-mesons reconstructed from different tracks
  - Select candidate with better 4-tracks vertex quality

- 96% out of the 15% corresponds to B^0 and $\overline{B}^0$ reconstructed from the same 4 tracks
  - No K/π identification at ATLAS => both Kπ and πK mass hypo on the two hadronic tracks pass the selection criteria
  - Select candidate with best K* mass significance: $|m(K^*)-m_{PDG}(K^*)| / \sigma_{m(K^*)}$
  - Statistically tends to provide right answer (checked at MC), but mis-tagging (wrong identification of B^0 or $\overline{B}^0$) leads to dilution of S_4, S_5 and S_9
    - Dilution factor $D = (1 - \omega - \overline{\omega})$
    - $\omega \sim \overline{\omega} \sim 11\%$ from signal MC
    - Parameters above corrected after fit

Background Studies

- Number of potentially significant backgrounds of similar topology studied:

$b\bar{b} -> \mu\mu X$ (Pythia)
$b\bar{b} -> \mu\mu X$ (EvtGen)
$b\bar{b} -> \mu\mu X$ (Pythia: AA)
$b\bar{b} -> \mu\mu X$ (Pythia: AB)
$b\bar{b} -> \mu\mu X$ (Pythia: BA)
$b\bar{b} -> \mu\mu X$ (Pythia: BB)
$c\bar{c} -> \mu\mu X$
$B_s \to J/\psi\phi$
$\Lambda_b \to \Lambda J/\psi$
$\overline{\Lambda}_b \to \overline{\Lambda} J/\psi$
$B_d \to J/\psi K^0_S$
$B_d \to \psi(2S) K^0_S$
$\Lambda_b \to \Lambda\psi(2S)$
$\overline{\Lambda}_b \to \overline{\Lambda}\psi(2S)$
$B^+ \to J/\psi K^+$ (Pythia)
$B^+ \to J/\psi \pi^+$ (Pythia)
$B^- \to J/\psi K^-$ (Pythia)
$B^\pm \to K^{*+}\mu\mu$ (EvtGen)
$B_s \to \phi\mu\mu$ (EvtGen)
$B_d \to K^*\mu\mu$ (EvtGen:PHSP)
$B_d \to K^*\mu\mu$ (EvtGen:SM)
$\overline{B}_d \to K^*\mu\mu$ (EvtGen:SM)
$B_d \to J/\psi K^*$ (EvtGen)
$B_d \to \psi(2S) K^*$ (EvtGen)
$B^\pm \to K^+\mu\mu$ (EvtGen)
$B^\pm \to K^+\pi^-\mu\mu$ (EvtGen; S-wave)
$B_s \to J/\psi K^*$
$B^0_d \to \phi K^*$
$\Lambda_b \to \Lambda\mu\mu$
$\Lambda_b \to Kp\mu\mu$ (non-resonant)

ATLAS
Internal

The only backgrounds with non-negligible contributions:

Peaking background	q^2 range					
	[0.04, 0.98]	[1.10, 2.00]	[2.00, 3.00]	[3.00, 4.00]	[4.00, 5.00]	[5.00, 6.00]
$B^+ \to K^{*+}\mu^+\mu^-$	0.17	0.12	0.03	0.25	0.12	0.22
$B^+ \to K^+\mu^+\mu^-$	0.89	0.81	1.00	1.30	1.50	1.90
$B^0_s \to \phi\mu^+\mu^-$	0.40	0.19	0.22	0.23	0.25	0.28
$\Lambda_b \to \Lambda(1520)\,\mu^+\mu^-$	1.83	1.88	0.61	0.66	0.09	0.08
$\Lambda_b \to pK^-\,\mu^+\mu^-$	0.99	0.87	0.46	0.48	0.10	0.11
Total	4.28	3.87	2.32	2.92	2.06	2.59

Two unexpected structures seen in the decay angles distributions after unblinding

- At $\cos(\theta_K) \sim 1.0$: source identified as $B^+ \to K\mu\mu$, $\pi\mu\mu$
- At $\cos(\theta_L) \sim 0.7$: source identified as $B \to DX$ decays, left B-mass side

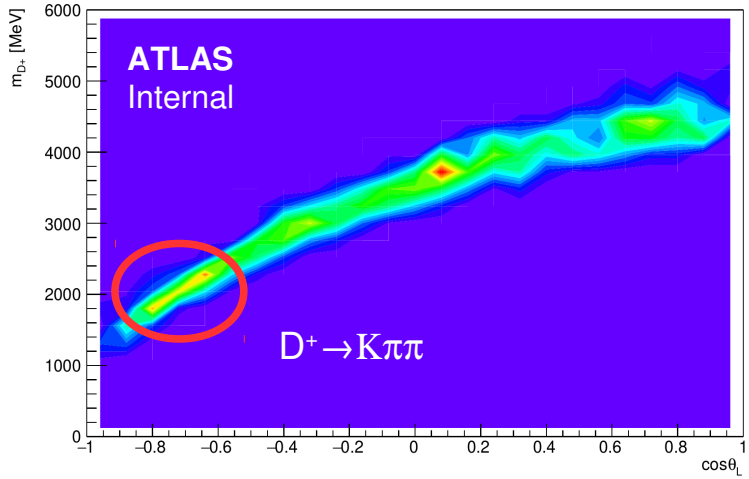

Fit

- Extended unbinned maximum likelihood fit of B-mass and helicity angles

$$\mathcal{L} = \frac{e^{-N}}{n!} \prod_{i=1}^{n} \sum_{j} n_j P_{ij}(m_{K\pi\mu\mu}, \cos\theta_K, \cos\theta_L, \phi; \widehat{p}, \widehat{\theta})$$

- Sequential: $m_{K\pi\mu\mu}$ pre-fit first, angular fit follows with fixed $P(m_{K\pi\mu\mu})$ parameters

- $P(m_{K\pi\mu\mu})$ gaussian;
  m_{B0} and resolution (scale factor) extracted from control channel $B^0 \to K^*(K\pi)J/\psi(\mu^+\mu^-)$

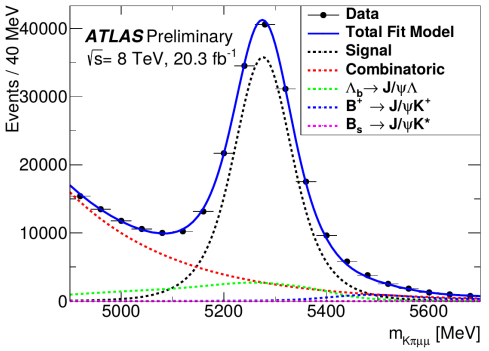

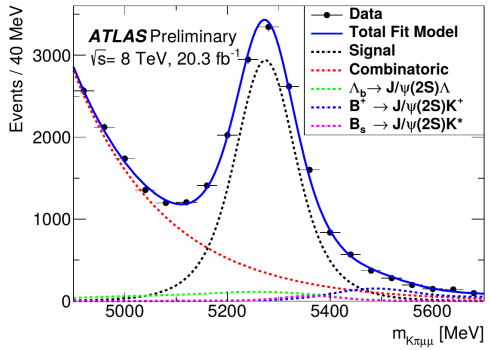

- Angular acceptance functions (polynomials) extracted from flat-angles signal MC and factorized:

$$P_{ij} = \varepsilon(\cos\theta_K)\varepsilon(\cos\theta_L)\varepsilon(\phi)g(\cos\theta_K, \cos\theta_L, \phi)$$

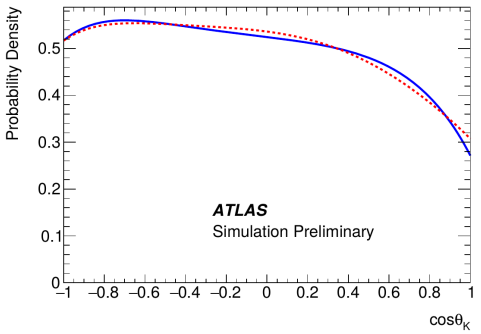

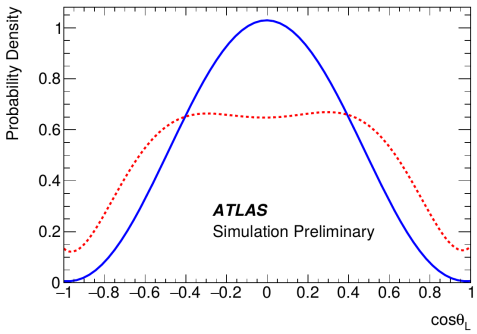

- Background $m_{K\pi\mu\mu}$ exponential
- Background angles 2nd order polynomial
- Peaking backgrounds (B^+, B_s, Λ_b) not included in default fit, but treated as systematics

Fit Result Example

q^2 [GeV^2]	n_{signal}	$n_{\text{background}}$
$[0.04, 2.0]$	128 ± 22	122 ± 22
$[2.0, 4.0]$	106 ± 23	113 ± 23
$[4.0, 6.0]$	114 ± 24	204 ± 26
$[0.04, 4.0]$	236 ± 31	233 ± 32
$[1.1, 6.0]$	275 ± 35	363 ± 36
$[0.04, 6.0]$	342 ± 39	445 ± 40

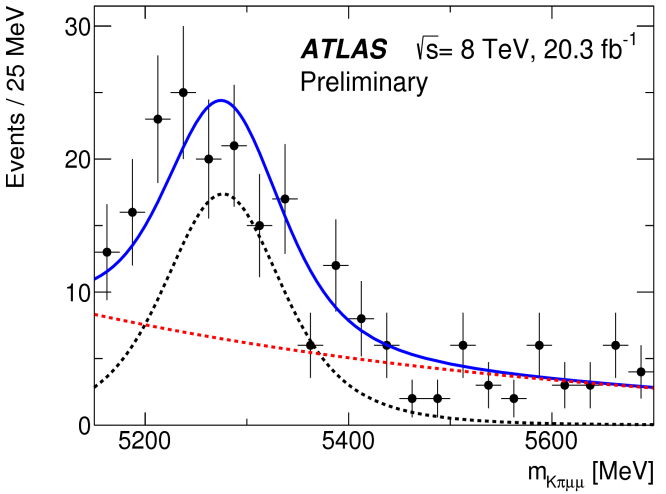

$2\ \text{GeV}^2 < q^2 = [m(\mu^+\mu^-)]^2 < 4\ \text{GeV}^2$

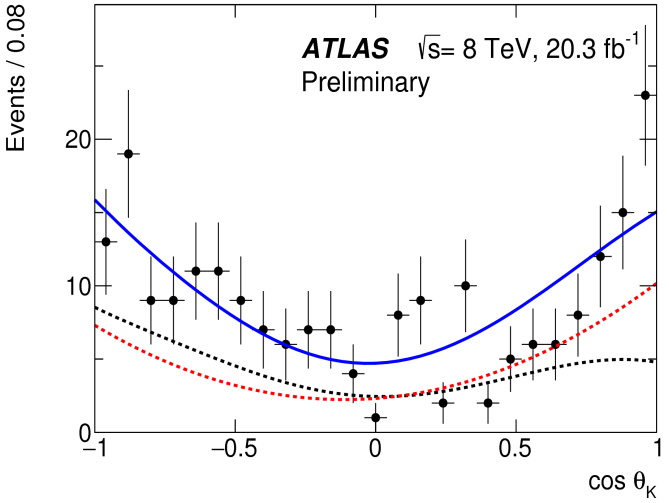

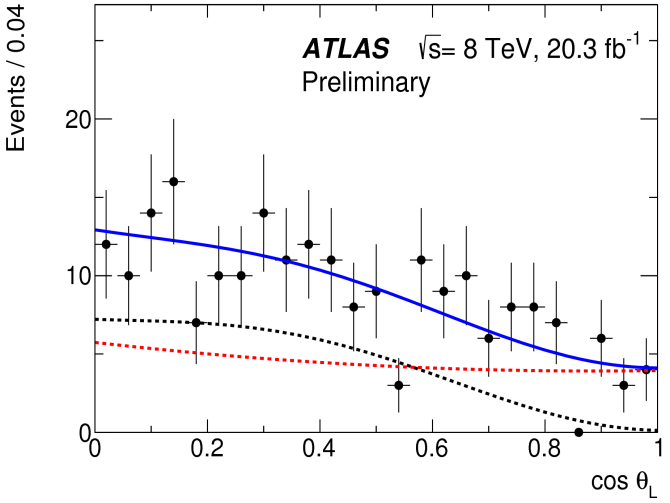

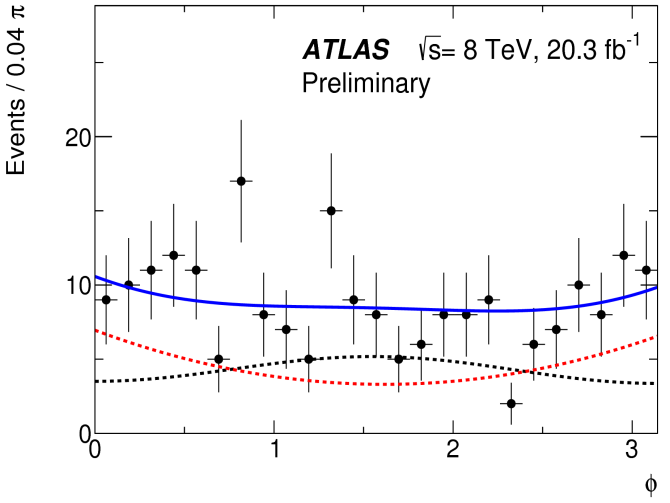

- Low statistics → large stat. uncertainties, but fit feasibility validated with toy-MC
- Extracted S_i parameters → transformed to P_i parameters (including correlations)
- Left sideband cut out to avoid contributions from partially reconstructed B-decays

Systematic Uncertainties

- Overall systematics typically at around ½ of the statistical uncertainties
- Largest systematics from background (mis)understanding

Source	F_L	S_3	S_4	S_5	S_7	S_8
Combinatoric $K\pi$ (fake K^*) background	0.03	0.03	0.05	0.03	0.06	0.13
D and B^+ veto	0.11	0.04	0.05	0.03	0.01	0.05
Background p.d.f. shape	0.04	0.04	0.03	0.02	0.03	0.01
Acceptance function	0.01	0.01	0.07	0.01	0.01	0.01
Partially reconstructed decay background	0.03	0.05	0.02	0.06	0.05	0.05
Alignment and B field calibration	0.02	0.04	0.05	0.03	0.04	0.03
Fit bias	0.01	0.01	0.02	0.02	0.01	0.04
Data/MC differences for p_T	0.02	0.02	0.01	0.01	0.01	0.01
S-wave	0.01	0.01	0.01	0.01	0.01	0.02
Nuisance parameters	0.01	0.01	0.01	0.01	0.01	0.01
Λ_b, B^+ and B_s background	0.01	0.01	0.01	0.01	0.01	0.01
Misreconstructed signal	0.01	0.01	0.01	0.01	0.01	0.01
Dilution	–	–	0.01	0.01	–	–

- $|\cos(\theta_K)| < 0.9$
- veto B^+/D hypothesis
- expo. / 3rd oder poly.
- factorization, signal MC test
- left B-sideband variation
- track p_T smearing
- toy-MC pulls
- data/MC B-p_T weights
- $B \to K\pi\mu\mu$, 5% fed to toy-MC
- control sample fit uncertainties
- toy-MC with peak. backgrounds
- B fit with $\overline{B}$ acceptance
- MC stat., ω vs. $\overline{\omega}$

Fit Results - ATLAS vs. Theory

- Results ~compatible with Standard Model predictions
- Largest deviation of 2.5(2.7) sigma in $P_4'(P_5')$ w.r.t DHWM model, follow LHCb observation

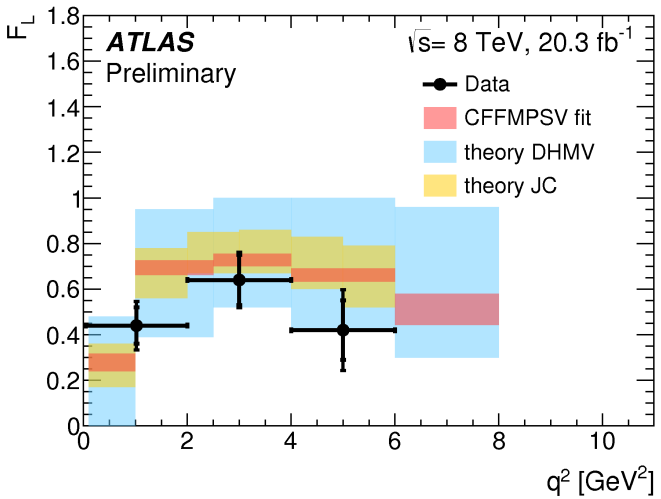

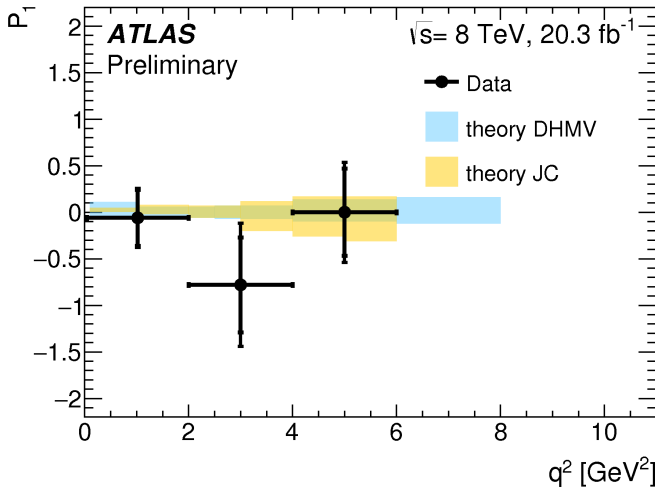

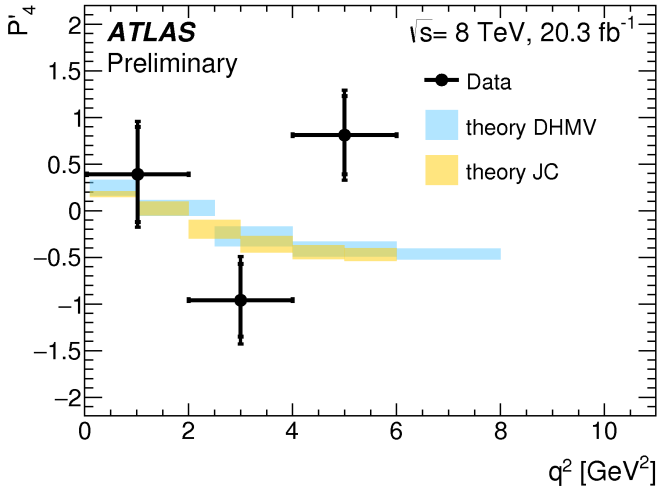

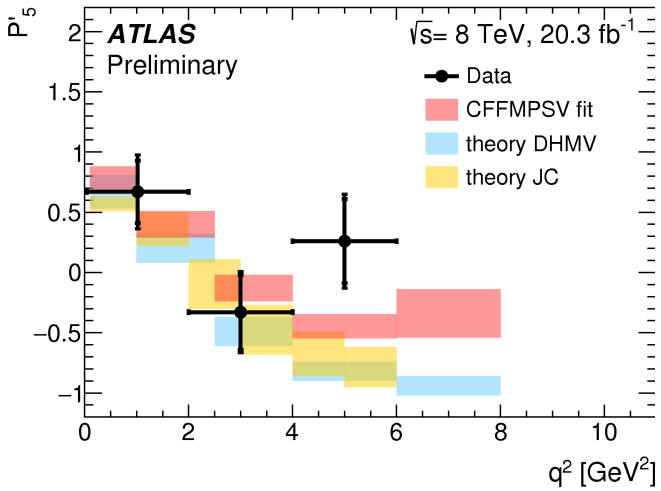

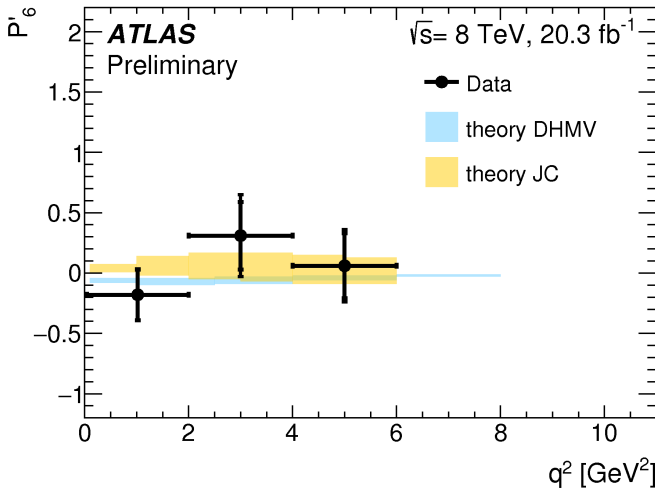

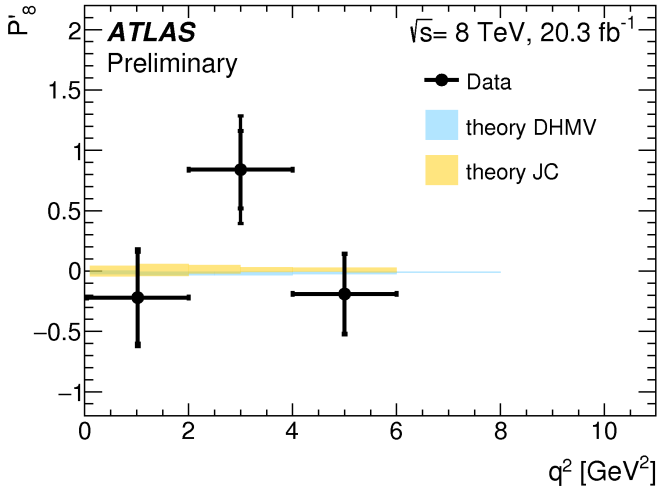

Fit Results - ATLAS vs. Experiments

- Results ~compatible with Standard Model predictions and compatible with other experiments
- Largest deviation of 2.5(2.7) sigma in $P_4'(P_5')$ w.r.t DHWM model, follow LHCb observation

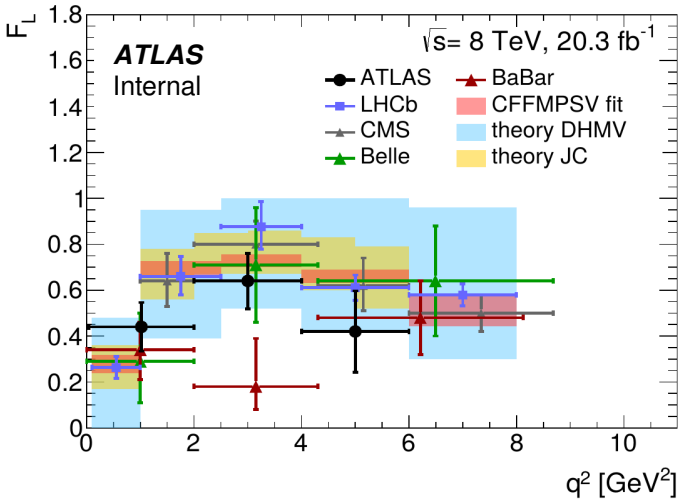

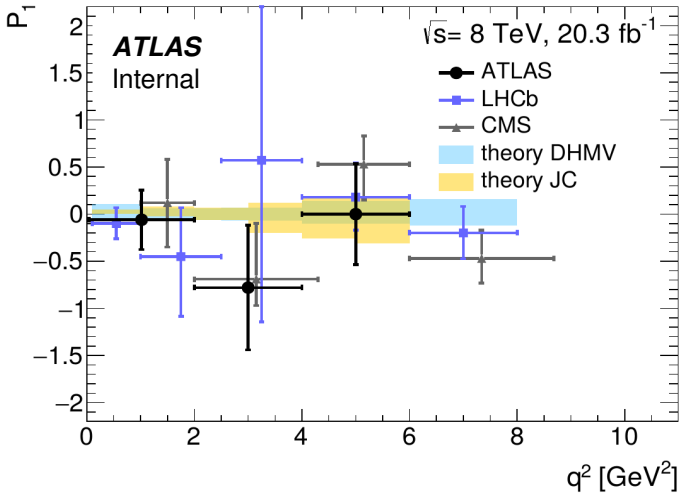

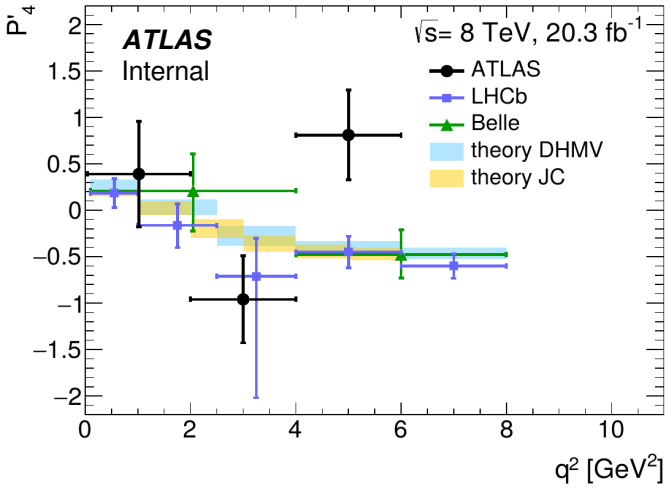

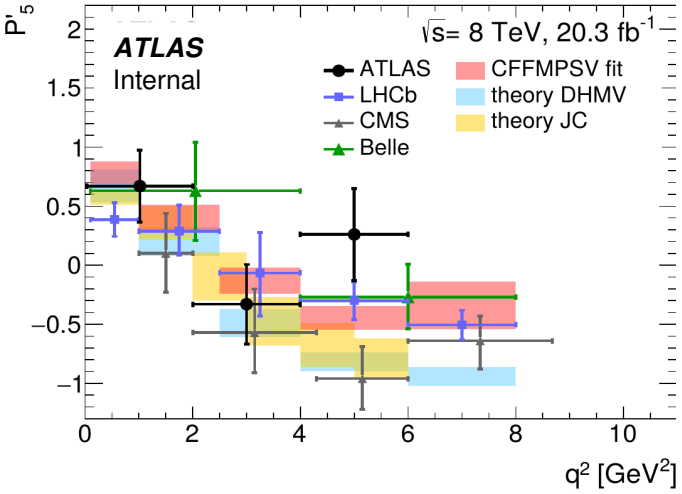

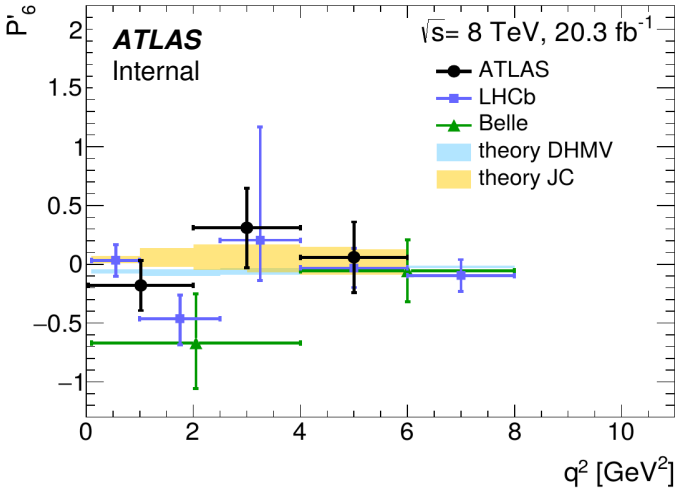

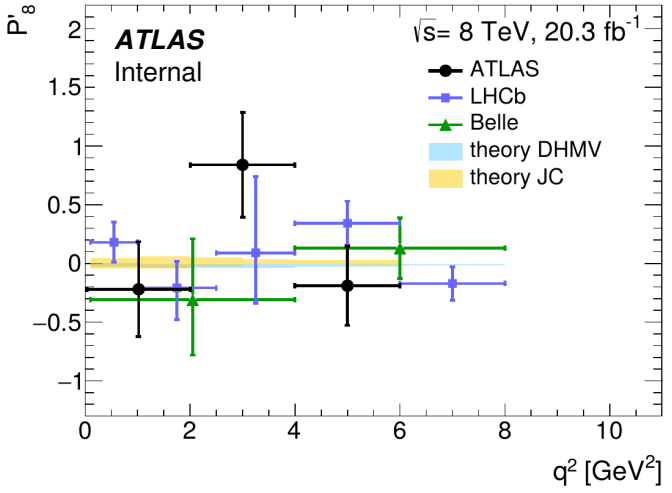

Conclusion + Run-2 And Beyond Prospects

- 2012 ATLAS data analysis of $B^0 \to K^* \mu^+ \mu^-$ gives results compatible with SM and other experiment measurements

ATLAS-CONF-2017-023

- Increase statistics in Run-2 and beyond and:
  - Benefit from better decay time (≥ Run-2) and mass (at HL-LHC) resolution
  - Use topological L1-trigger (≥ Run-2) to cope with high instantaneous luminosity, possibly rely on future trigger features (FTK, track triggers, partial event building, ...)
  - Fit & Systematics improvement: S-wave fit, mistagged $B^0/\overline{B^0}$ in fit, full q^2 spectrum, peaking backgrounds, CP-sensitive parametrization, …
  - Possibly analyze other decay channels to cross-check observed tensions:

JHEP 02 (2016) 104
Angular analysis of
$B^0 \to K^* \mu\mu$

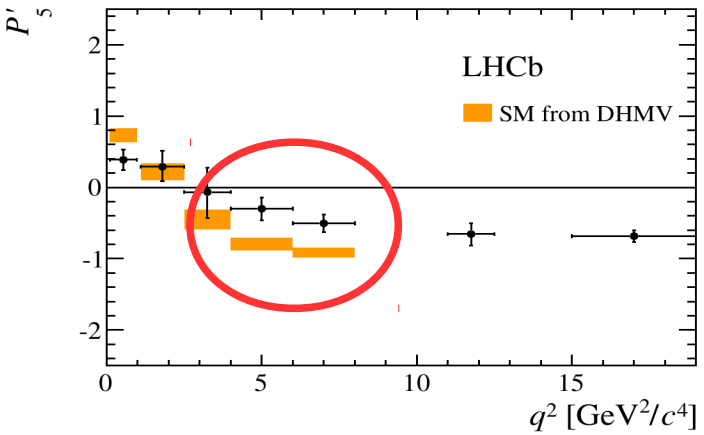

JHEP 09 (2015) 179
Differential decay rate
$B_s \to \phi\mu\mu$

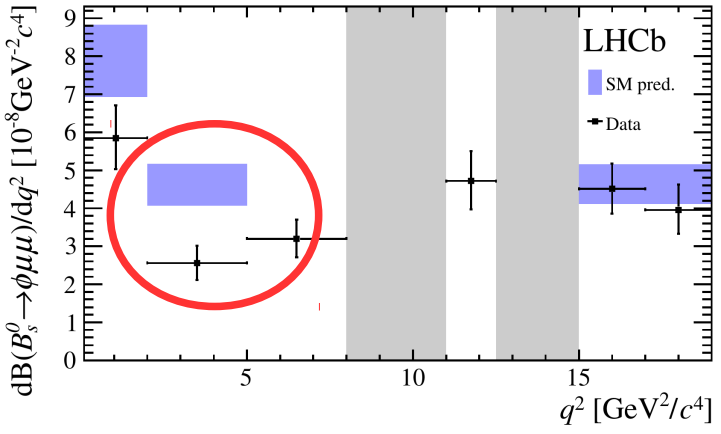

arXiv:1705.05802
Relative production of
$B^0 \to K^* \mu\mu$ / $B^0 \to K^* ee$

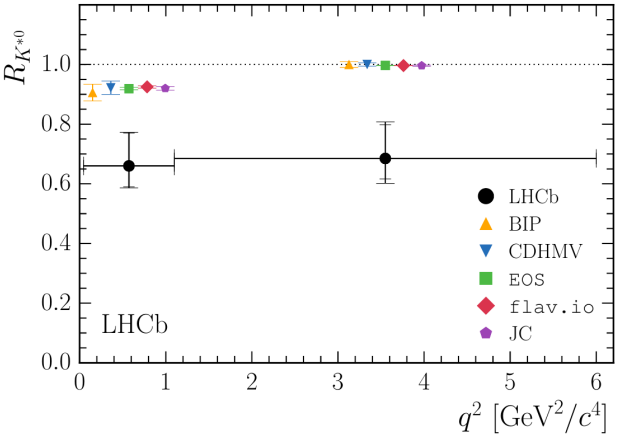

Backup

Paper

ATLAS Paper Draft
BPHY-2013-02
Version 1.06

Comments are due by: tbc May 2017

Supporting internal notes

ATL-COM-PHYS-2014-898: https://cds.cern.ch/record/1745005
ATL-COM-PHYS-2015-1368 (Backgrounds): https://cds.cern.ch/record/2066759

Angular analysis of $B_d^0 \to K^*\mu^+\mu^-$ decays in pp collisions at $\sqrt{s} = 8$ TeV with the ATLAS detector

An angular analysis of the decay $B_d^0 \to K^*\mu^+\mu^-$ is presented using proton-proton collisions at $\sqrt{s} = 8$ TeV from LHC data analysed with the ATLAS detector. The study is based on 20.3 fb^{-1} of integrated luminosity collected during 2012. Measurements of the K^* longitudinal polarisation fraction and a set of angular parameters obtained for this decay are presented. The results are compatible with theoretical predictions.

To be submitted to: JHEP

Analysis Team

[*email:* atlas-bphy-2013-02-editors@cern.ch]

Adrian Bevan, Marcella Bona, Ina Carli, Patrick Jussel, Emmerich Kneringer, Tamsin Nooney, Pavel Reznicek, Semen Turchikhin, Anna Usanova

Editorial Board

[*email:* atlas-bphy-2013-02-editorial-board@cern.ch]

David Rousseau (chair)
Stefano Rosati
Thomas LeCompte
Philippe Grenier

Data Samples

- Full 2012 (8 TeV) dataset of 20.3 fb^{-1} using GRL:
  data12_8TeV.periodAllYear_DetStatus-v61-pro14-02_DQDefects-00-01-00_PHYS_StandardGRL_All_Good.xml
- Events from “Muon” and “B-Physics” streams
  - B-Physics stream allowed more bandwidth for B-physics events, but with delayed processing (reconstruction)
- 79 selected events per fb in $q^2 < 6$ GeV^2 and 4.90 GeV < $m(K\pi\mu\mu)$ < 5.70 GeV
  17 signal events pdf fb in $q^2 < 6$ GeV^2 and 5.15 GeV < $m(K\pi\mu\mu)$ < 5.70 GeV

ATLAS Internal

Period	Streams	L_{int}/fb^{-1}	Yield	Yield / fb^{-1}
A	Muon	0.794	13390	16864
B	Muon + B	5.095	88335	17338
C	Muon + B	1.406	28550	20306
D	Muon + B	3.288	67671	20581
E	Muon + B	2.526	51251	20289
G	Muon + B	1.275	26009	20399
H	Muon + B	1.445	29411	20354
I	Muon + B	1.016	20822	20494
J	Muon + B	2.596	53378	20562
L	Muon + B	0.840	17460	20786
All	Muon + B	20.281	396277	19539
$q^2 < 6$	Muon + B	20.281	1603	79

Triggers

- Combination (OR) of triggers requiring >1, >2 or >3 muons
  overall triggering (mind the overlaps) 21.1% 88.8% 4.5% of the selected events
- Luminosity/prescale weights applied on MC to match data
- Main trigger: di-muon at L1, searching for the full $B^0 \to K^*(K\pi)\mu^+\mu^-$ decay at HLT

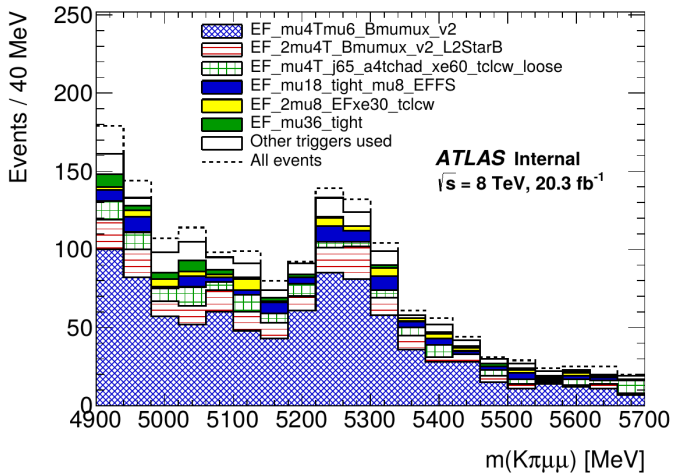

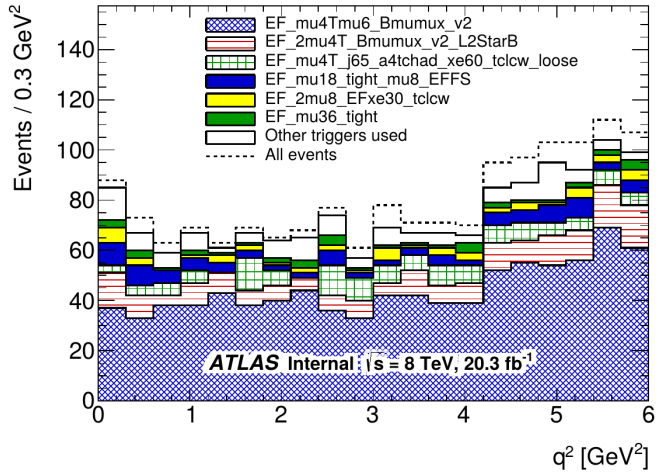

Iteration	Trigger chain	# events selected	# events left
	Total		1603
1	EF_mu4Tmu6_Bmumux_v2	889	714
2	EF_2mu4T_Bmumux_v2_L2StarB	182	532
3	EF_mu4T_j65_a4tchad_xe60_tclcw_loose	120	412
4	EF_mu18_tight_mu8_EFFS	90	322
5	EF_2mu8_EFxe30_tclcw	50	272
6	EF_mu36_tight	40	232
7	EF_2mu4T_Bmumux_v2	23	209
8	EF_3mu4T	23	186
9	EF_2mu4T_Bmumux_BarrelOnly_v2_L2StarB	22	164
10	EF_mu24_j65_a4tchad_EFxe40_tclcw	20	144
11	EF_mu24_tight_mu6_EFFS	9	135
12	EF_mu24_tight	7	128
13	EF_2mu6_Bmumux_v2_L2StarB	7	121
14	EF_mu40_MSonly_barrel_tight	7	114
15	EF_2mu6_DiMu_noVtx_noOS	5	109
	EF_2mu6_Bmumux_v2	1	108
	EF_mu4Tmu6_Bmumux_v2_L2StarB	1	107
	EF_2mu4T_Bmumux_Barrel_v2_L2StarB	1	106
	EF_mu4Tmu6_Bmumux_Barrel_v2_L2StarB	0	106

ATLAS Internal

Backgrounds After Unblinding

- Two unexpected structures seen in the decay angles distributions after unblinding
  - At $\cos(\theta_K) \sim 1.0$: most probable source identified as $B^+ \to K\mu\mu$, $\pi\mu\mu$
  - At $\cos(\theta_L) \sim 0.7$: most probable source identified as $B \to DX$ decays, left B-mass side

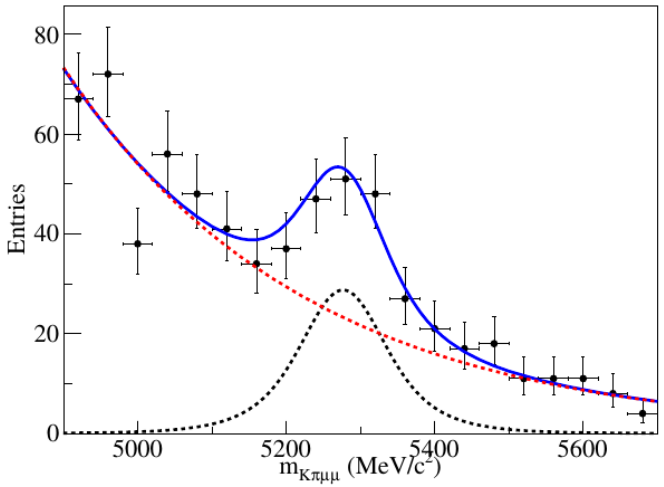

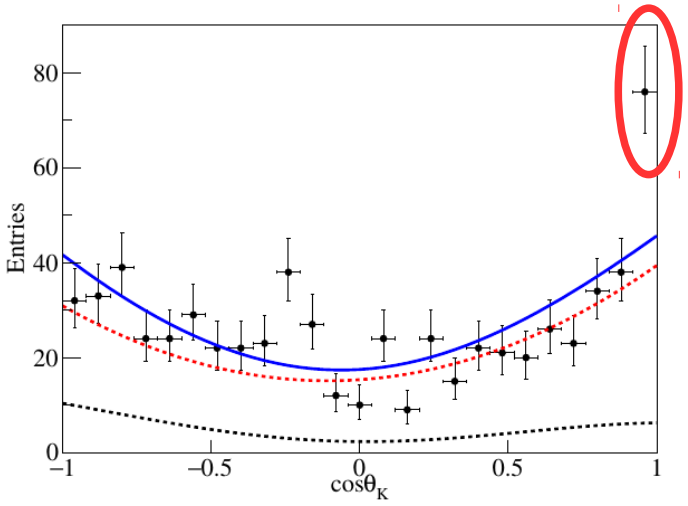

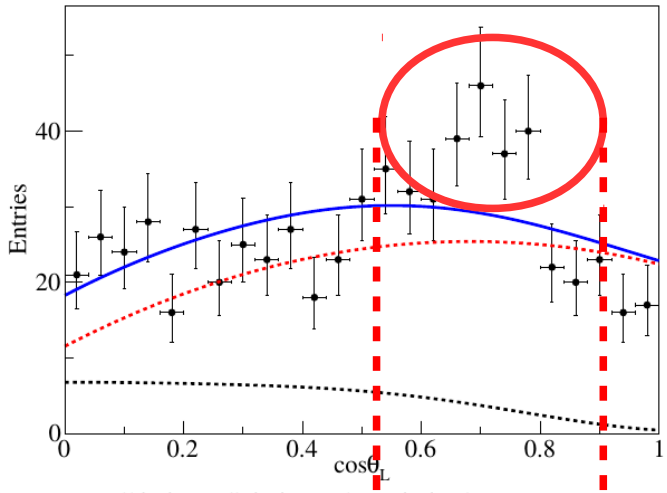

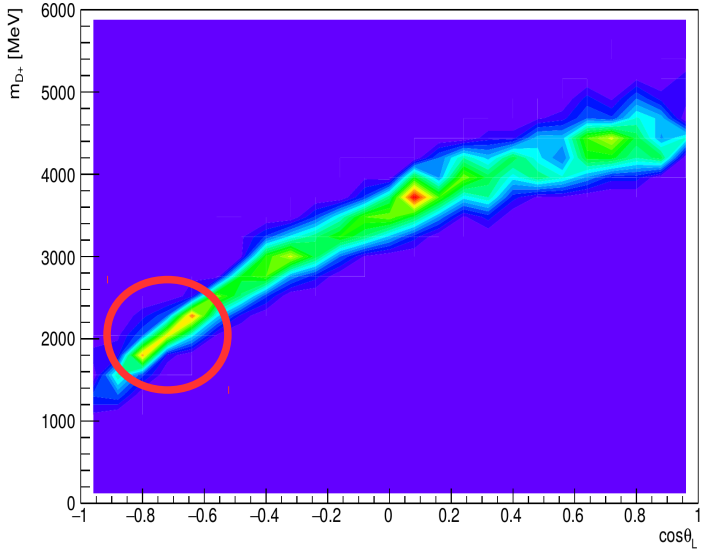

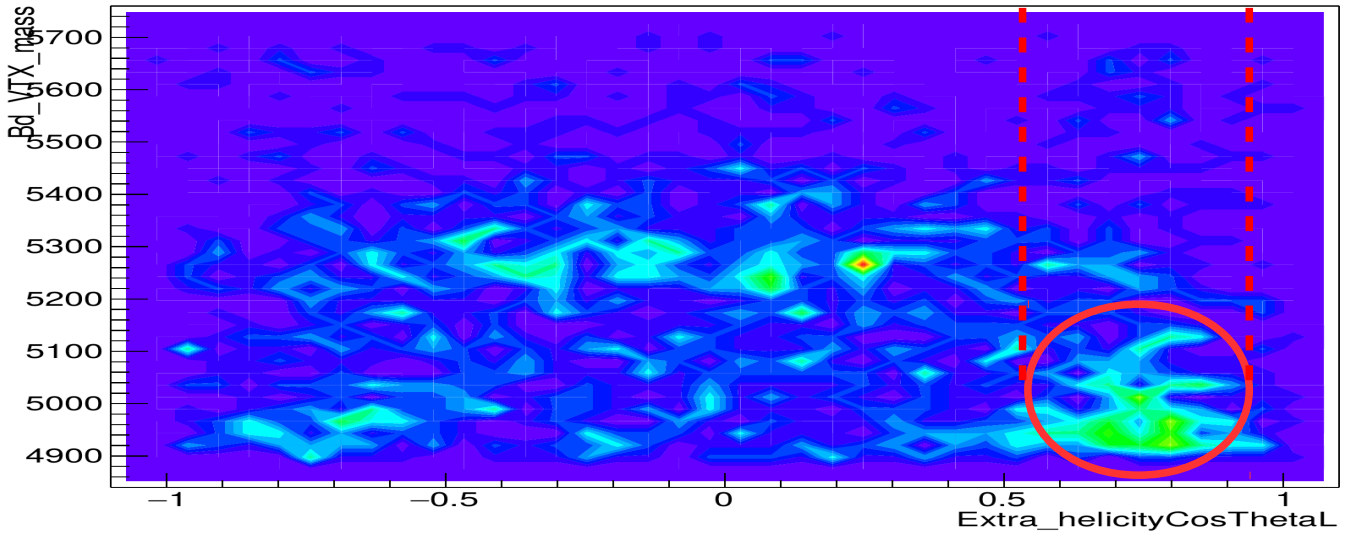

Fit Results – ATLAS vs. Theory (S_i)

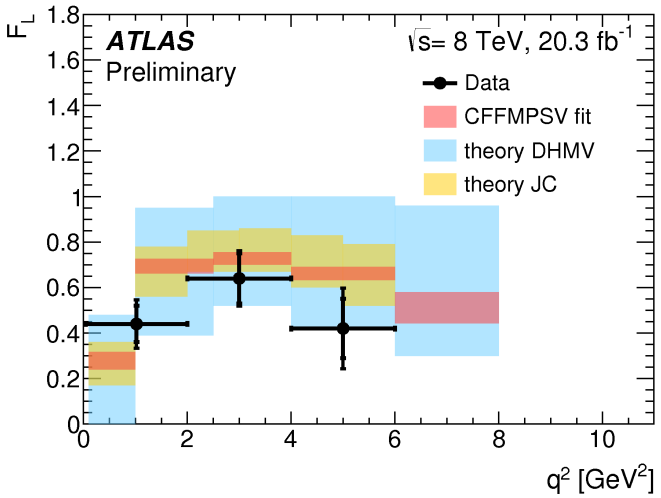

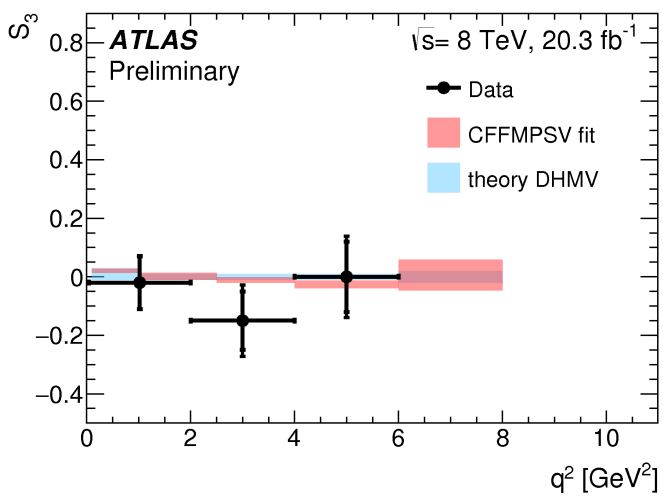

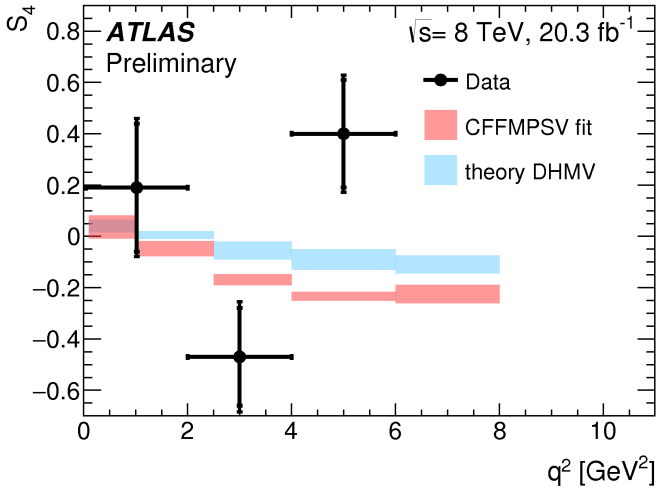

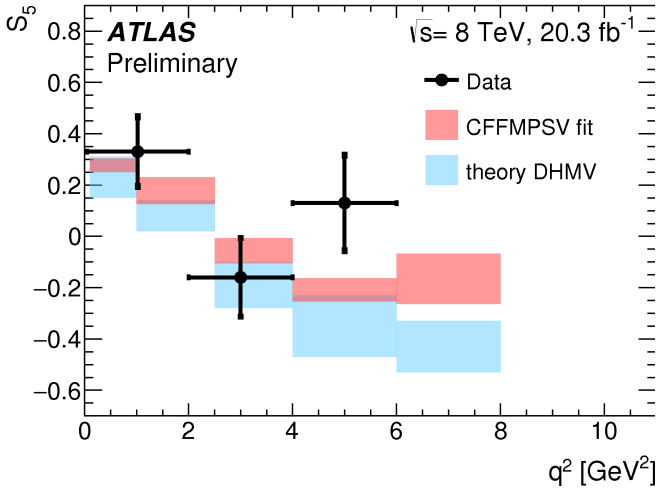

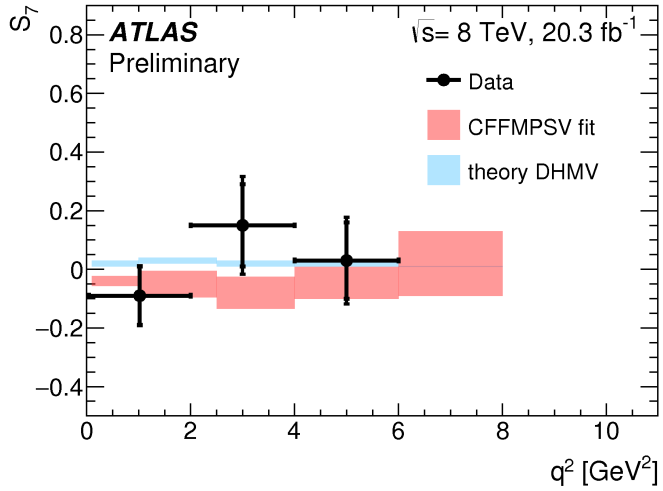

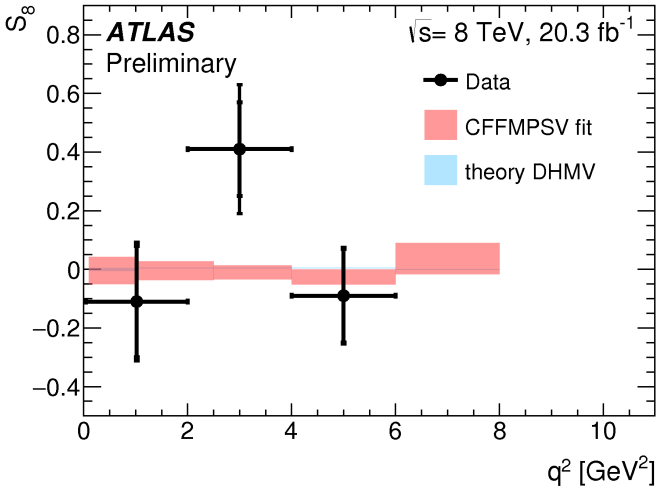

Fit Results – ATLAS vs. Experiments (S_i)

ATLAS
Internal

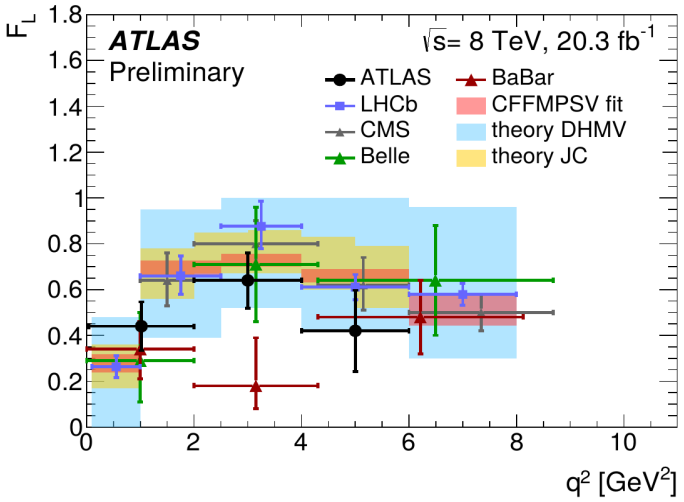

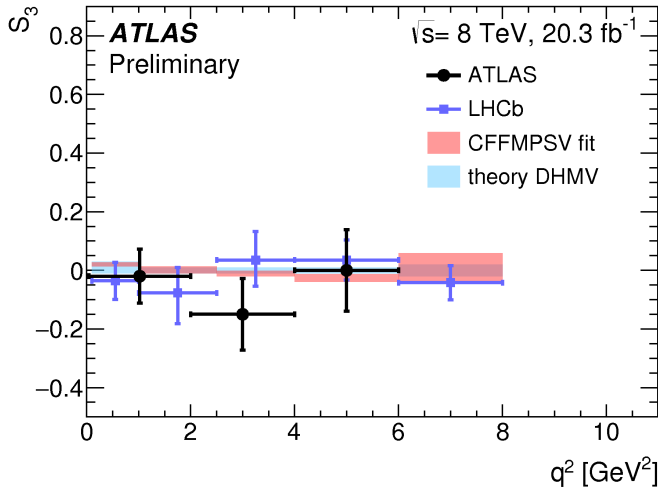

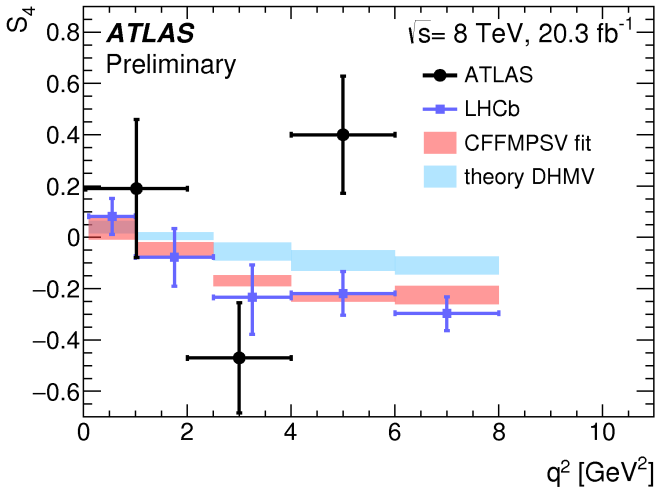

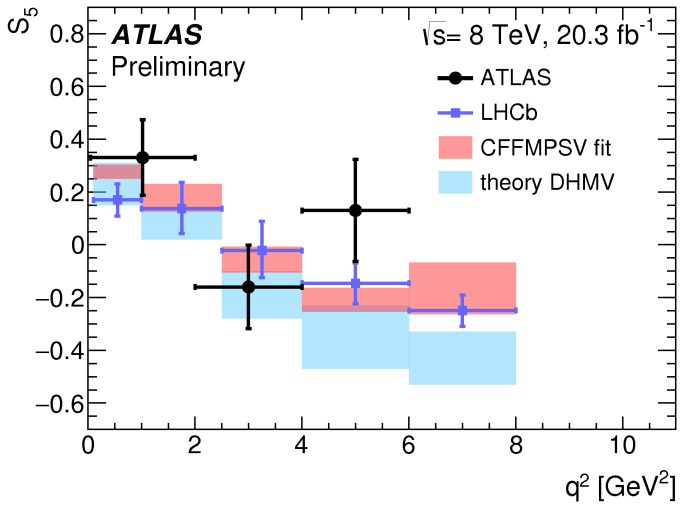

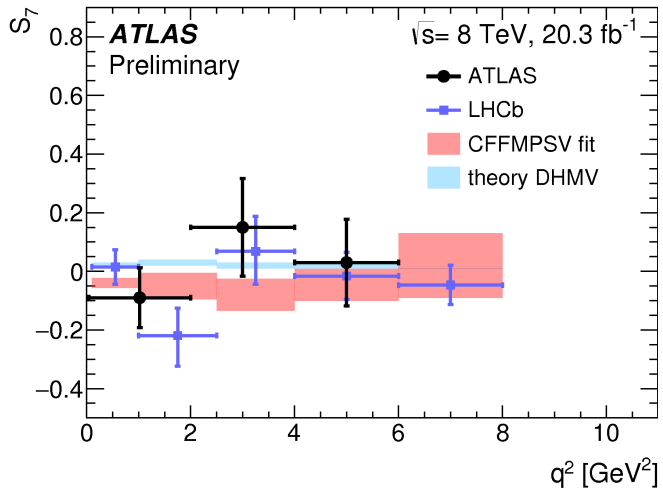

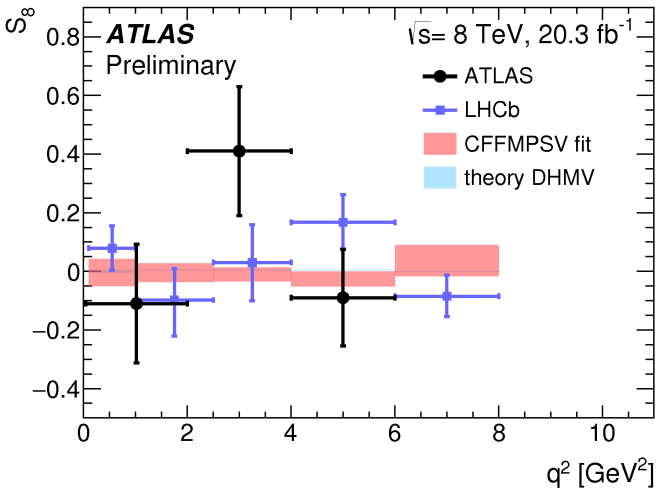

Tabulated Results

q^2 [GeV^2]	n_{signal}	$n_{\text{background}}$
$[0.04, 2.0]$	128 ± 22	122 ± 22
$[2.0, 4.0]$	106 ± 23	113 ± 23
$[4.0, 6.0]$	114 ± 24	204 ± 26
$[0.04, 4.0]$	236 ± 31	233 ± 32
$[1.1, 6.0]$	275 ± 35	363 ± 36
$[0.04, 6.0]$	342 ± 39	445 ± 40

q^2 [GeV^2]	F_L	S_3	S_4	S_5	S_7	S_8
$[0.04, 2.0]$	$0.44 \pm 0.08 \pm 0.07$	$-0.02 \pm 0.09 \pm 0.02$	$0.19 \pm 0.25 \pm 0.10$	$0.33 \pm 0.13 \pm 0.06$	$-0.09 \pm 0.10 \pm 0.02$	$-0.11 \pm 0.19 \pm 0.07$
$[2.0, 4.0]$	$0.64 \pm 0.11 \pm 0.05$	$-0.15 \pm 0.10 \pm 0.07$	$-0.47 \pm 0.19 \pm 0.10$	$-0.16 \pm 0.15 \pm 0.05$	$0.15 \pm 0.14 \pm 0.09$	$0.41 \pm 0.16 \pm 0.15$
$[4.0, 6.0]$	$0.42 \pm 0.13 \pm 0.12$	$0.00 \pm 0.12 \pm 0.07$	$0.40 \pm 0.21 \pm 0.09$	$0.13 \pm 0.18 \pm 0.07$	$0.03 \pm 0.13 \pm 0.07$	$-0.09 \pm 0.16 \pm 0.04$
$[0.04, 4.0]$	$0.52 \pm 0.07 \pm 0.06$	$-0.05 \pm 0.06 \pm 0.04$	$-0.19 \pm 0.16 \pm 0.09$	$0.16 \pm 0.10 \pm 0.04$	$0.01 \pm 0.08 \pm 0.05$	$0.15 \pm 0.13 \pm 0.10$
$[1.1, 6.0]$	$0.56 \pm 0.07 \pm 0.06$	$-0.04 \pm 0.07 \pm 0.03$	$0.03 \pm 0.14 \pm 0.07$	$0.00 \pm 0.10 \pm 0.03$	$0.02 \pm 0.08 \pm 0.06$	$0.09 \pm 0.11 \pm 0.08$
$[0.04, 6.0]$	$0.50 \pm 0.06 \pm 0.04$	$-0.04 \pm 0.06 \pm 0.03$	$0.03 \pm 0.13 \pm 0.07$	$0.14 \pm 0.09 \pm 0.03$	$0.02 \pm 0.07 \pm 0.05$	$0.05 \pm 0.10 \pm 0.07$

q^2 [GeV^2]	P_1	P_4'	P_5'	P_6'	P_8'
$[0.04, 2.0]$	$-0.06 \pm 0.30 \pm 0.10$	$0.39 \pm 0.51 \pm 0.25$	$0.67 \pm 0.26 \pm 0.16$	$-0.18 \pm 0.21 \pm 0.04$	$-0.22 \pm 0.38 \pm 0.14$
$[2.0, 4.0]$	$-0.78 \pm 0.51 \pm 0.42$	$-0.96 \pm 0.39 \pm 0.26$	$-0.33 \pm 0.31 \pm 0.13$	$0.31 \pm 0.28 \pm 0.19$	$0.84 \pm 0.32 \pm 0.31$
$[4.0, 6.0]$	$0.00 \pm 0.47 \pm 0.26$	$0.81 \pm 0.42 \pm 0.24$	$0.26 \pm 0.35 \pm 0.17$	$0.06 \pm 0.27 \pm 0.13$	$-0.19 \pm 0.33 \pm 0.07$
$[0.04, 4.0]$	$-0.22 \pm 0.26 \pm 0.16$	$-0.38 \pm 0.31 \pm 0.22$	$0.32 \pm 0.21 \pm 0.10$	$0.01 \pm 0.17 \pm 0.10$	$0.30 \pm 0.26 \pm 0.19$
$[1.1, 6.0]$	$-0.17 \pm 0.31 \pm 0.14$	$0.07 \pm 0.28 \pm 0.18$	$0.01 \pm 0.21 \pm 0.07$	$0.03 \pm 0.17 \pm 0.11$	$0.18 \pm 0.22 \pm 0.16$
$[0.04, 6.0]$	$-0.15 \pm 0.23 \pm 0.10$	$0.07 \pm 0.26 \pm 0.18$	$0.27 \pm 0.19 \pm 0.07$	$0.03 \pm 0.15 \pm 0.10$	$0.11 \pm 0.21 \pm 0.14$

P_i' Parameter Correlations

ATLAS
Internal

Table 5: Correlation matrix for the $P^{(\prime)}$ parameters obtained for $q^2 \in [0.04, 2.0]$.

	P_1	P_4'	P_5'	P_6'	P_8'
P_1	1.00	0.04	0.31	0.62	0.39
P_4'		1.00	0.57	−0.08	0.09
P_5'			1.00	0.10	0.30
P_6'				1.00	0.59
P_8'					1.00

Table 7: Correlation matrix for the $P^{(\prime)}$ parameters obtained for $q^2 \in [2.0, 4.0]$.

	P_1	P_4'	P_5'	P_6'	P_8'
P_1	1.00	−0.12	−0.24	0.05	0.01
P_4'		1.00	0.62	0.08	−0.11
P_5'			1.00	−0.22	−0.30
P_6'				1.00	0.63
P_8'					1.00

Table 9: Correlation matrix for the $P^{(\prime)}$ parameters obtained for $q^2 \in [4.0, 6.0]$.

	P_1	P_4'	P_5'	P_6'	P_8'
P_1	1.00	0.11	0.23	0.41	0.14
P_4'		1.00	0.50	0.06	0.02
P_5'			1.00	0.31	0.29
P_6'				1.00	0.61
P_8'					1.00

Table 11: Correlation matrix for the $P^{(\prime)}$ parameters obtained for $q^2 \in [0.04, 4.0]$.

	P_1	P_4'	P_5'	P_6'	P_8'
P_1	1.00	−0.07	0.00	0.21	0.10
P_4'		1.00	0.78	0.08	0.02
P_5'			1.00	0.03	−0.03
P_6'				1.00	0.60
P_8'					1.00

Table 13: Correlation matrix for the $P^{(\prime)}$ parameters obtained for $q^2 \in [1.1, 6.0]$.

	P_1	P_4'	P_5'	P_6'	P_8'
P_1	1.00	0.23	0.07	0.08	−0.07
P_4'		1.00	0.61	0.15	0.08
P_5'			1.00	0.31	0.27
P_6'				1.00	0.67
P_8'					1.00

Table 15: Correlation matrix for the $P^{(\prime)}$ parameters obtained for $q^2 \in [0.04, 6.0]$.

	P_1	P_4'	P_5'	P_6'	P_8'
P_1	1.00	−0.02	−0.13	0.17	0.02
P_4'		1.00	0.67	0.00	0.04
P_5'			1.00	−0.05	0.07
P_6'				1.00	0.63
P_8'					1.00

S_i Parameter Correlations

ATLAS
Internal

Table 4: Correlation matrix for the F_L and S parameters obtained for $q^2 \in [0.04, 2.0]$.

	F_L	S_3	S_4	S_5	S_7	S_8
F_L	1.00	0.11	−0.13	0.03	0.16	0.24
S_3		1.00	0.31	0.28	0.73	0.45
S_4			1.00	0.58	0.19	0.22
S_5				1.00	0.14	0.28
S_7					1.00	0.59
S_8						1.00

Table 6: Correlation matrix for the F_L and S parameters obtained for $q^2 \in [2.0, 4.0]$.

	F_L	S_3	S_4	S_5	S_7	S_8
F_L	1.00	0.27	0.35	−0.04	−0.15	−0.37
S_3		1.00	−0.08	−0.44	−0.09	−0.20
S_4			1.00	0.60	−0.02	−0.12
S_5				1.00	−0.11	−0.20
S_7					1.00	0.63
S_8						1.00

Table 8: Correlation matrix for the F_L and S parameters obtained for $q^2 \in [4.0, 6.0]$.

	F_L	S_3	S_4	S_5	S_7	S_8
F_L	1.00	0.33	−0.18	0.04	0.22	0.28
S_3		1.00	0.15	0.23	0.60	0.05
S_4			1.00	0.52	0.03	0.01
S_5				1.00	0.28	0.27
S_7					1.00	0.60
S_8						1.00

Table 10: Correlation matrix for the F_L and S parameters obtained for $q^2 \in [0.04, 4.0]$.

	F_L	S_3	S_4	S_5	S_7	S_8
F_L	1.00	0.08	0.05	0.01	0.18	0.14
S_3		1.00	−0.04	0.03	0.29	−0.16
S_4			1.00	0.79	0.08	0.03
S_5				1.00	0.03	−0.02
S_7					1.00	0.60
S_8						1.00

Table 12: Correlation matrix for the F_L and S parameters obtained for $q^2 \in [1.1, 6.0]$.

	F_L	S_3	S_4	S_5	S_7	S_8
F_L	1.00	0.05	0.00	0.07	0.18	−0.03
S_3		1.00	0.41	0.46	0.32	−0.01
S_4			1.00	0.60	0.09	0.03
S_5				1.00	0.17	0.24
S_7					1.00	0.67
S_8						1.00

Table 14: Correlation matrix for the F_L and S parameters obtained for $q^2 \in [0.04, 6.0]$.

	F_L	S_3	S_4	S_5	S_7	S_8
F_L	1.00	0.03	0.01	−0.10	0.13	0.06
S_3		1.00	−0.02	−0.09	0.32	−0.01
S_4			1.00	0.68	0.00	0.04
S_5				1.00	−0.05	0.03
S_7					1.00	0.65
S_8						1.00

Measurements in Run-2 and Beyond

LHC / HL-LHC Plan

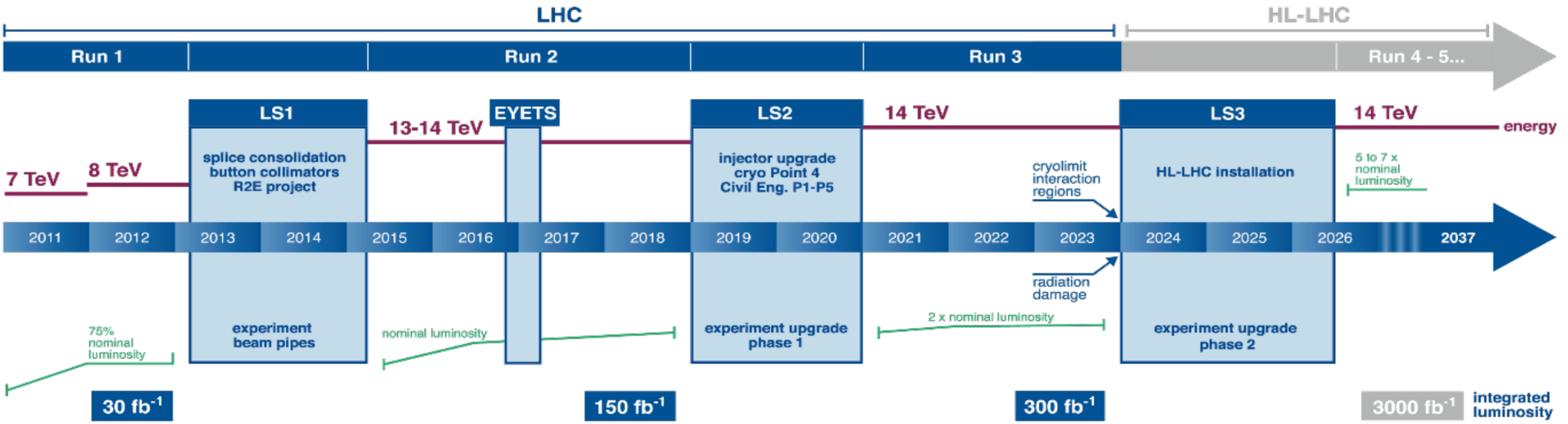

- New pixel layer (IBL, 32-38 mm) + small radius Be beam pipe
- Topological L1 trigger

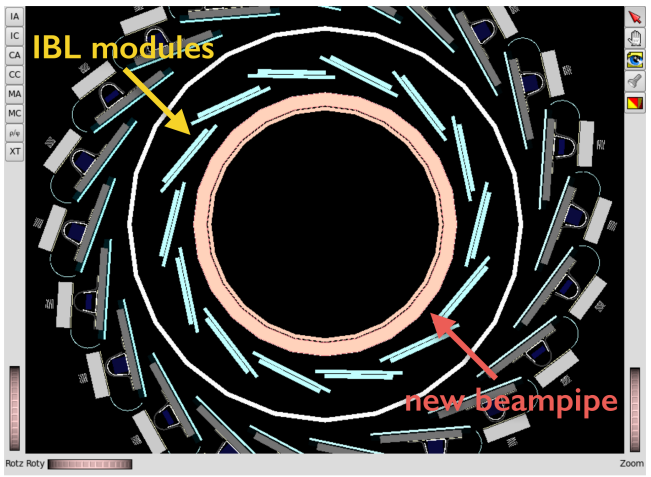

- New small muon wheel
- Fast tracking trigger (FTK) at LVL 1.5; available in Run-2

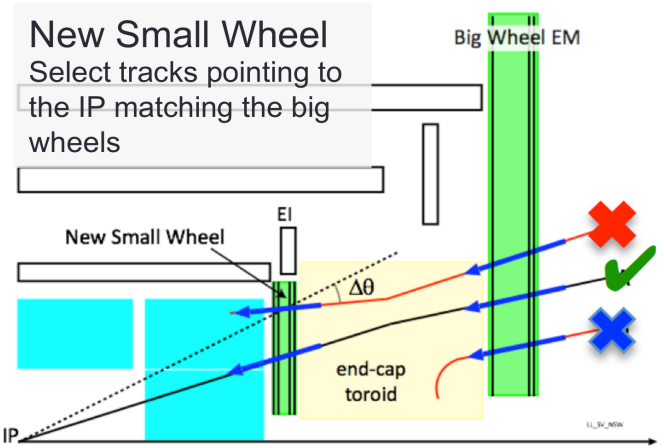

- Completely new Si based tracker (ITK)

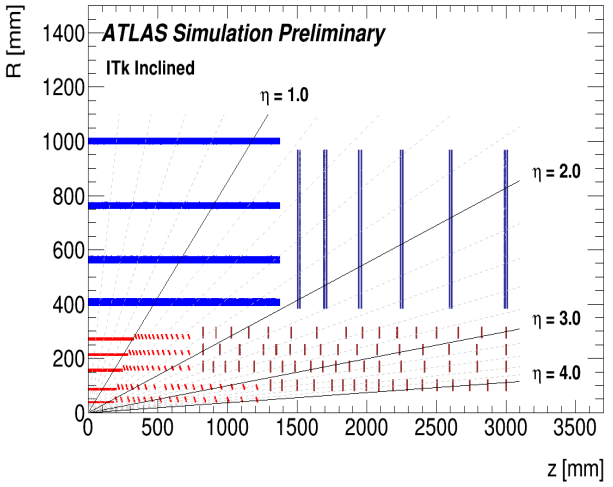

Detector Performance in Run-2 and Beyond

ATL-PHYS-PUB-2016-025

- **Resolution:** invariant mass in decay $B_s \to \mu^+\mu^-$, proper decay time in $B_s \to J/\psi(\mu^+\mu^-)\phi(K^+K^-)$ decay
- Comparison of Run-1, Run-2 (IBL) and HL-LHC (ITk) performances
- **Trigger:** use L1-topo (keep low thresholds at L1) and complicated HLT with full $B_s \to J/\psi(\mu^+\mu^-)\phi(K^+K^-)$ decay topology reconstruction at trigger level

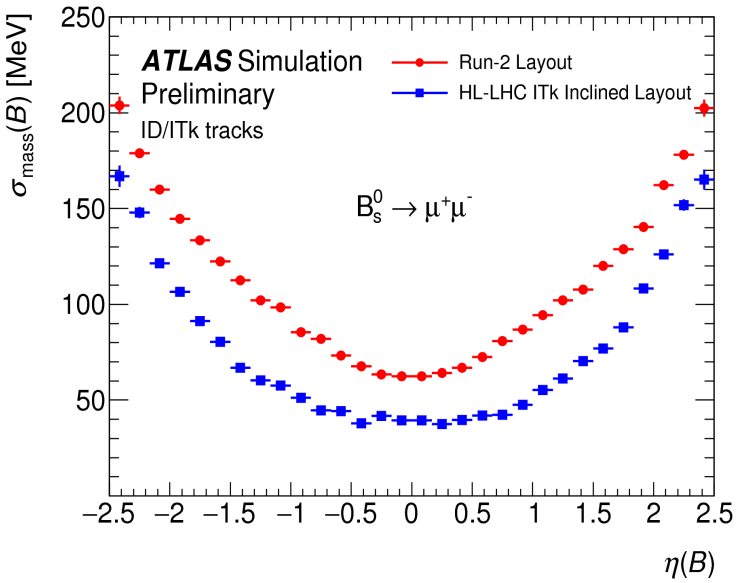

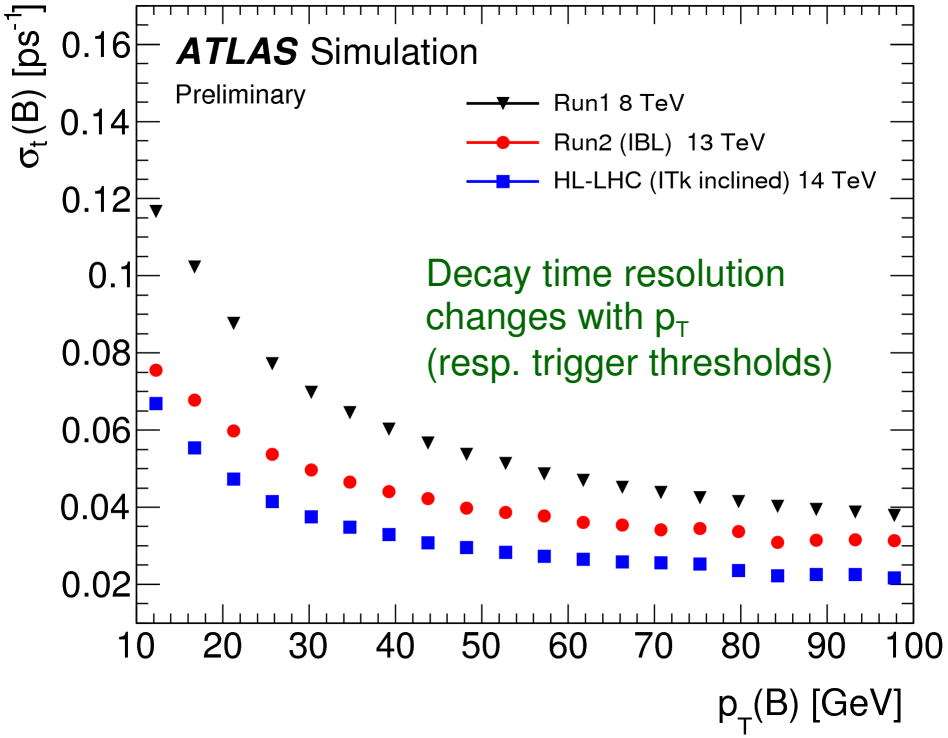

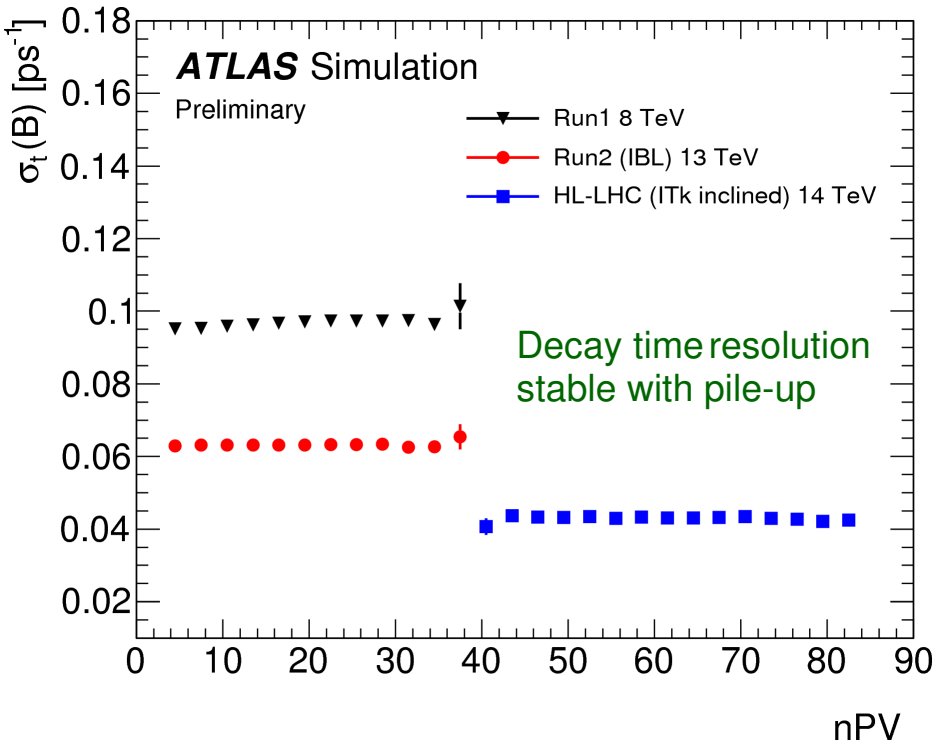

CKM 2016

9th International Workshop on the CKM Unitarity Triangle

28th November – 2nd December 2016

Tata Institute of Fundamental Research, Mumbai

Latest ATLAS Results on ϕ_s

Pavel Řezníček *(Charles University, Prague)*, on behalf of the ATLAS collaboration

The ATLAS Experiment

General purpose detector

Calorimeter System

EM and Hadronic energy
- LAr EM barrel and EC
- LAr Had. EC
- Tile Calorimeter (Fe-Scin.) hadronic barrel

Muon Specrometer

Toroid Magnets
Precision μ tracking:
- MDT (Monitored Drift Tubes)
- CSC (Cathode Strip Chambers)

Trigger:
- RPC (Resistive Plate Chamber)
- TGC (Thin Gas Chamber)

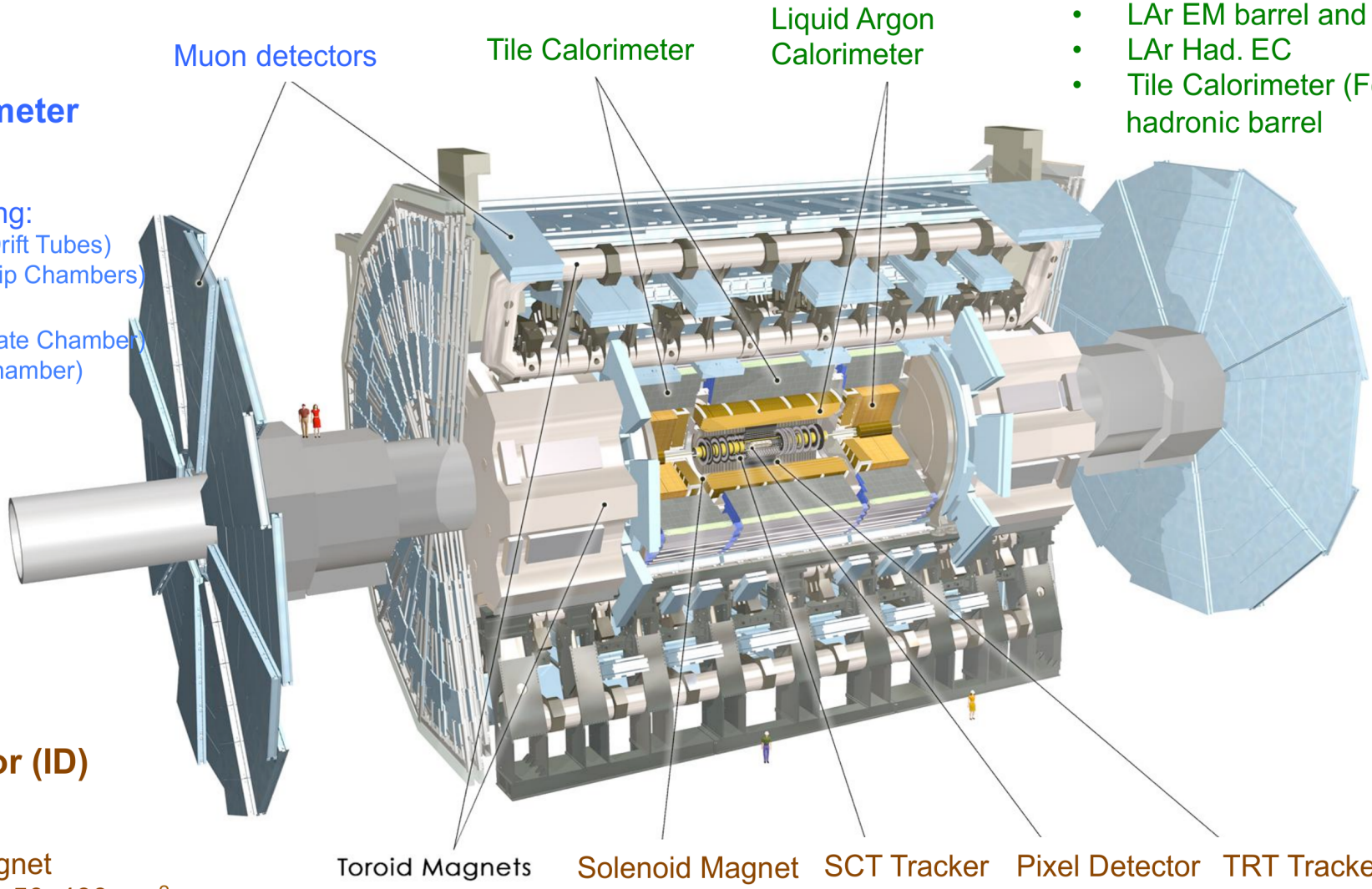

Inner Detector (ID)

Tracking
2T Solenoid Magnet
- Silicon Pixels, 50x400 μm^2
- Silicon Strips (SCT), 80 μm stereo
- Transition Ratiation Tracker (TRT) 36 points/track

The ATLAS Experiment

- Triggering $|\eta| < 2.4$
- Precision Tracking $|\eta| < 2.7$

B-Physics

Calorimeter System

EM and Hadronic energy
- LAr EM barrel and EC
- LAr Had. EC
- Tile Calorimeter (Fe-Scin.) hadronic barrel

Muon detectors

Tile Calorimeter

Liquid Argon Calorimeter

Muon Specrometer

Toroid Magnets

Precision μ tracking:
- MDT (Monitored Drift Tubes)
- CSC (Cathode Strip Chambers)

Trigger:
- RPC (Resistive Plate Chamber)
- TGC (Thin Gas Chamber)

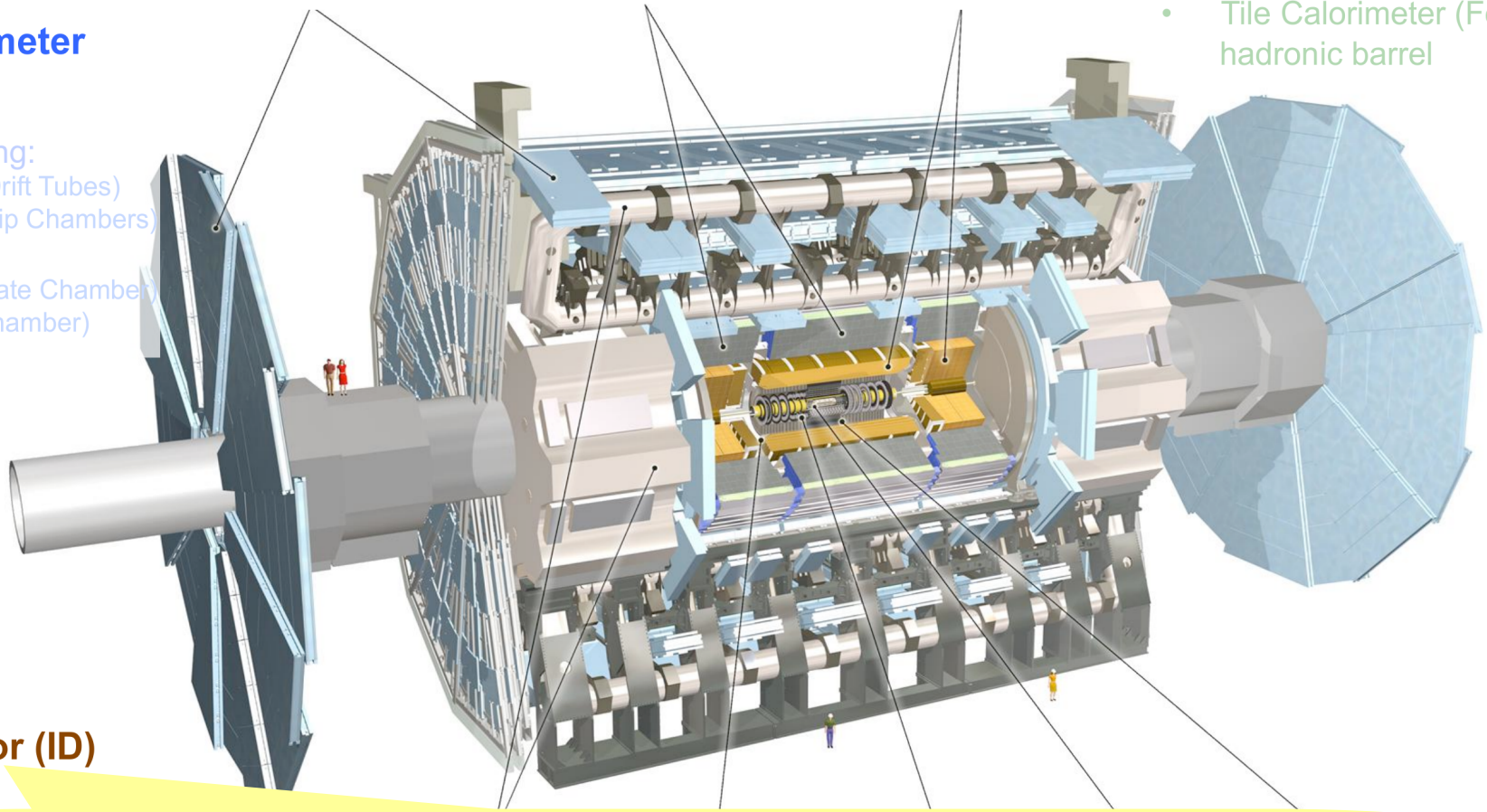

Inner Detector (ID)

- $p_T > 0.4$ GeV, $|\eta| < 2.5$
- New for Run2: Insertable B-Layer (IBL) an additional inner-most pixel layer ($r = 33$mm) and lower x/X_0 beam pipe
- Resolution in $m_{\mu+\mu-}$: around 50 MeV for J/ψ and 150 MeV for ϒ(nS)
- Resolution in b-hadron proper decay time in Run-1 data around 100 fs (~30% improvement with IBL in Run-2)

Measurement of $\Delta\Gamma_s$ and ϕ_s in $B_s \to J/\psi(\mu\mu)\phi(KK)$

- CP violation in $B_s \to J/\psi\phi$ occurs through the interference in mixing and decay

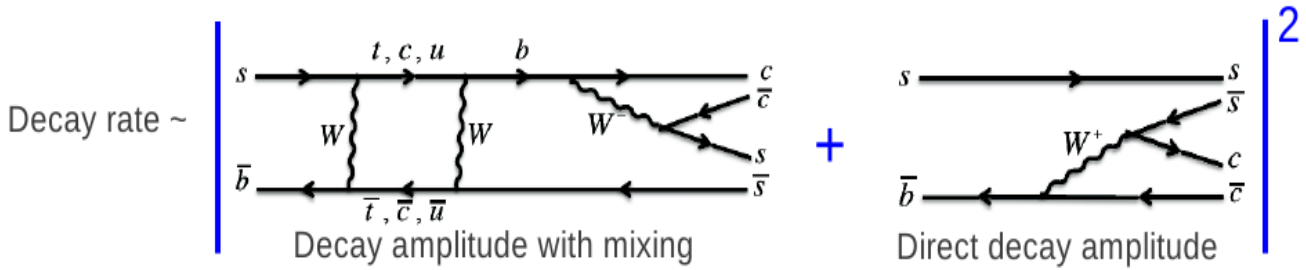

B_s mixing:
- Mass difference $\Delta m = m_H - m_L$
- Mixing phase ϕ_s
- Decay width difference $\Delta\Gamma_s = \Gamma_L - \Gamma_H$

$$|B_s^H\rangle = p|B_s^0\rangle - q|\bar{B}_s^0\rangle$$
$$|B_s^L\rangle = p|B_s^0\rangle + q|\bar{B}_s^0\rangle$$

- Time evolution of flavour tagged $B_s \to J/\psi\phi$ very sensitive to New Physics
- 9 physics parameters to describe $B_s \to J/\psi\phi$ decay

Γ_s, $\Delta\Gamma_s$	decay with and decay width difference
ϕ_s ($\approx 2\beta_s$)	CP violating phase
$\lvert A_0\rvert^2$, $\lvert A_{\lvert\rvert}\rvert^2$	CP state amplitudes
$\delta_{\lvert\rvert}$, $\delta_\perp$	Strong phases
$\lvert A_S\rvert^2$, δ_S	S-wave parameters

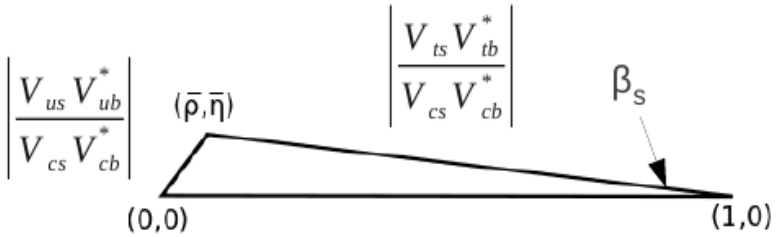

ϕ_s small in SM, clear to see potential excess from NP

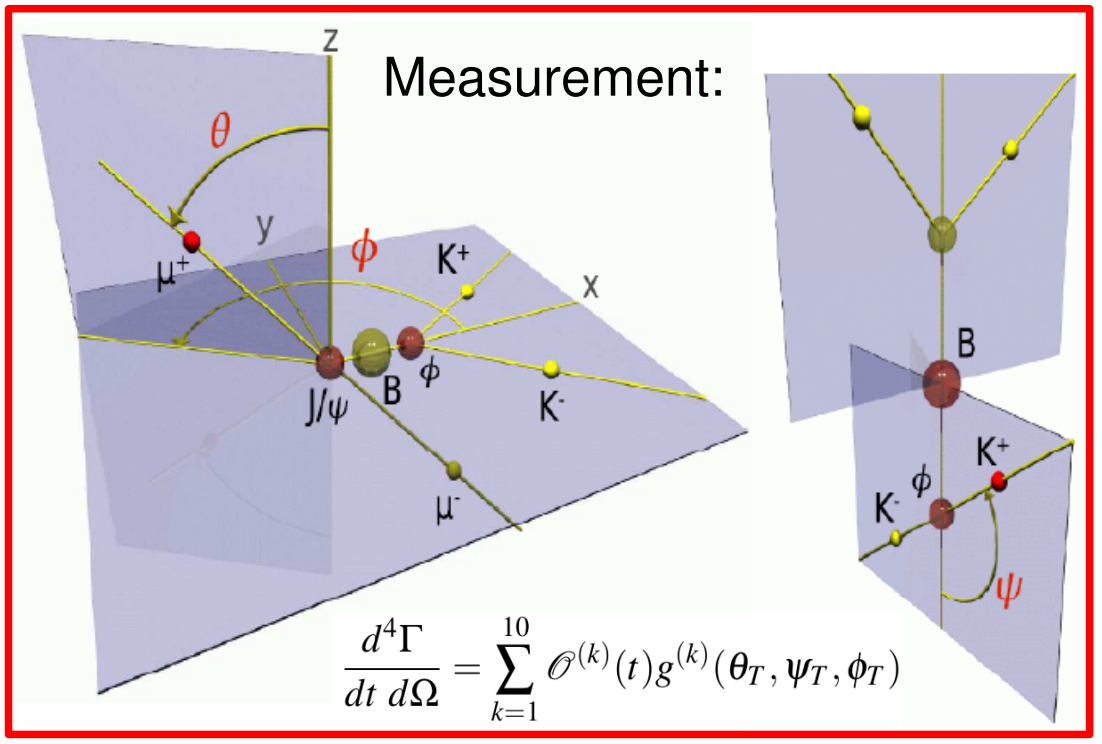

Datasets and Selection

- Latest result using Run-1 pp collision data at 8 TeV, combined with previous 7 TeV analysis

JHEP 1608 (2016) 147 | PRD 90 (2014) 052007

- **Datasets (pp):** 7 TeV data, 5.08 fb^{-1} (used 4.9 fb^{-1}), $L_{max} = 3.7 \times 10^{33}\, cm^{-2}s^{-1}$
  8 TeV data, 21.3 fb^{-1} (used 14.3 fb^{-1}), $L_{max} = 7.7 \times 10^{33}\, cm^{-2}s^{-1}$

- **Trigger:** 20 MHz collision rate → ~400 Hz recording
  - B-physics concentrates on low-p_T di-muon signatures, in this case $J/\psi \to \mu\mu$
  - Trigger on low-p_T (4,6 GeV) di-muon
    - 2 muons at L1 (HW-based)
    - Confirmed at HLT
    - Track vertex fit and J/ψ mass cuts at HLT
  - 8 TeV data: low-p_T maintained introducing barrel triggers at L1

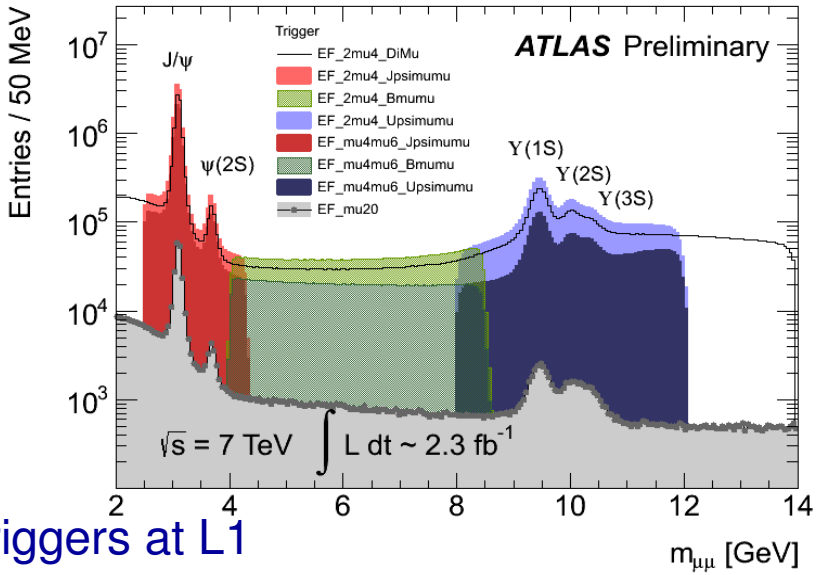

- **Selection:** full $B_s \to J/\psi(\mu^+\mu^-)\phi(K^+K^-)$ decay chain reconstruction with Inner Detector, no K/π separation
  - J/ψ selection – di-muon vertex $\chi^2/_{NDF}$<10, J/ψ invariant mass windows width 0.27 ... 0.48 GeV (barrel → endcap)
  - ϕ selection – $p_T(K^{\pm}) > 1$ GeV, ϕ invariant mass window 22 MeV
  - B_s candidates – 4-track vertex $\chi^2/_{NDF}$<3, $J/\psi\phi$ invariant mass range for analysis (5.15 – 5.65) GeV, no proper decay time cut

B-Flavour Tagging in $B_s \to J/\psi\phi$

- Knowledge of $B_s/\bar{B}_s$ flavour at production significantly increases signal PDF sensitivity to ϕ_s
- Three taggers: muon, electron, b-tagged jet
- Key variable: charge of p_T-weighted tracks in a cone (ΔR) around the opposite side primary object (μ, e, b-jet), used to build per-candidates B_s tag probability

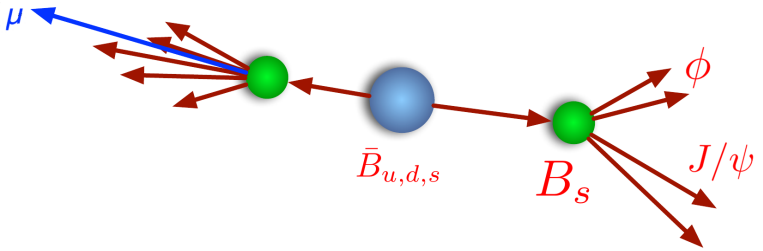

Muon tagger:
- muon p_T > 2.5 GeV
- $\Delta z(\mu)$ w.r.t. PV < 5 mm
- ΔR (cone) = 0.5
- κ = 1.1
- tracks p_{Ti} > 0.5 GeV

Electron tagger:
- electron p_T > 0.5 GeV
- $\Delta z(e)$ w.r.t. PV < 5 mm
- $\Delta R(e^{\pm}, B_s)$ > 0.4
- ΔR (cone) = 0.5
- κ = 1.0
- tracks p_{Ti} > 0.5 GeV

b-jet tagger:
- b-tag weight 0.7 maximizing the tagging power on $B^{\pm}$ sample
- anti-k_T (R = 0.8)
- κ = 1.1
- using all tracks associated to the jet

$$Q_{\text{jet}} = \frac{\sum_i^{N\ \text{tracks}} q_i \cdot (p_{\text{T}i})^{\kappa}}{\sum_i^{N\ \text{tracks}} (p_{\text{T}i})^{\kappa}}$$

$$Q_{\mu} = \frac{\sum_i^{N\ \text{tracks}} q_i \cdot (p_{\text{T}i})^{\kappa}}{\sum_i^{N\ \text{tracks}} (p_{\text{T}i})^{\kappa}}$$

- Calibration on self-tagged $B^{\pm} \to J/\psi K^{\pm}$ channel:
  3-track vertex, $p_T(K)$ > 1 GeV, Lxy > 0.1 mm

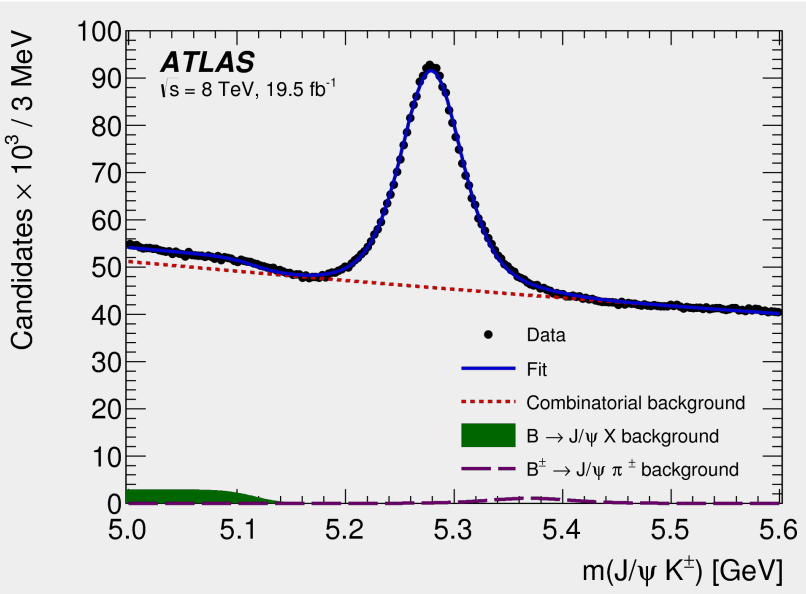

B-Flavour Tagging Results

Tagger	Efficiency [%]	Dilution [%]	Tagging Power [%]
Combined μ	4.12 ± 0.02	47.4 ± 0.2	0.92 ± 0.02
Electron	1.19 ± 0.01	49.2 ± 0.3	0.29 ± 0.01
Segment-tagged μ	1.20 ± 0.01	28.6 ± 0.2	0.10 ± 0.01
Jet-charge	13.15 ± 0.03	11.85 ± 0.03	0.19 ± 0.01
Total	19.66 ± 0.04	27.56 ± 0.06	1.49 ± 0.02

- Per each B_s-candidate, only one out of the available taggers is selected – the one with the highest Dilution

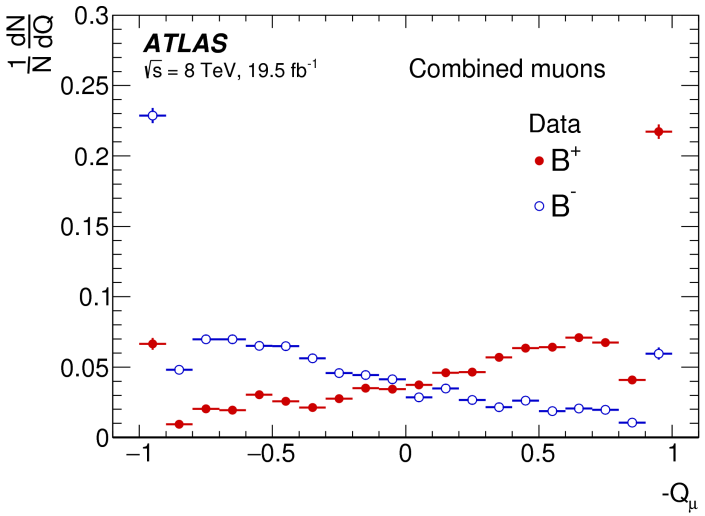

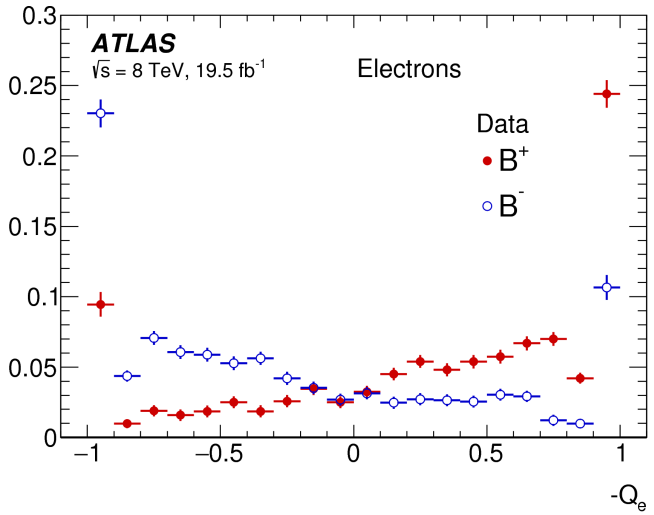

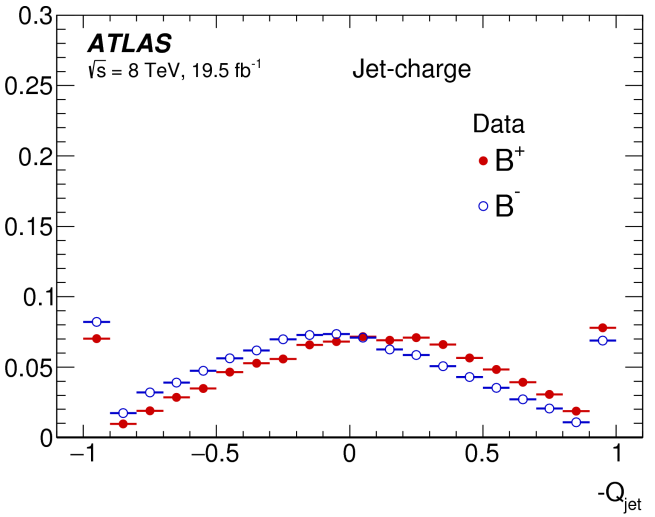

Unbinned Maximum Likelihood Fit

$$\ln \mathcal{L} = \sum_{i=1}^{N} \{ w_i \cdot \ln(f_s \cdot \mathcal{F}_s (m_i, t_i, \sigma_{t_i}, \Omega_i, P(B|Q), p_{T_i}) + f_s \cdot f_{B^0} \cdot \mathcal{F}_{B^0}(m_i, t_i, \sigma_{t_i}, \Omega_i, P(B|Q), p_{T_i}) + f_s \cdot f_{\Lambda_b} \cdot \mathcal{F}_{\Lambda_b}(m_i, t_i, \sigma_{t_i}, \Omega_i, P(B|Q), p_{T_i}) + (1 - f_s \cdot (1 + f_{B^0} + f_{\Lambda_b})) \mathcal{F}_{\mathrm{bkg}}(m_i, t_i, \sigma_{t_i}, \Omega_i, P(B|Q), p_{T_i})) \}$$

Measured variables:

- B_s mass m_i
- B_s proper decay time t_i and its uncertainty σ_{ti}
- 3 angles Ω_i (θ_{Ti}, φ_{Ti}, ψ_{Ti})
- B_s momentum p_{Ti}
- B_s tag probability $p_{B|Qi}$
- tagging method M_i

Signal and background PDFs for conditional observables determined from data using sidebands subtraction; PDFs fixed in the fit

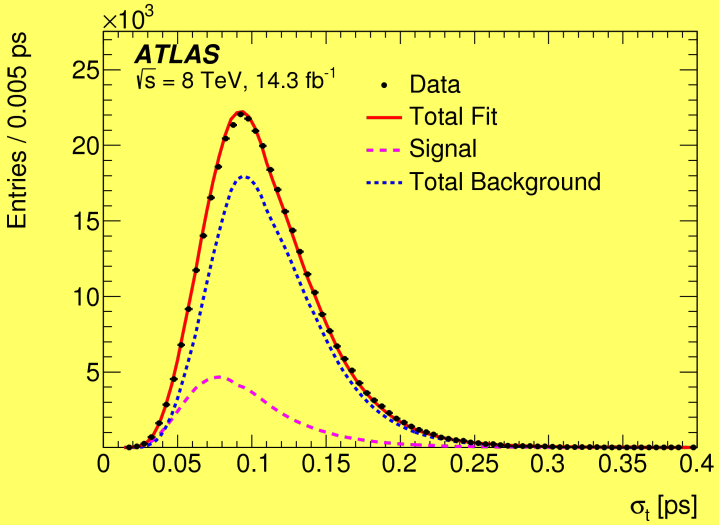

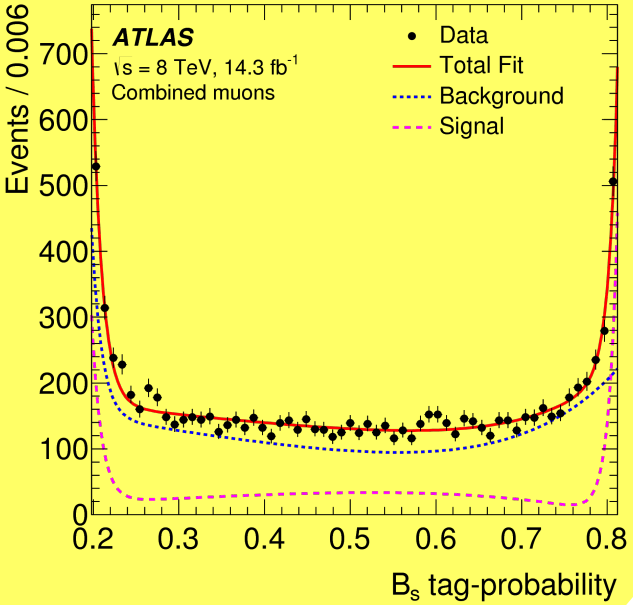

Unbinned Maximum Likelihood Fit

$$\ln \mathcal{L} = \sum_{i=1}^{N} \{ w_i \cdot \ln(f_s \cdot \mathcal{F}_s \quad (m_i, t_i, \sigma_{t_i}, \Omega_i, P(B|Q), p_{T_i}) + f_s \cdot f_{B^0} \cdot \mathcal{F}_{B^0}(m_i, t_i, \sigma_{t_i}, \Omega_i, P(B|Q), p_{T_i}) + f_s \cdot f_{\Lambda_b} \cdot \mathcal{F}_{\Lambda_b}(m_i, t_i, \sigma_{t_i}, \Omega_i, P(B|Q), p_{T_i}) + (1 - f_s \cdot (1 + f_{B^0} + f_{\Lambda_b})) \mathcal{F}_{\text{bkg}}(m_i, t_i, \sigma_{t_i}, \Omega_i, P(B|Q), p_{T_i})) \}$$

Signal decay main parameters:

- CP violating phase ϕ_s
- Decay width $\Gamma_s = (\Gamma_H + \Gamma_L)/2$
- Decay width difference $\Delta\Gamma = \Gamma_H - \Gamma_L$
- CP state amplitudes $|A_0(0)|^2$ and $|A_{||}(0)|^2$
- Strong phases $\delta_{||}$ and $\delta_\perp$
- S-wave amplitude $|A_S(0)|^2$ and phase δ_S (fitting $\delta_S - \delta_\perp$ to avoid high correlations)
- B_s mean mass
- (Δm_s fixed to 17.77 ps^{-1})

$B_d \to J/\psi K^*(K\pi)$ and $\Lambda_b \to J/\psi \Lambda^*(Kp)$ decay reflections, derived from MC, PDG and the LHCb $\Lambda_b \to J/\psi Kp$ measurement; fixed shape and relative contribution in the fit

Combinatorial background description, derived from data sidebands; angular distribution described by spherical harmonics and fixed in the fit

Weights accounting for **proper decay time trigger efficiency** (muons track d_0 reconstruction efficiency bias); estimated from MC

Fit Projections

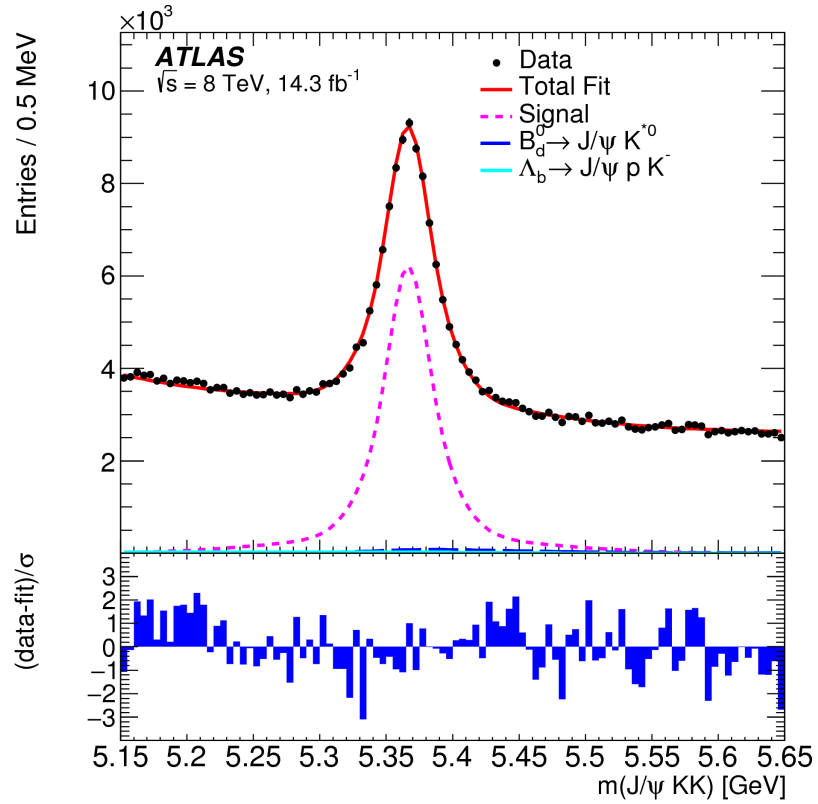

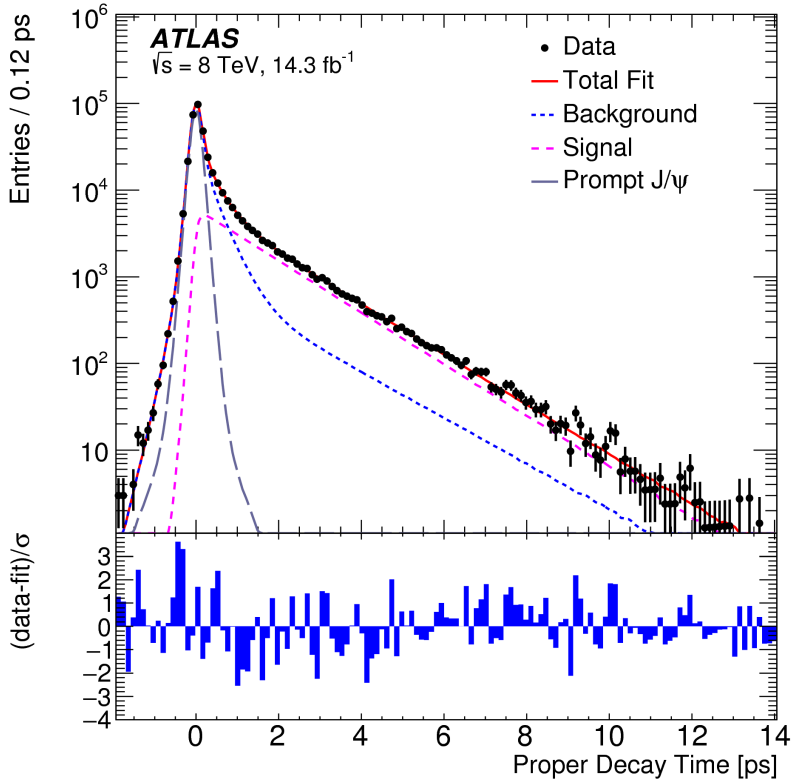

$$\ln \mathcal{L} = \sum_{i=1}^{N} \{ w_i \cdot \ln(f_s \cdot \mathcal{F}_s + f_s \cdot f_{B^0} \cdot \mathcal{F}_{B^0} + f_s \cdot f_{\Lambda_b} \cdot \mathcal{F}_{\Lambda_b} + (1 - f_{s,B^0,\Lambda_b}) \mathcal{F}_{\text{bkg}}) \}$$

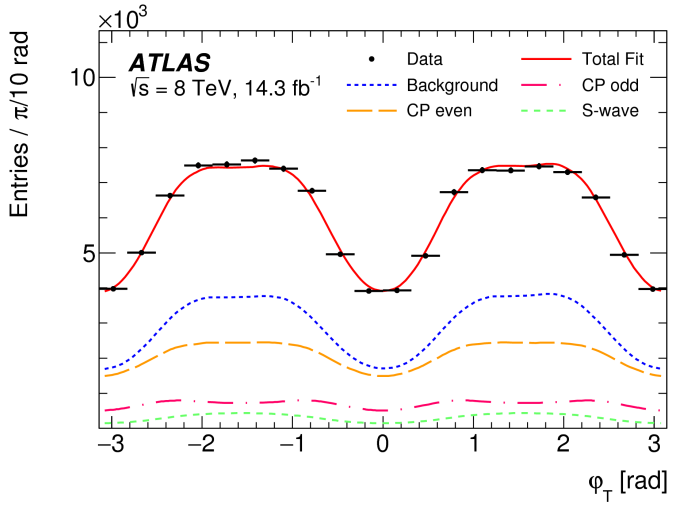

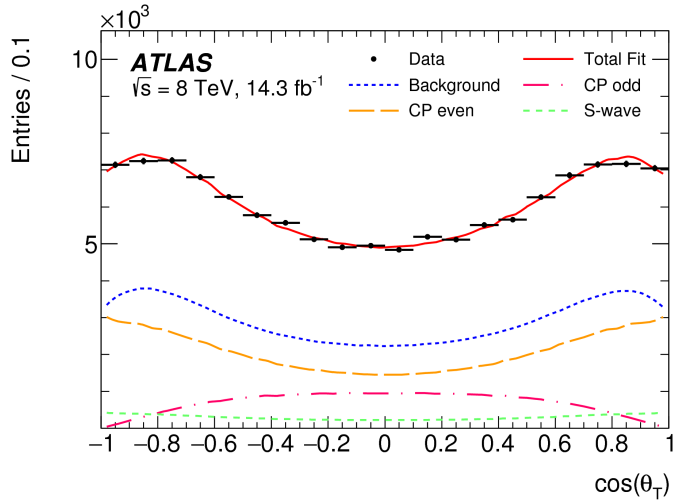

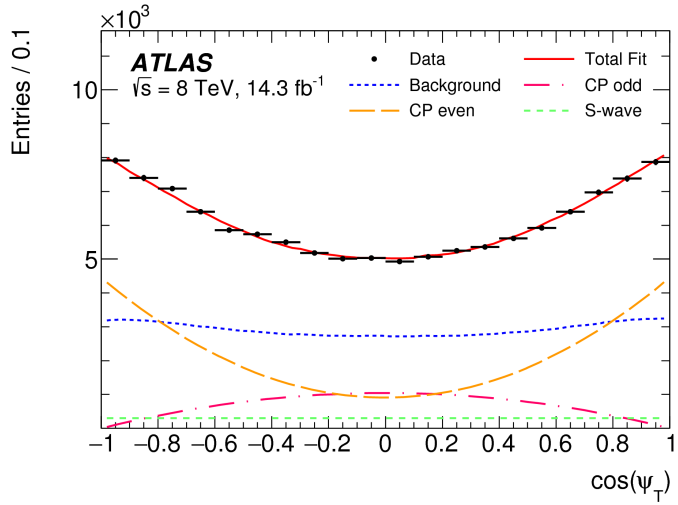

Systematic Uncertainties

	ϕ_s [rad]	$\Delta\Gamma_s$ [ps^{-1}]	Γ_s [ps^{-1}]	$\lvert A_\parallel(0)\rvert^2$	$\lvert A_0(0)\rvert^2$	$\lvert A_S(0)\rvert^2$	$\delta_\perp$ [rad]	$\delta_\parallel$ [rad]	$\delta_\perp - \delta_S$ [rad]
Tagging	0.025	0.003	$<10^{-3}$	$<10^{-3}$	$<10^{-3}$	0.001	0.236	0.014	0.004
Acceptance	$<10^{-3}$	$<10^{-3}$	$<10^{-3}$	0.003	$<10^{-3}$	0.001	0.004	0.008	$<10^{-3}$
Inner detector alignment	0.005	$<10^{-3}$	0.002	$<10^{-3}$	$<10^{-3}$	$<10^{-3}$	0.134	0.007	$<10^{-3}$
Background angles model:									
Choice of p_T bins	0.020	0.006	0.003	0.003	$<10^{-3}$	0.008	0.004	0.006	0.008
Choice of mass interval	0.008	0.001	0.001	$<10^{-3}$	$<10^{-3}$	0.002	0.021	0.005	0.003
B_d^0 background model	0.023	0.001	$<10^{-3}$	0.002	0.002	0.017	0.090	0.011	0.009
Λ_b background model	0.011	0.002	0.001	0.001	0.007	0.009	0.045	0.006	0.007
Fit model:									
Mass signal model	0.004	$<10^{-3}$	$<10^{-3}$	0.002	$<10^{-3}$	0.001	0.015	0.017	$<10^{-3}$
Mass background model	$<10^{-3}$	0.002	$<10^{-3}$	0.002	$<10^{-3}$	0.002	0.027	0.038	$<10^{-3}$
Time resolution model	0.003	$<10^{-3}$	0.001	0.002	$<10^{-3}$	0.002	0.057	0.011	0.001
Default fit model	0.001	0.002	$<10^{-3}$	0.002	$<10^{-3}$	0.002	0.025	0.015	0.002
Total	0.042	0.007	0.004	0.006	0.007	0.022	0.30	0.05	0.01

- Uncertainty in the calibration of the B_s-tag probability; MC statistical uncertainty included in fit stat. error
- Alternative detector acceptance fit-functions and binning determined from MC
- Radial expansion uncertainties determined from their effect on tracks d_0 in the data
- Background angles model (fixed in UML fit) extracted from data with varying sidebands size and binning
- Uncertainties of relative fraction; fit-model and P-wave contribution
- Uncertainties of relative fraction; fit-model and contributions from $\Lambda_b \to \Lambda^* J/\psi$ decays
- Toy-MC studies; pulls of the default fit model, default fit on toy-data generated with modified PDFs
- (Trigger efficiency modeling in MC found negligible)

Result of the CPV $B_s \to J/\psi\phi$ Study

- Result with 8 TeV data

Parameter	Value	Statistical uncertainty	Systematic uncertainty
ϕ_s[rad]	−0.110	0.082	0.042
$\Delta\Gamma_s$[ps^{-1}]	0.101	0.013	0.007
Γ_s[ps^{-1}]	0.676	0.004	0.004
$\lvert A_{\parallel}(0)\rvert^2$	0.230	0.005	0.006
$\lvert A_0(0)\rvert^2$	0.520	0.004	0.007
$\lvert A_S(0)\rvert^2$	0.097	0.008	0.022
$\delta_\perp$ [rad]	4.50	0.45	0.30
$\delta_{\parallel}$ [rad]	3.15	0.10	0.05
$\delta_\perp - \delta_S$ [rad]	−0.08	0.03	0.01

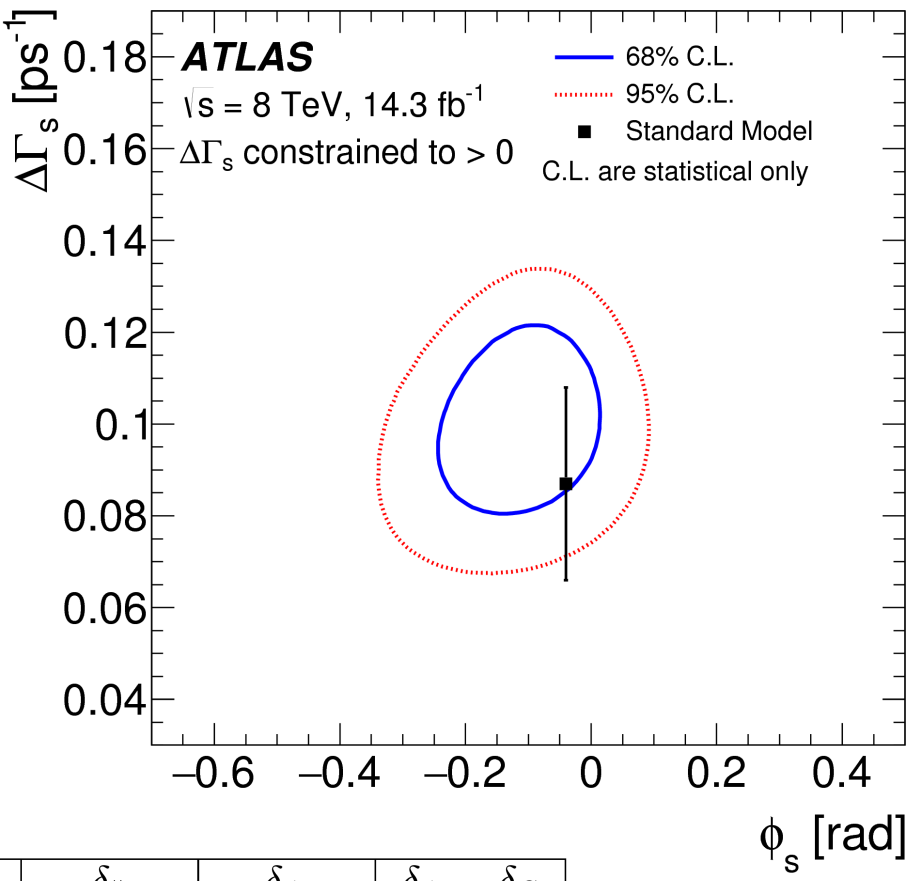

- Fit correlation matrix:

	$\Delta\Gamma$	Γ_s	$\lvert A_{\parallel}(0)\rvert^2$	$\lvert A_0(0)\rvert^2$	$\lvert A_S(0)\rvert^2$	$\delta_{\parallel}$	$\delta_\perp$	$\delta_\perp - \delta_S$
ϕ_s	0.097	−0.085	0.030	0.029	0.048	0.067	0.035	−0.008
$\Delta\Gamma$	1	−0.414	0.098	0.136	0.045	0.009	0.008	−0.011
Γ_s		1	−0.119	−0.042	0.167	−0.027	−0.009	0.018
$\lvert A_{\parallel}(0)\rvert^2$			1	−0.330	0.072	0.105	0.025	−0.018
$\lvert A_0(0)\rvert^2$				1	0.234	−0.011	0.007	0.014
$\lvert A_S(0)\rvert^2$					1	−0.046	0.004	0.052
$\delta_{\parallel}$						1	0.158	−0.006
$\delta_\perp$							1	0.018

Result of the CPV $B_s \to J/\psi\phi$ Study

- Combination of 7 & 8 TeV results (BLUE comb.)

Par	Run1 combined Value	Stat	Syst
ϕ_s[rad]	−0.090	0.078	0.041
$\Delta\Gamma_s$[ps^{-1}]	0.085	0.011	0.007
Γ_s[ps^{-1}]	0.675	0.003	0.003
$\lvert A_\parallel(0)\rvert^2$	0.227	0.004	0.006
$\lvert A_0(0)\rvert^2$	0.522	0.003	0.007
$\lvert A_S\rvert^2$	0.072	0.007	0.018
$\delta_\perp$ [rad]	4.15	0.32	0.16
$\delta_\parallel$ [rad]	3.15	0.10	0.05
$\delta_\perp - \delta_S$ [rad]	−0.08	0.03	0.01

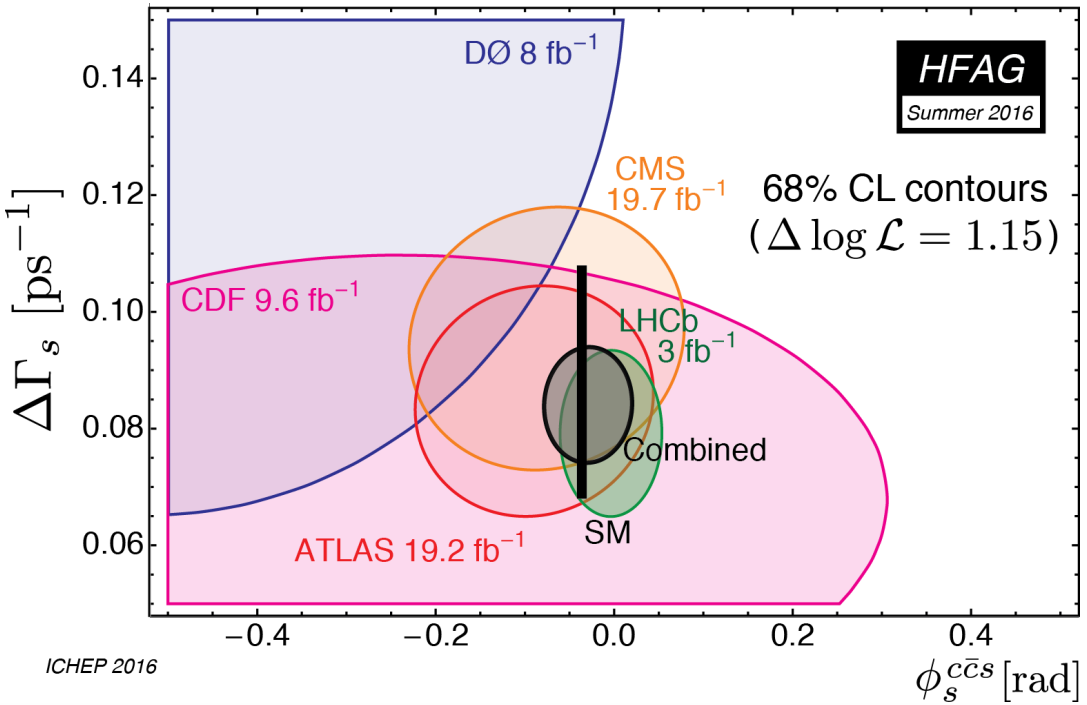

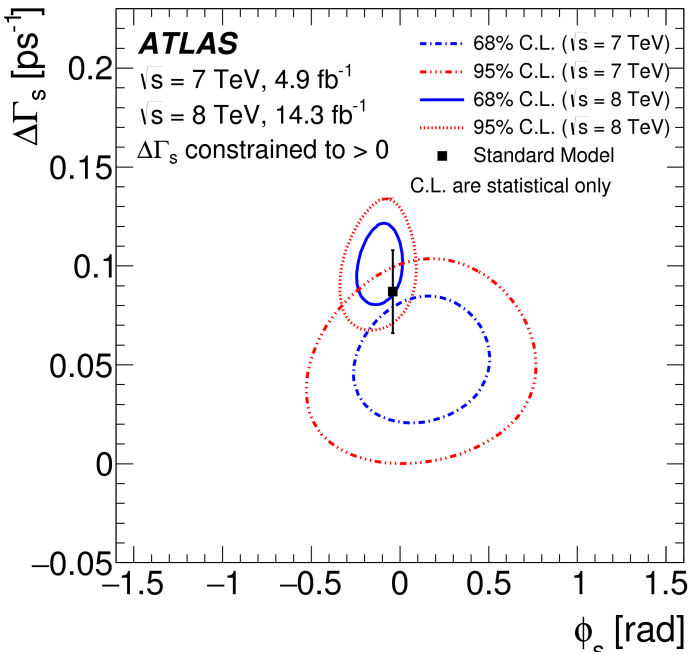

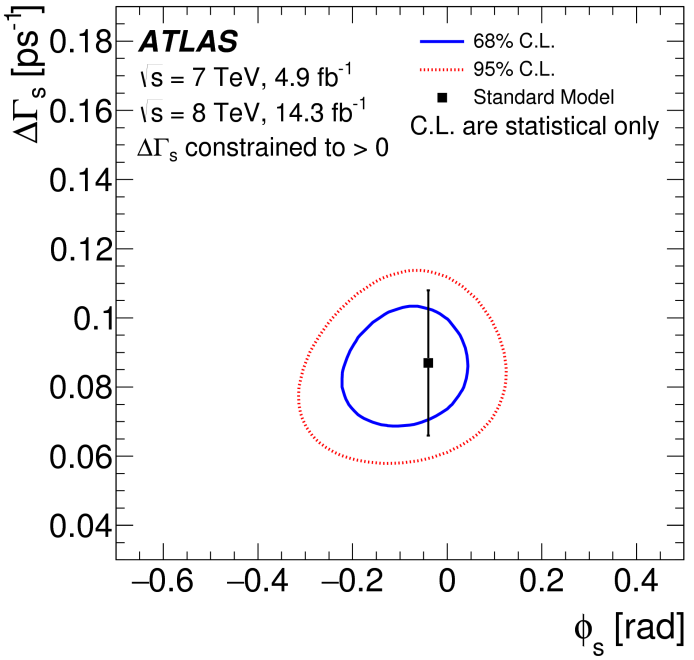

Measurements in Run-2 and Beyond

LHC / HL-LHC Plan

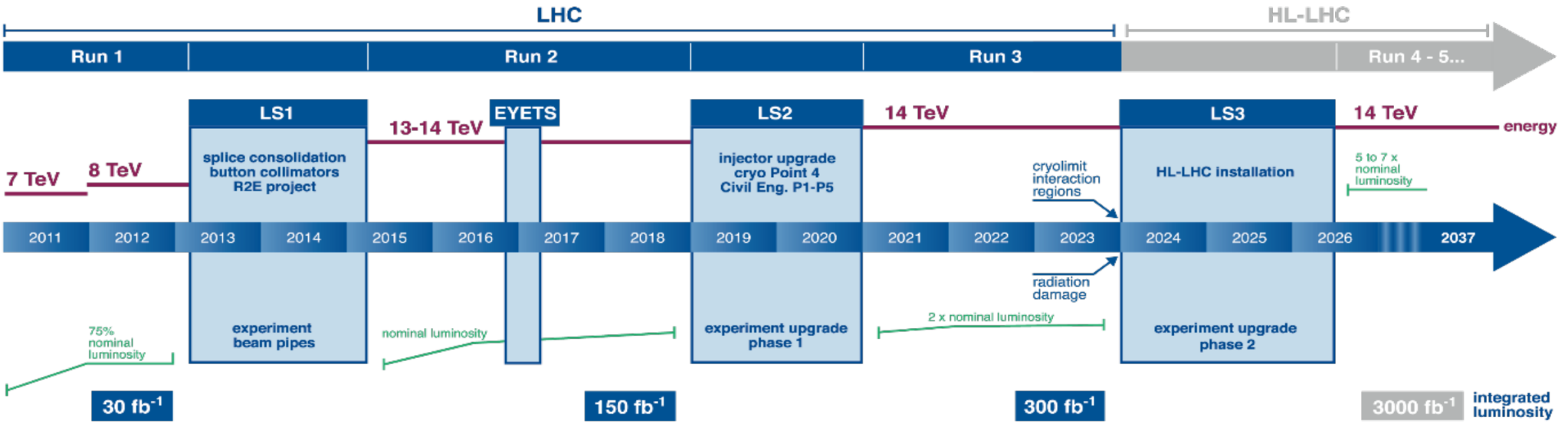

- New pixel layer (IBL, 32-38 mm) + small radius Be beam pipe
- Topological L1 trigger

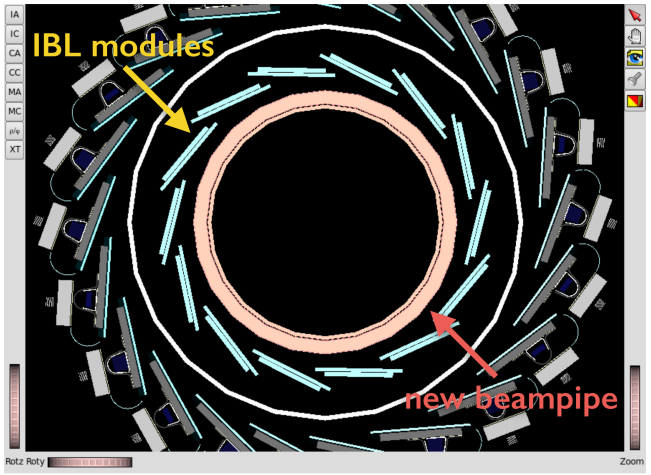

- New small muon wheel
- Fast tracking trigger (FTK) at LVL 1.5; available in Run-2

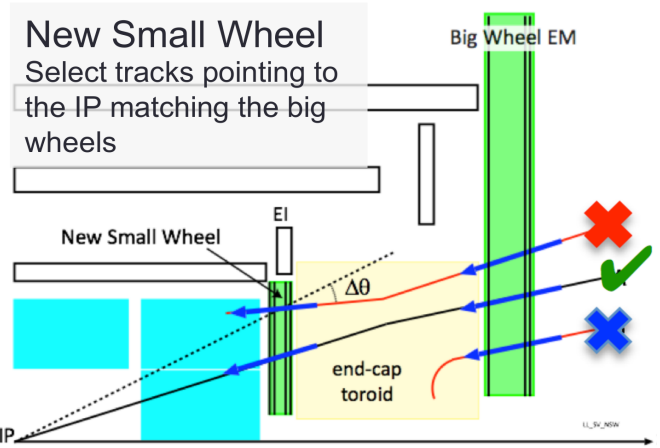

- Completely new Si based tracker (ITK)

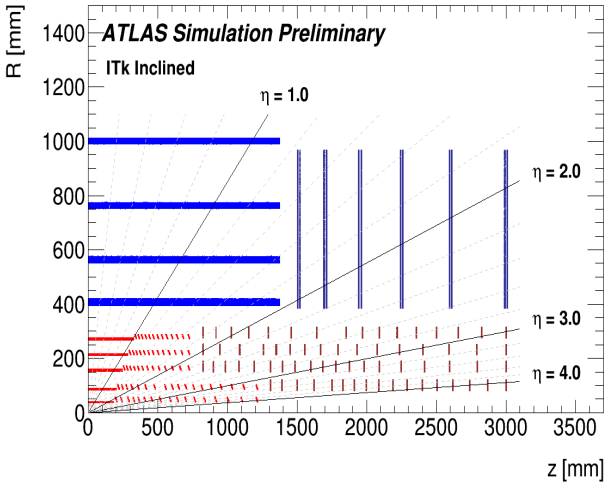

Detector Performance in Run-2 and Beyond

ATL-PHYS-PUB-2016-025

- **Resolution:** invariant mass in decay $B_s \to \mu^+\mu^-$, proper decay time in $B_s \to J/\psi(\mu^+\mu^-)\phi(K^+K^-)$ decay
- Comparison of Run-1, Run-2 (IBL) and HL-LHC (ITk) performances
- **Trigger:** use L1-topo (keep low thresholds at L1) and complicated HLT with full $B_s \to J/\psi(\mu^+\mu^-)\phi(K^+K^-)$ decay topology reconstruction at trigger level

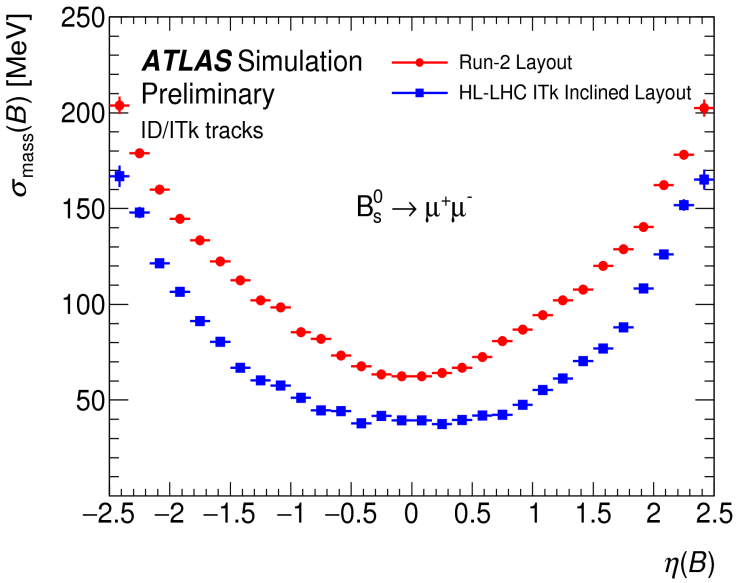

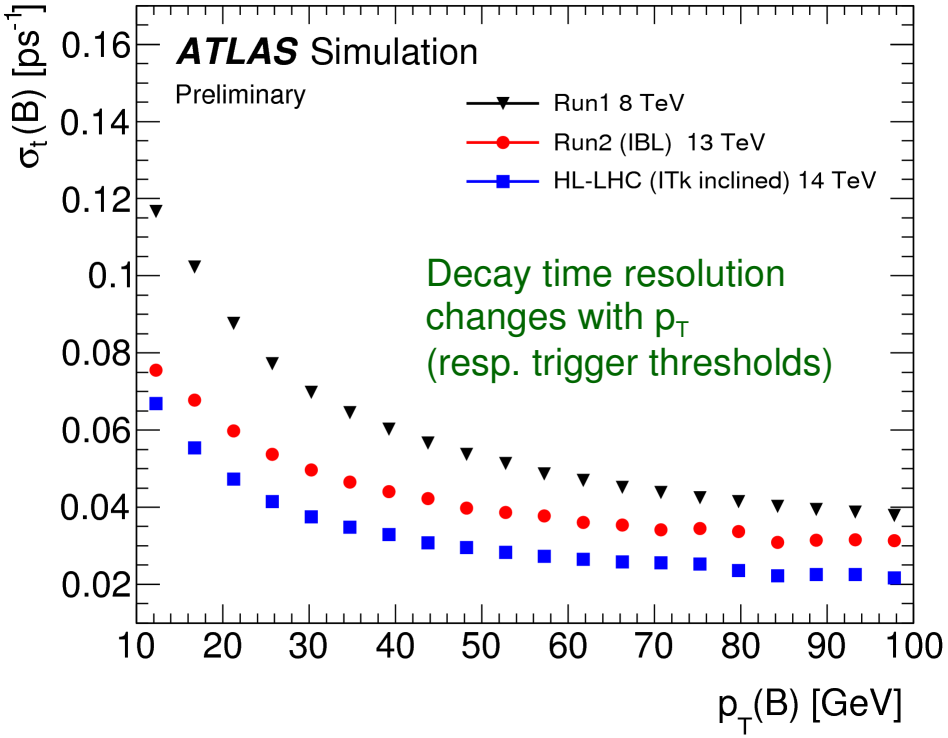

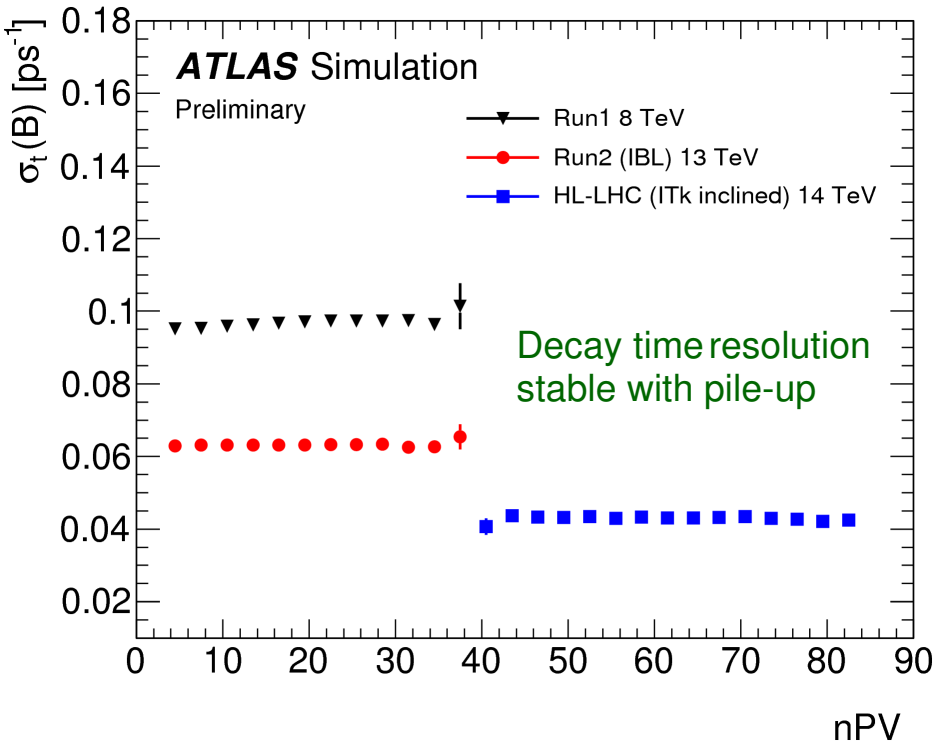

Summary

- ATLAS has measured ϕ_s with full Run-1 dataset, combining 7 & 8 TeV pp collision data, in the decay channel $B_s \to J/\psi(\mu^+\mu^-)\,\phi(K^+K^-)$
  - Results are consistent with Standard Model prediction as well as with other measurements:

$$\begin{aligned} \phi_s &= -0.090 \pm 0.078\ (\text{stat.}) \pm 0.041\ (\text{syst.})\ \text{rad} \\ \Delta\Gamma_s &= 0.085 \pm 0.011\ (\text{stat.}) \pm 0.007\ (\text{syst.})\ \text{ps}^{-1} \\ \Gamma_s &= 0.675 \pm 0.003\ (\text{stat.}) \pm 0.003\ (\text{syst.})\ \text{ps}^{-1} \end{aligned}$$

JHEP 1608 (2016) 147

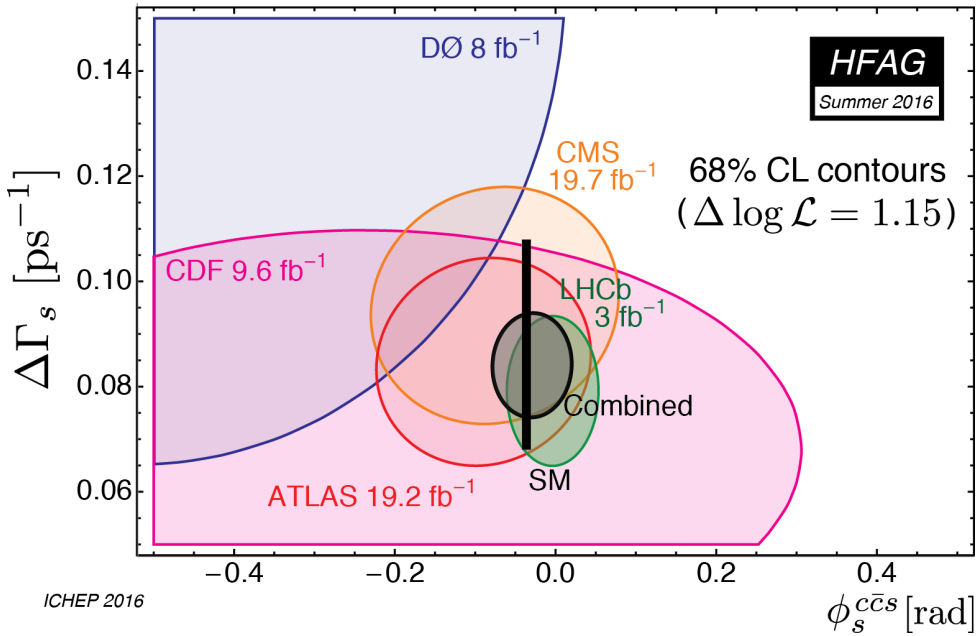

- The analysis is continuing in Run-2 and will continue also in the future stages of the LHC
  - Detector upgrades (namely in **tracking** and **muon system**) and new **trigger strategies** and tools will help to cope with the high-luminosity environment and achieve precision needed to examine possible beyond-SM effects

Backup

Comparison with Other Experiments

- $B_s \to J/\psi\phi(KK)$ channel: ATLAS **JHEP 1608 (2016) 147**, CMS **PLB 757 (2016) 97**, LHCb **PRL 114 (2015) 041801**

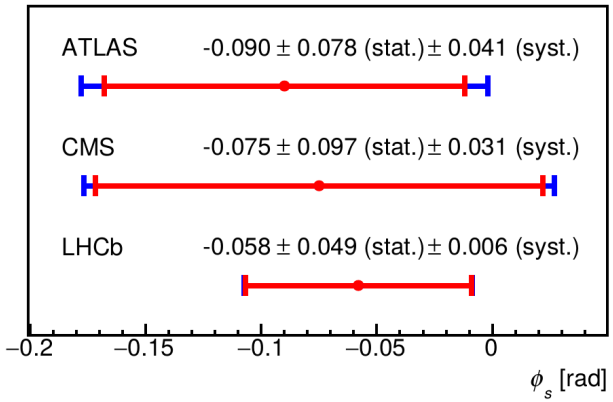

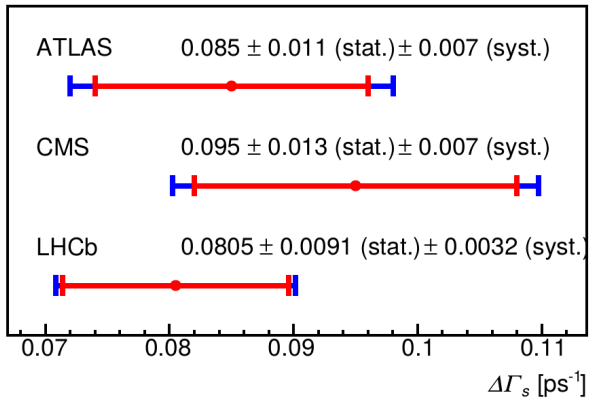

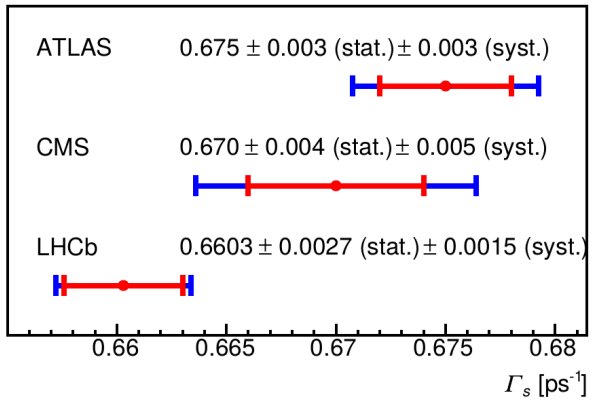

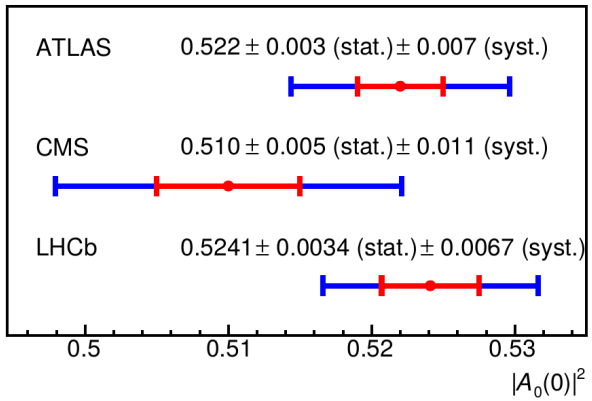

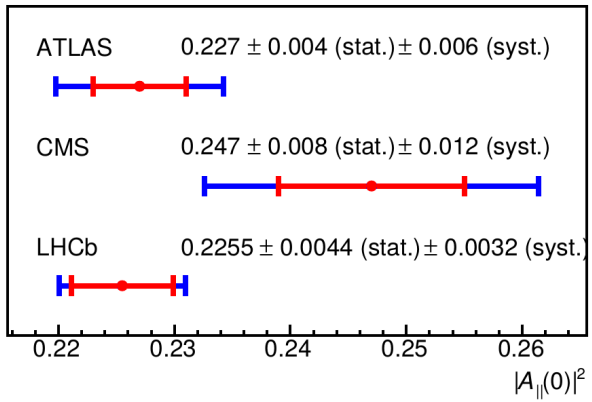

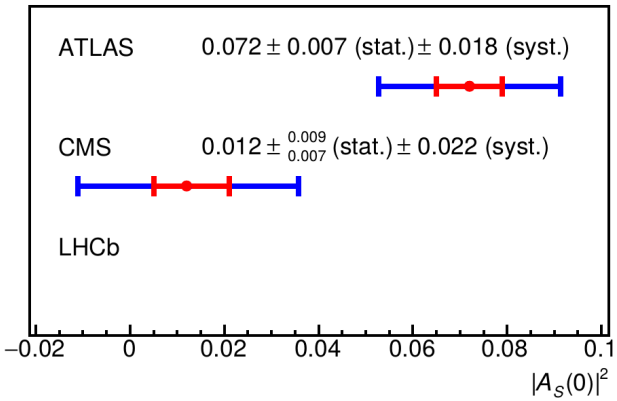

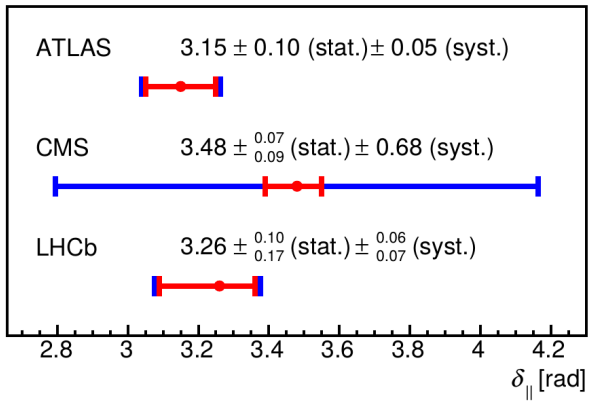

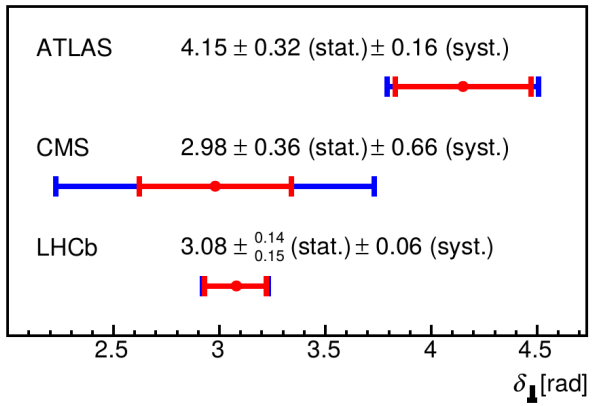

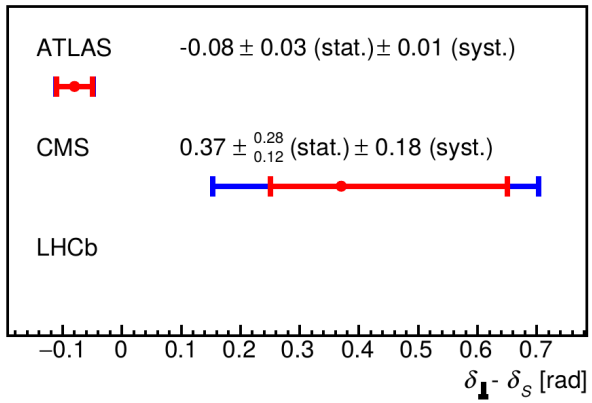

Signal PDF

- **Signal time-angular PDF:**
  (convolved with detector resolution)

$$\frac{d^4\Gamma}{dt\, d\Omega} = \sum_{k=1}^{10} O^{(k)}(t) g^{(k)}(\theta_T, \psi_T, \phi_T)$$

2 PDFs for B_s and $\overline{B}_s$(alternative ± signs): PDF(B_s), PDF($\overline{B}_s$)
Tagged fit: Prob(B_s-tag)*PDF(B_s) + (1-Prob(B_s-tag))*PDF($\overline{B}_s$)
Untagged fit: Prob(B_s-tag) = 0.5

Symmetries: $\{\phi_s, \Delta\Gamma_s, \delta_\perp, \delta_\parallel\} \to \{\pi - \phi_s, -\Delta\Gamma_s, \pi - \delta_\perp, 2\pi - \delta_\parallel\}$

~~$\{\phi_s, \Delta\Gamma_s, \delta_\perp, \delta_\parallel, \delta_S\} \to \{\phi_s, \Delta\Gamma_s, \pi - \delta_\perp, -\delta_\parallel, -\delta_S\}$~~ (untagged fit only)

	k	$\mathcal{O}^{(k)}(t)$	$g^{(k)}(\theta_T, \psi_T, \phi_T)$
CP +1	1	$\frac{1}{2}\lvert A_0(0)\rvert^2 \left[(1+\cos\phi_s)\, e^{-\Gamma_L^{(s)} t} + (1-\cos\phi_s)\, e^{-\Gamma_H^{(s)} t} \pm 2e^{-\Gamma_s t}\sin(\Delta m_s t)\sin\phi_s\right]$	$2\cos^2\psi_T(1-\sin^2\theta_T\cos^2\phi_T)$
CP +1	2	$\frac{1}{2}\lvert A_\parallel(0)\rvert^2 \left[(1+\cos\phi_s)\, e^{-\Gamma_L^{(s)} t} + (1-\cos\phi_s)\, e^{-\Gamma_H^{(s)} t} \pm 2e^{-\Gamma_s t}\sin(\Delta m_s t)\sin\phi_s\right]$	$\sin^2\psi_T(1-\sin^2\theta_T\sin^2\phi_T)$
CP -1	3	$\frac{1}{2}\lvert A_\perp(0)\rvert^2 \left[(1-\cos\phi_s)\, e^{-\Gamma_L^{(s)} t} + (1+\cos\phi_s)\, e^{-\Gamma_H^{(s)} t} \mp 2e^{-\Gamma_s t}\sin(\Delta m_s t)\sin\phi_s\right]$	$\sin^2\psi_T\sin^2\theta_T$
Inter-ference terms	4	$\frac{1}{2}\lvert A_0(0)\rvert\lvert A_\parallel(0)\rvert\cos\delta_\parallel \left[(1+\cos\phi_s)\, e^{-\Gamma_L^{(s)} t} + (1-\cos\phi_s)\, e^{-\Gamma_H^{(s)} t} \pm 2e^{-\Gamma_s t}\sin(\Delta m_s t)\sin\phi_s\right]$	$\frac{1}{\sqrt{2}}\sin 2\psi_T\sin^2\theta_T\sin 2\phi_T$
	5	$\lvert A_\parallel(0)\rvert\lvert A_\perp(0)\rvert[\frac{1}{2}(e^{-\Gamma_L^{(s)} t} - e^{-\Gamma_H^{(s)} t})\cos(\delta_\perp-\delta_\parallel)\sin\phi_s \pm e^{-\Gamma_s t}(\sin(\delta_\perp-\delta_\parallel)\cos(\Delta m_s t) - \cos(\delta_\perp-\delta_\parallel)\cos\phi_s\sin(\Delta m_s t))]$	$-\sin^2\psi_T\sin 2\theta_T\sin\phi_T$
	6	$\lvert A_0(0)\rvert\lvert A_\perp(0)\rvert[\frac{1}{2}(e^{-\Gamma_L^{(s)} t} - e^{-\Gamma_H^{(s)} t})\cos\delta_\perp\sin\phi_s \pm e^{-\Gamma_s t}(\sin\delta_\perp\cos(\Delta m_s t) - \cos\delta_\perp\cos\phi_s\sin(\Delta m_s t))]$	$\frac{1}{\sqrt{2}}\sin 2\psi_T\sin 2\theta_T\cos\phi_T$
S-wave terms	7	$\frac{1}{2}\lvert A_S(0)\rvert^2 \left[(1-\cos\phi_s)\, e^{-\Gamma_L^{(s)} t} + (1+\cos\phi_s)\, e^{-\Gamma_H^{(s)} t} \mp 2e^{-\Gamma_s t}\sin(\Delta m_s t)\sin\phi_s\right]$	$\frac{2}{3}\left(1-\sin^2\theta_T\cos^2\phi_T\right)$
	8	$\lvert A_S(0)\rvert\lvert A_\parallel(0)\rvert[\frac{1}{2}(e^{-\Gamma_L^{(s)} t} - e^{-\Gamma_H^{(s)} t})\sin(\delta_\parallel-\delta_S)\sin\phi_s \pm e^{-\Gamma_s t}(\cos(\delta_\parallel-\delta_S)\cos(\Delta m_s t) - \sin(\delta_\parallel-\delta_S)\cos\phi_s\sin(\Delta m_s t))]$	$\frac{1}{3}\sqrt{6}\sin\psi_T\sin^2\theta_T\sin 2\phi_T$
	9	$\frac{1}{2}\lvert A_S(0)\rvert\lvert A_\perp(0)\rvert\sin(\delta_\perp-\delta_S) \left[(1-\cos\phi_s)\, e^{-\Gamma_L^{(s)} t} + (1+\cos\phi_s)\, e^{-\Gamma_H^{(s)} t} \mp 2e^{-\Gamma_s t}\sin(\Delta m_s t)\sin\phi_s\right]$	$\frac{1}{3}\sqrt{6}\sin\psi_T\sin 2\theta_T\cos\phi_T$
	10	$\lvert A_0(0)\rvert\lvert A_S(0)\rvert[\frac{1}{2}(e^{-\Gamma_H^{(s)} t} - e^{-\Gamma_L^{(s)} t})\sin\delta_S\sin\phi_s \pm e^{-\Gamma_s t}(\cos\delta_S\cos(\Delta m_s t) + \sin\delta_S\cos\phi_s\sin(\Delta m_s t))]$	$\frac{4}{3}\sqrt{3}\cos\psi_T\left(1-\sin^2\theta_T\cos^2\phi_T\right)$

Unbinned Maximum Likelihood Fit

$$\ln \mathcal{L} = \sum_{i=1}^{N} \{ w_i \cdot \ln(f_s \cdot \mathcal{F}_s (m_i, t_i, \sigma_{t_i}, \Omega_i, P(B|Q), p_{T_i}) + f_s \cdot f_{B^0} \cdot \mathcal{F}_{B^0}(m_i, t_i, \sigma_{t_i}, \Omega_i, P(B|Q), p_{T_i}) + f_s \cdot f_{\Lambda_b} \cdot \mathcal{F}_{\Lambda_b}(m_i, t_i, \sigma_{t_i}, \Omega_i, P(B|Q), p_{T_i}) + (1 - f_s \cdot (1 + f_{B^0} + f_{\Lambda_b})) \mathcal{F}_{\mathrm{bkg}}(m_i, t_i, \sigma_{t_i}, \Omega_i, P(B|Q), p_{T_i}) \}$$

Measured variables:
- B_s mass m_i
- B_s proper decay time t_i and its uncertainty σ_{ti}
- 3 angles Ω_i (θ_{Ti}, φ_{Ti}, ψ_{Ti})
- B_s momentum p_{Ti}
- B_s tag probability $p_{B|Qi}$
- tagging method M_i

Signal decay main parameters:
- CP violating phase ϕ_s
- Decay width $\Gamma_s = (\Gamma_H + \Gamma_L)/2$
- Decay width difference $\Delta\Gamma = \Gamma_H - \Gamma_L$
- CP state amplitudes $|A_0(0)|^2$ and $|A_{||}(0)|^2$
- Strong phases $\delta_{||}$ and $\delta_\perp$
- S-wave amplitude $|A_S(0)|^2$ and phase δ_S (fitting $\delta_S - \delta_\perp$ to avoid high correlations)
- B_s mean mass
- (Δm_s fixed to 17.77 ps^{-1})

$B_d \to J/\psi K^*(K\pi)$ and $\Lambda_b \to J/\psi \Lambda^*(Kp)$ decay reflections, derived from MC, PDG and the LHCb $\Lambda_b \to J/\psi Kp$ measurement; fixed shape and relative contribution in the fit

Weights accounting for **proper decay time trigger efficiency** (muons track d_0 reconstruction efficiency bias); estimated from MC

Signal and background PDFs for conditional observables determined from data using sidebands subtraction; PDFs fixed in the fit

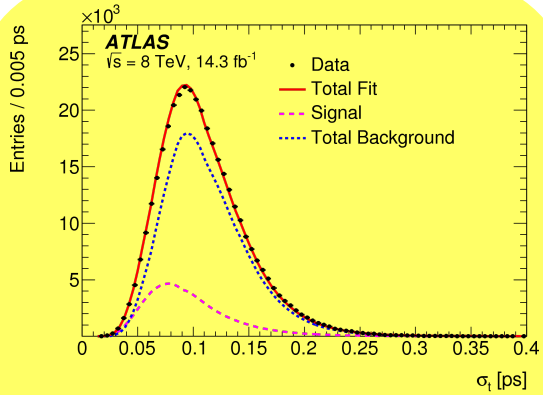

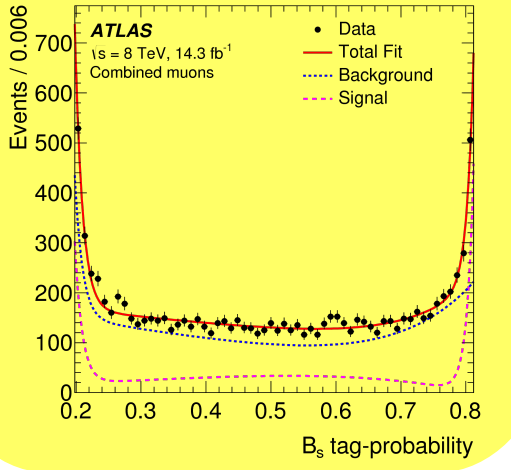

Combinatorial background description, derived from data sidebands; angular distribution described by spherical harmonics and fixed in the fit

B-Flavour Tagging Distributions

- Cone charge for the calibration B^+ and B^- data samples

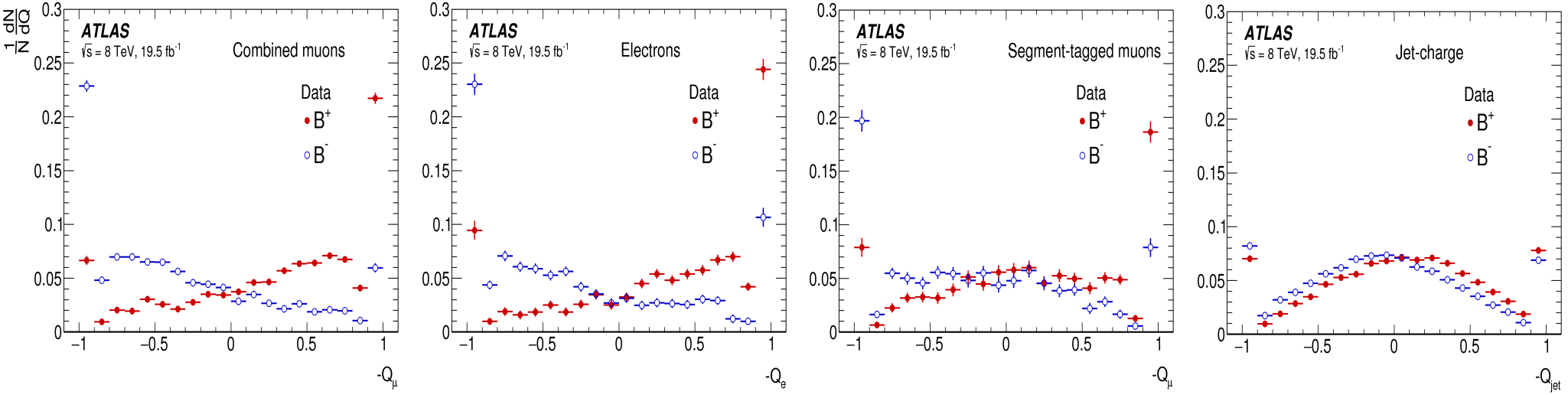

- B_s-tag probablity distribution in the fit, signal & background obtained using sidebands-subtraction method on the real data

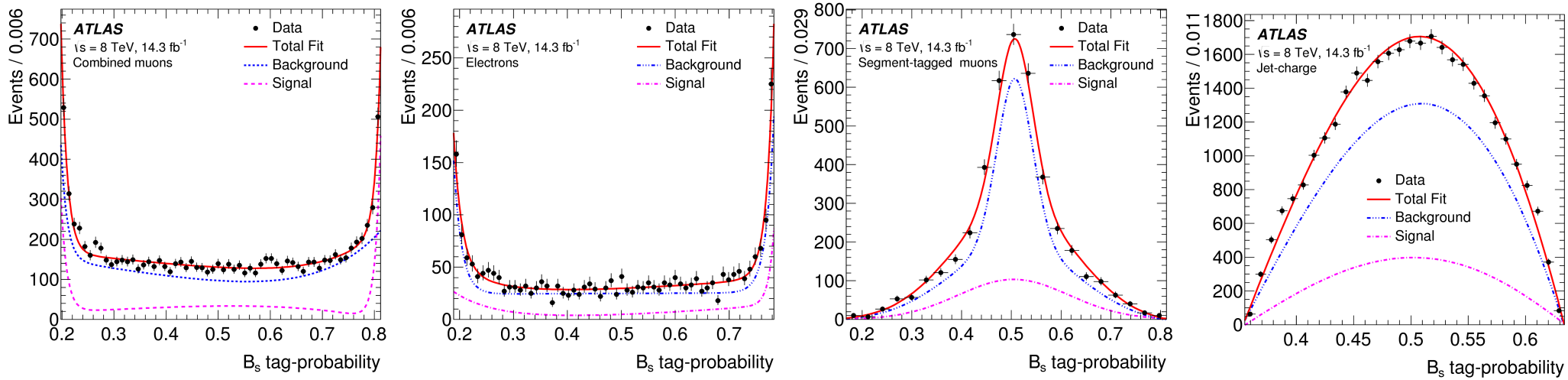

1D Likelihood Scans

- Cross-check of the Gaussian behavior of the likelihood, resp. asymmetry of the errors

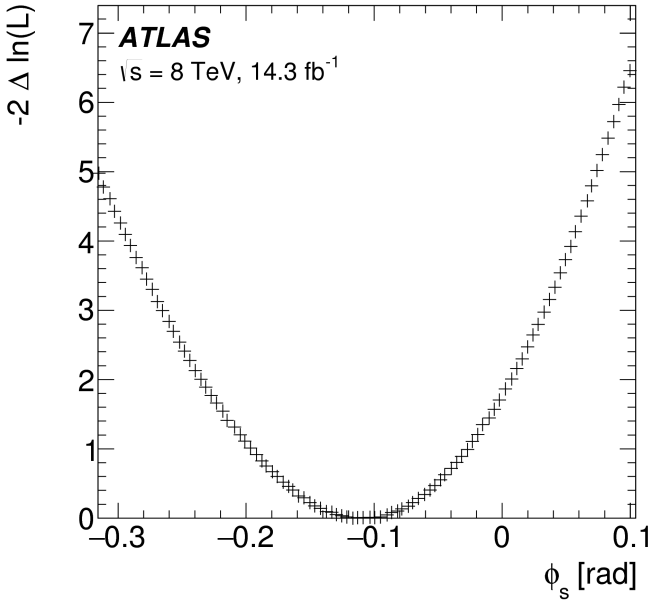

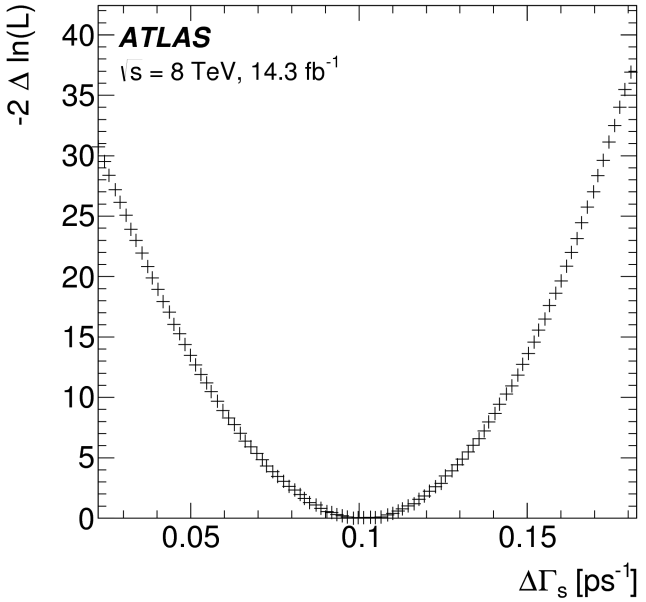

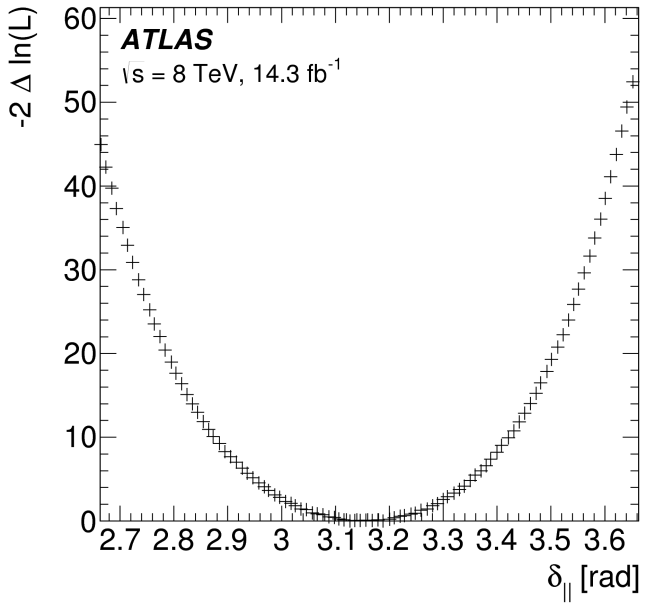

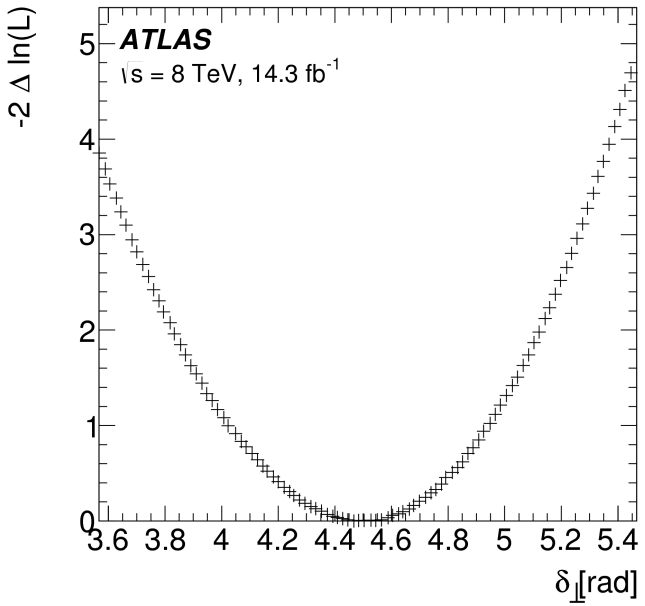

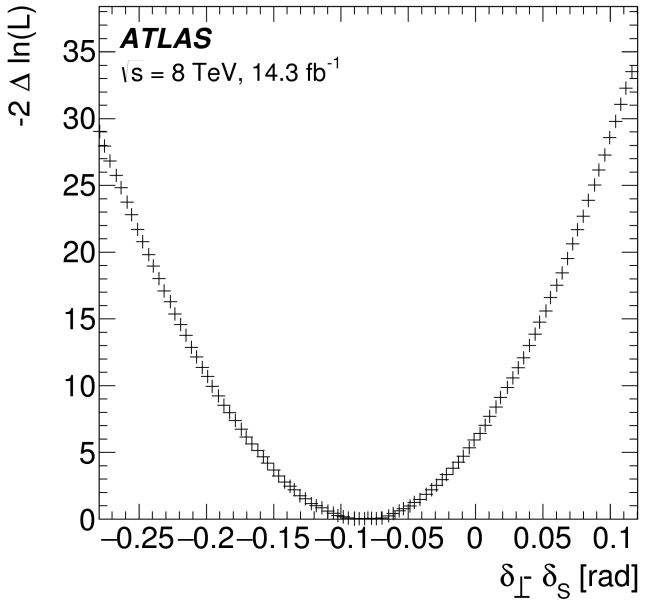

UML Fit Pulls

- Cross-check of the self-consistency of the Unbinned Maximum Likelihood fit

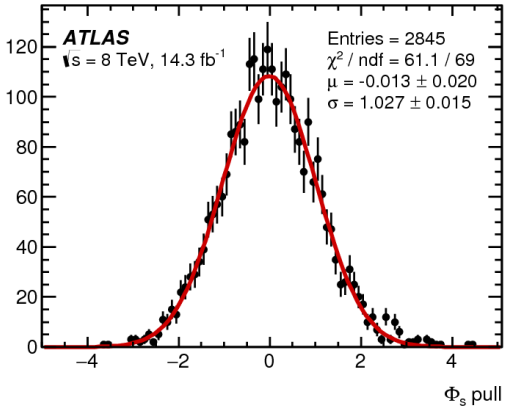

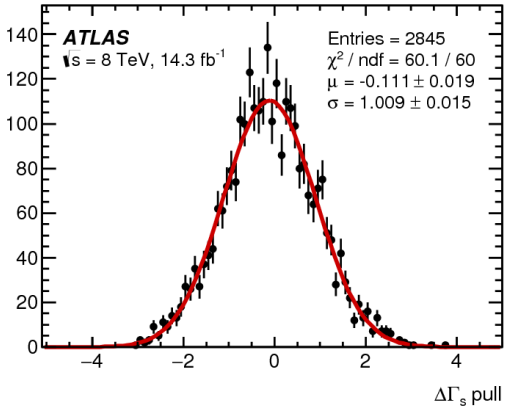

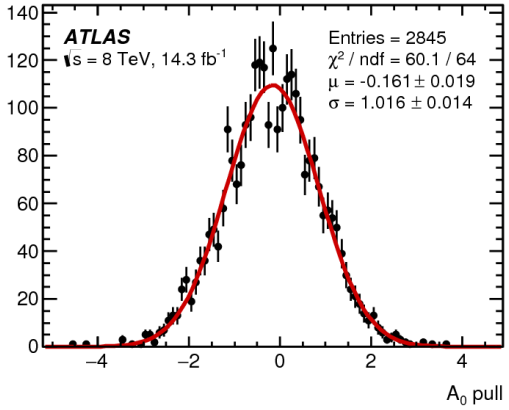

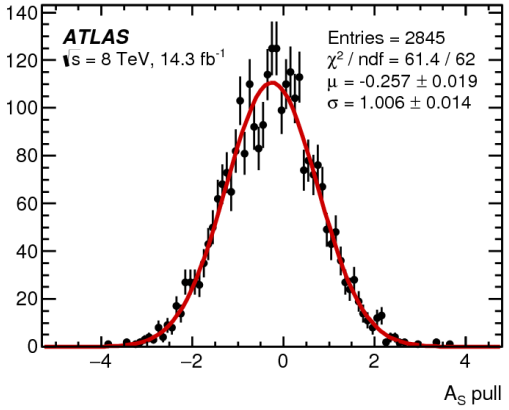

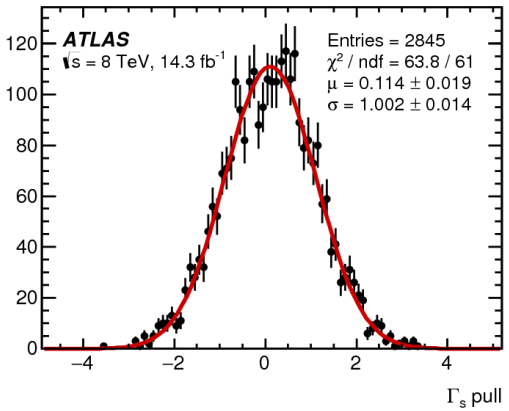

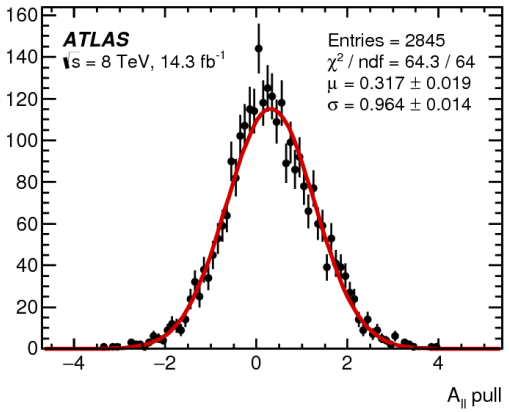

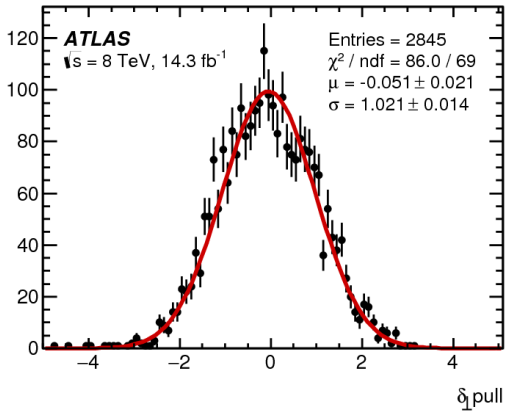

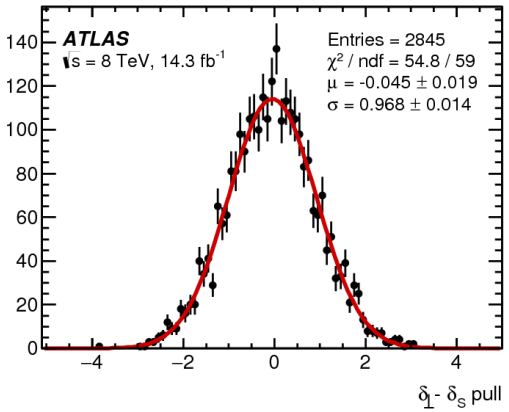

ATLAS ϕ_s Measurements in Run-1

- Comparison of the 7 and 8 TeV tagged analyses with the combination

Par	8 TeV data			7 TeV data			Run1 combined		
	Value	Stat	Syst	Value	Stat	Syst	Value	Stat	Syst
ϕ_s[rad]	-0.110	0.082	0.042	0.12	0.25	0.05	-0.090	0.078	0.041
$\Delta\Gamma_s[\mathrm{ps}^{-1}]$	0.101	0.013	0.007	0.053	0.021	0.010	0.085	0.011	0.007
$\Gamma_s[\mathrm{ps}^{-1}]$	0.676	0.004	0.004	0.677	0.007	0.004	0.675	0.003	0.003
$\lvert A_\parallel(0)\rvert^2$	0.230	0.005	0.006	0.220	0.008	0.009	0.227	0.004	0.006
$\lvert A_0(0)\rvert^2$	0.520	0.004	0.007	0.529	0.006	0.012	0.522	0.003	0.007
$\lvert A_S\rvert^2$	0.097	0.008	0.022	0.024	0.014	0.028	0.072	0.007	0.018
$\delta_\perp$ [rad]	4.50	0.45	0.30	3.89	0.47	0.11	4.15	0.32	0.16
$\delta_\parallel$ [rad]	3.15	0.10	0.05	[3.04, 3.23]		0.09	3.15	0.10	0.05
$\delta_\perp - \delta_S$ [rad]	-0.08	0.03	0.01	[3.02, 3.25]		0.04	-0.08	0.03	0.01

7 & 8 TeV
JHEP 1608 (2016) 147

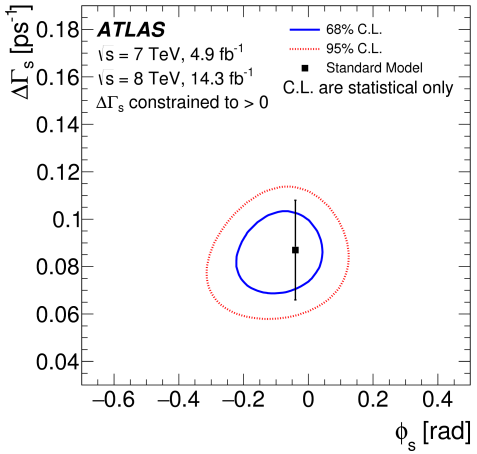

8 TeV
JHEP 1608 (2016) 147

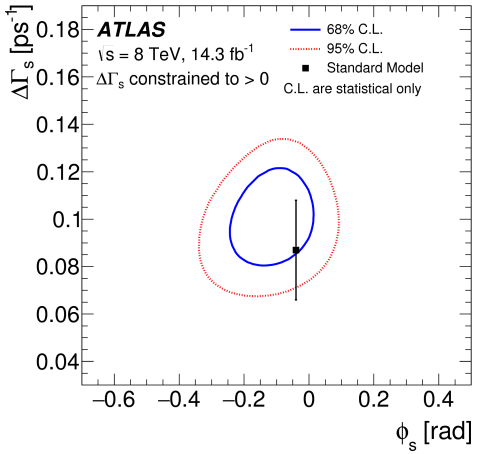

7 TeV
PRD 90 (2014) 052007

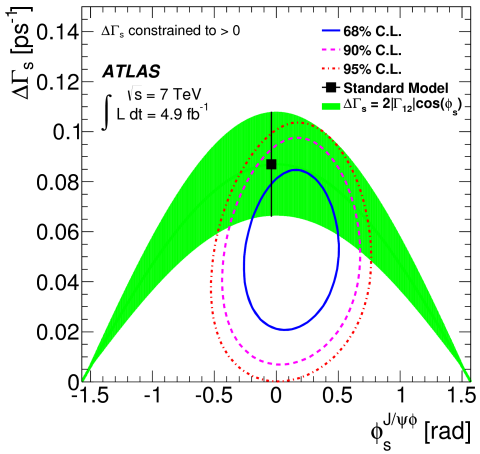

7 TeV (untagged)
JHEP 12 (2012) 072

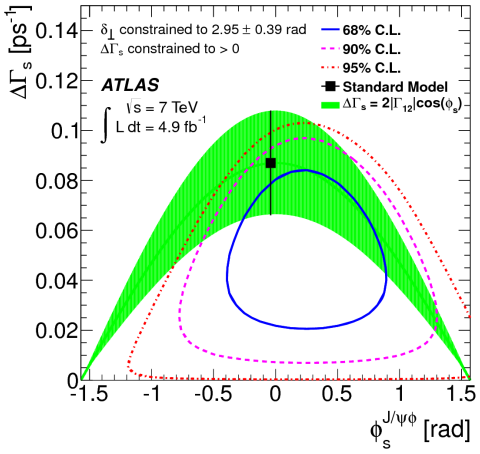

Data Taking (pp): Run-1 and Run-2

- 7 TeV data, 5.08 fb^{-1} — 50ns, 3.7×10^{33} $cm^{-2}s^{-1}$
- 8 TeV, 21.3 fb^{-1} — 50ns, 7.7×10^{33} $cm^{-2}s^{-1}$
- 13 TeV (2015), 3.9 fb^{-1} — 50/25ns, 5.0×10^{33} $cm^{-2}s^{-1}$
- 13 TeV (2016), 36.0 fb^{-1} — 25ns, 13.7×10^{33} $cm^{-2}s^{-1}$

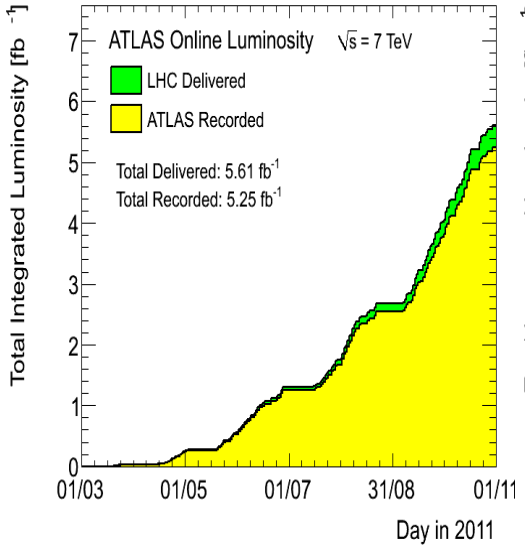

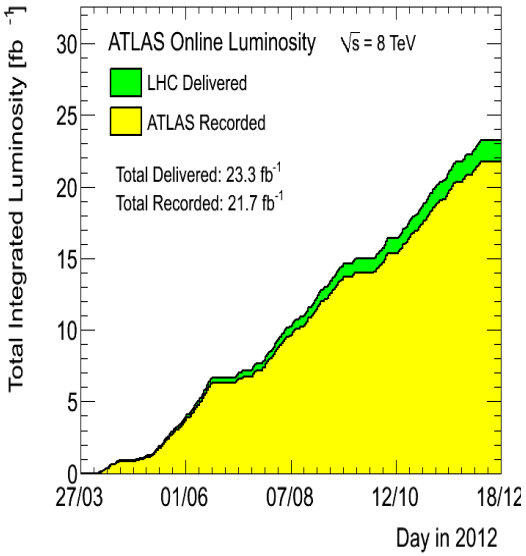

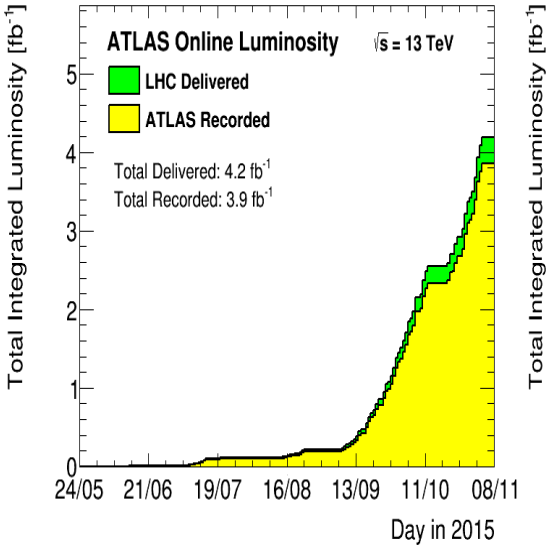

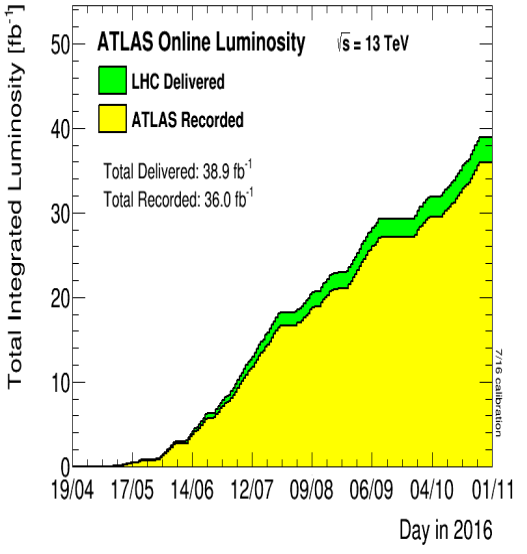

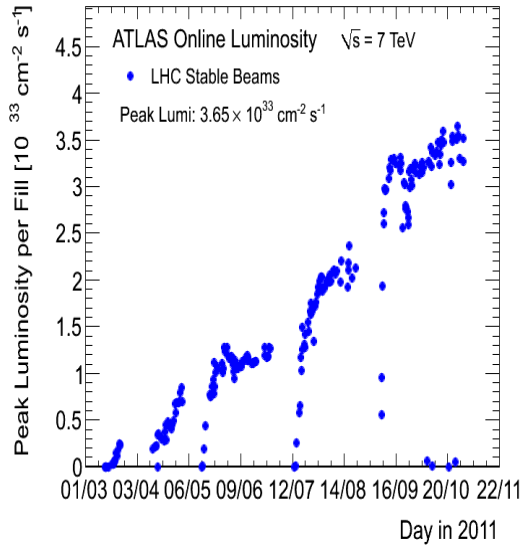

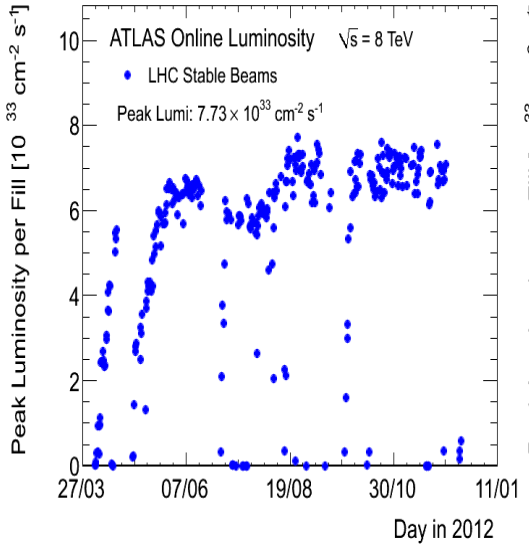

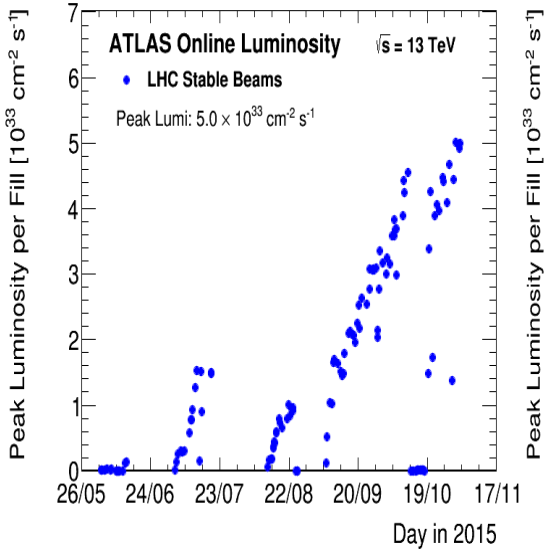

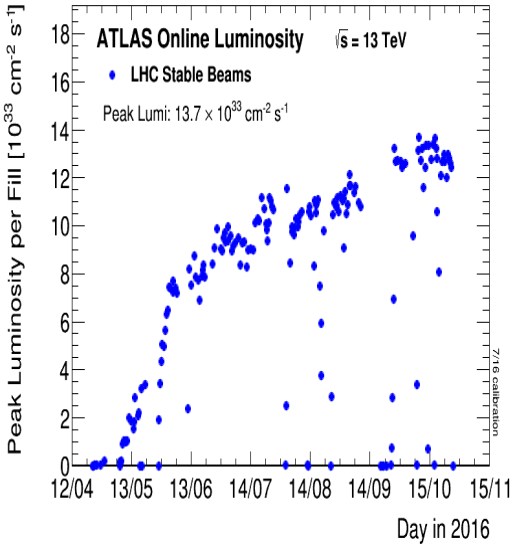

Proper Decay Time Resolution in Real Data

- Comparison of the proper decay time resolution distributions in Run-1 and Run-2 data:

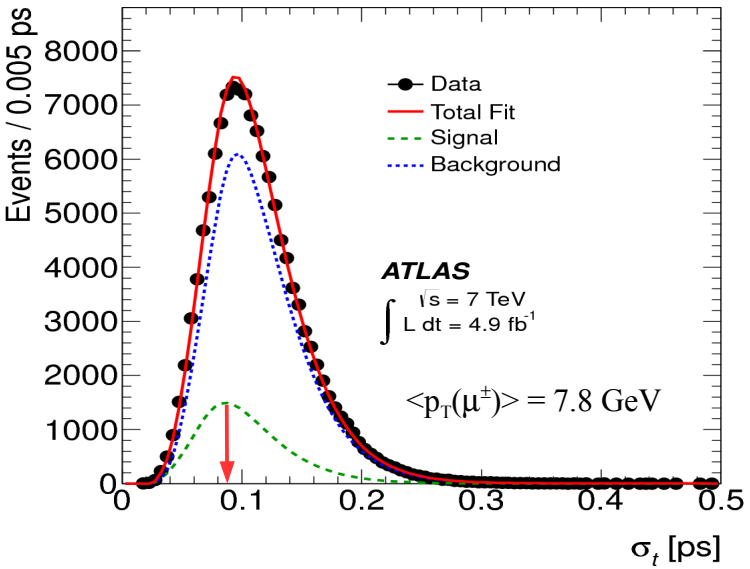

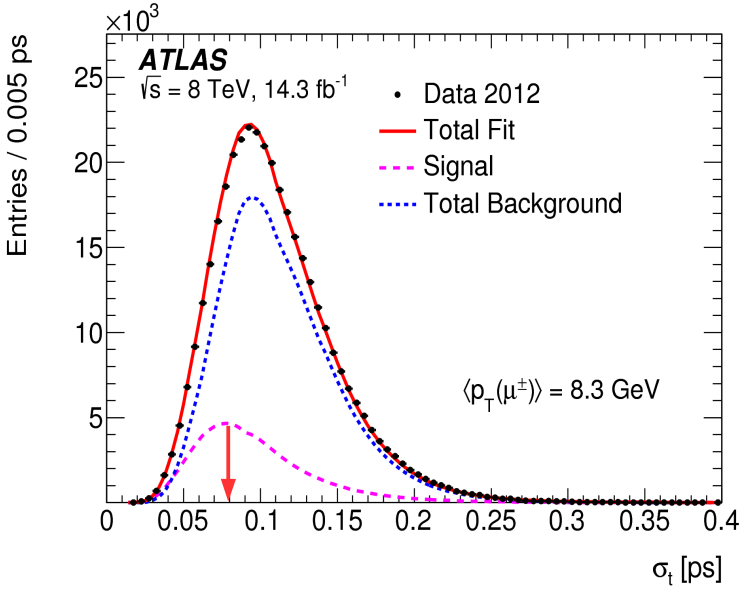

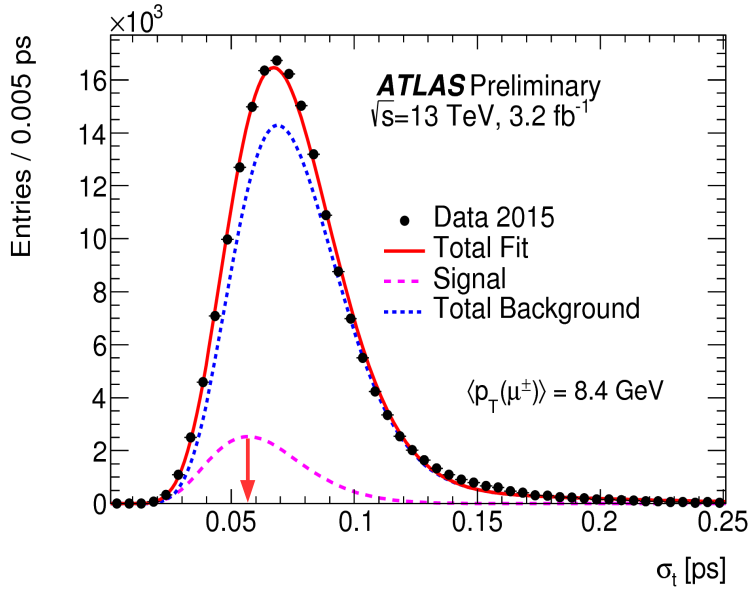

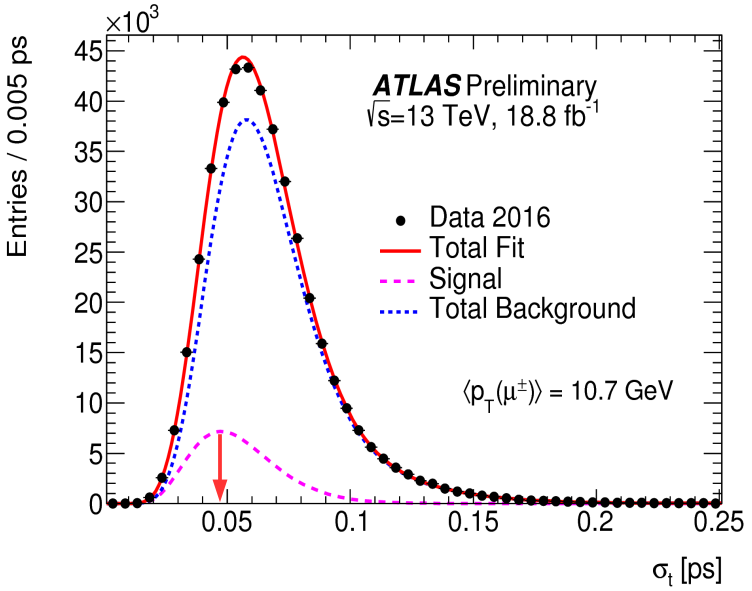

Average proper decay time distribution driven by:

- Tracking performance (with or without IBL)
- Trigger muon p_T thresholds → average B_s-meson momentum

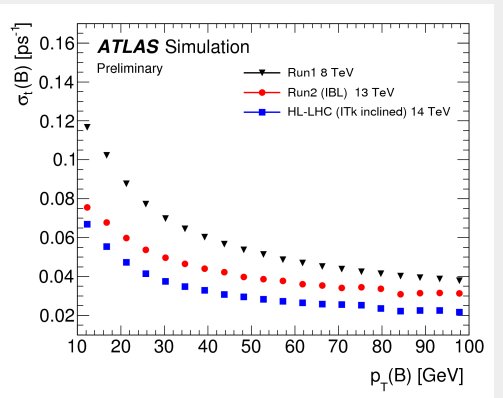

etector & Trigger Upgrades - Phase 0

SLIGHTLY OBSOLETE

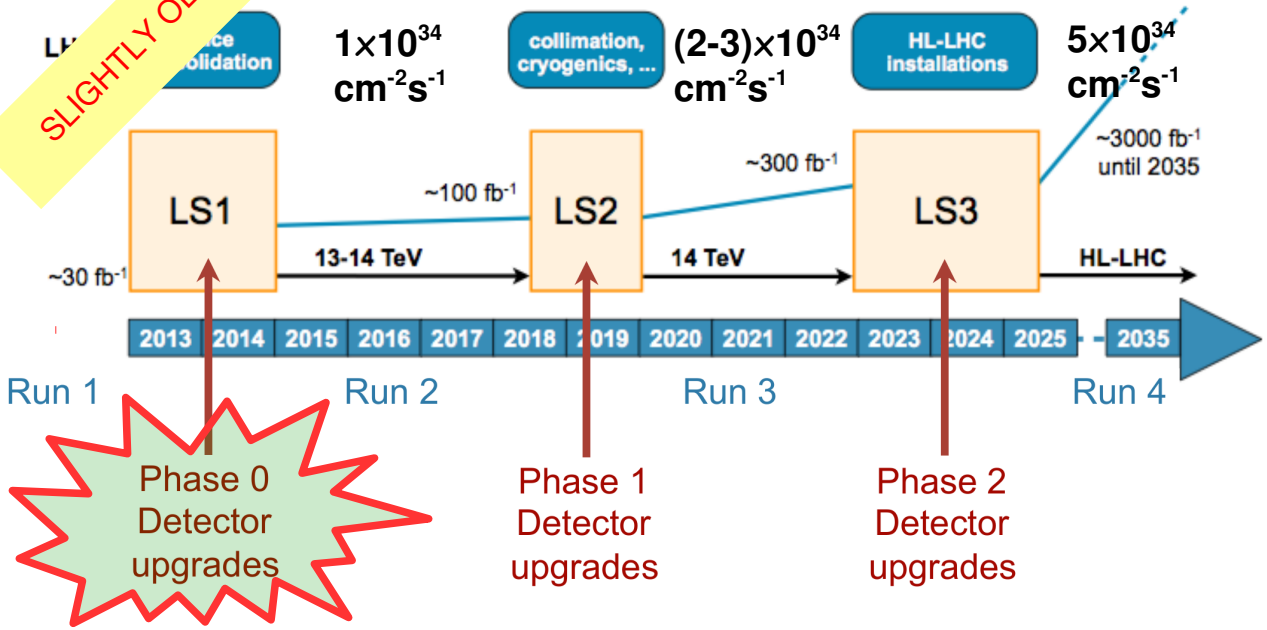

- Long Shutdown (LS) 1 almost over, LHC starts providing physics data in Spring 2015
- **Additional Pixel Layer (IBL)** and Be small radius beam pipe
- **Topological L1 trigger**
- Improved coverage of Muon spectrometer ($1.0 < |\eta| < 1.3$)
- Diamond Beam Monitor, consolidation of some parts of the detector (cooling etc.)

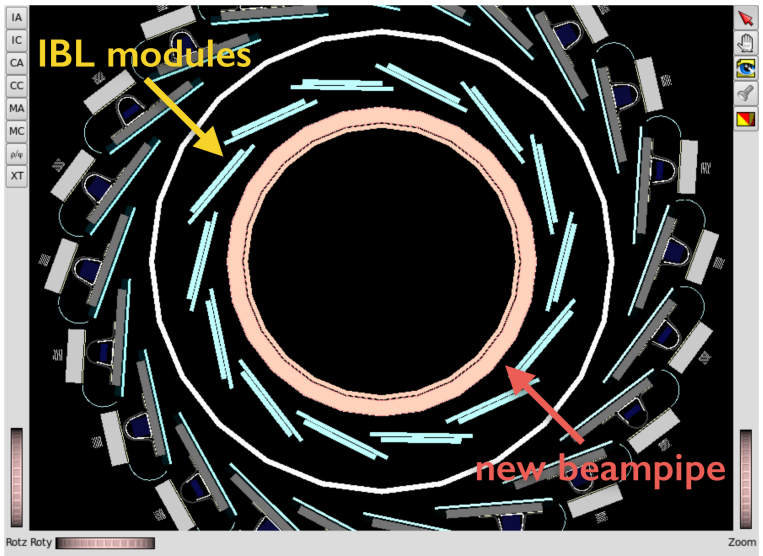

- Small radius (32-38 mm; current B-layer at 50.5 mm), small material budget
- 4th pixel layer => more robust track reconstruction, better impact parameter d_0 and z_0 resolution
- Better θ and ϕ resolution at low p_T ~ 1 GeV

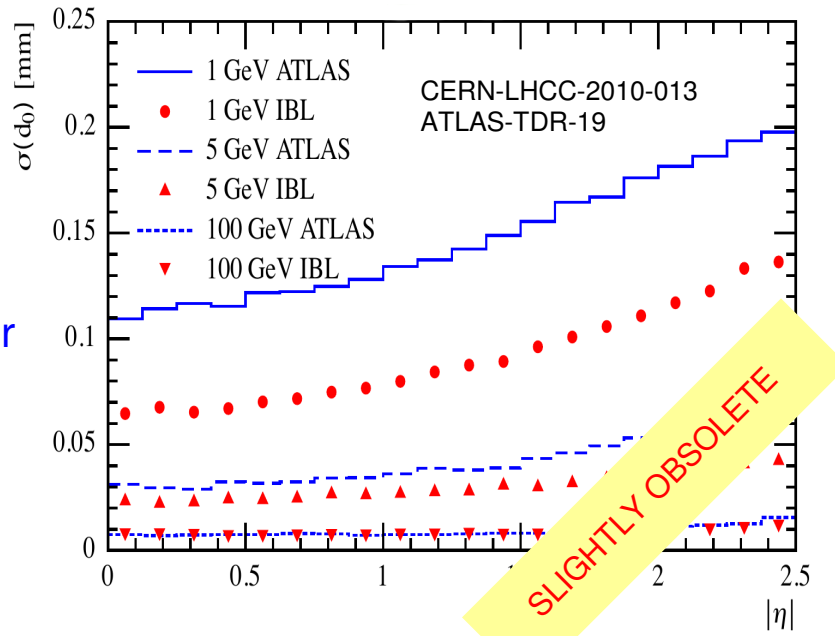

SLIGHTLY OBSOLETE

etector & Trigger Upgrades - Phase 1

SLIGHTLY OBSOLETE

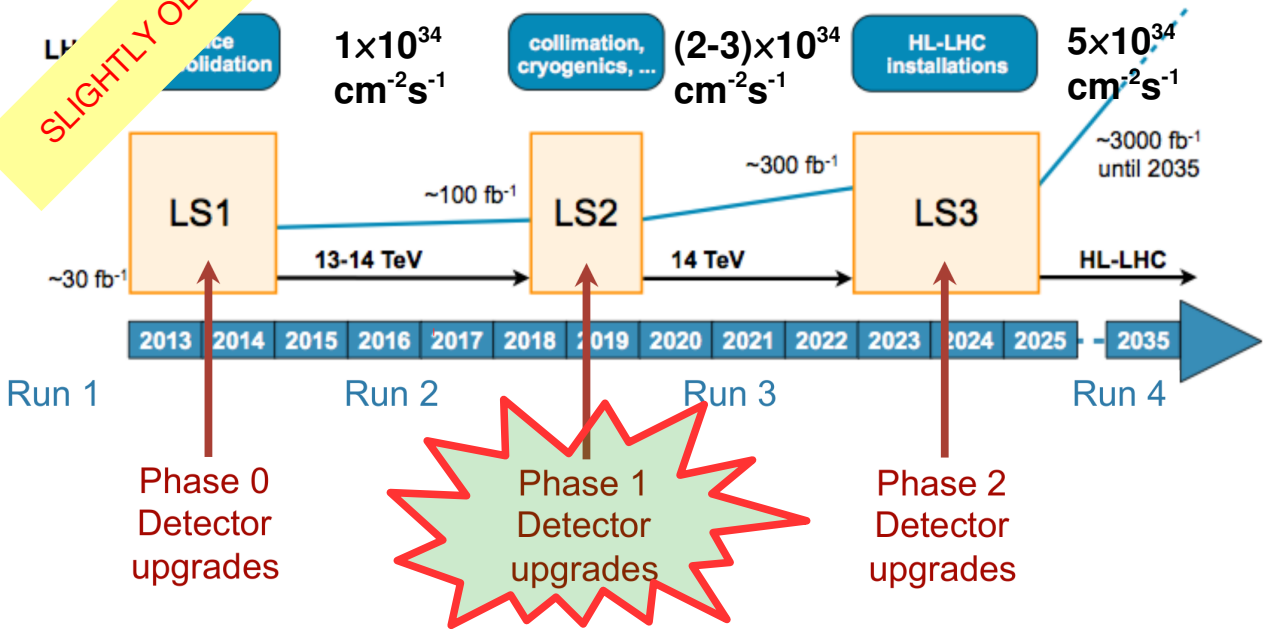

- Goal: no loss of performance when going above LHC nominal luminosity
- **New small muon wheel**
- **New fast-tracking (FTK) at trigger level 1.5. Gradually implemented already during Run 2**
- Higher granularity and precision L1 trigger for calorimeter
- TDAQ improved performance

Fast tracking trigger:

- HW based track finder in the Inner Detector silicon layers at “offline precision”
- Provides tracks already before the L2 trigger (first SW based trigger layer)
- Two-step processing: hit pattern matching & subsequent linear fitting in FPGAs

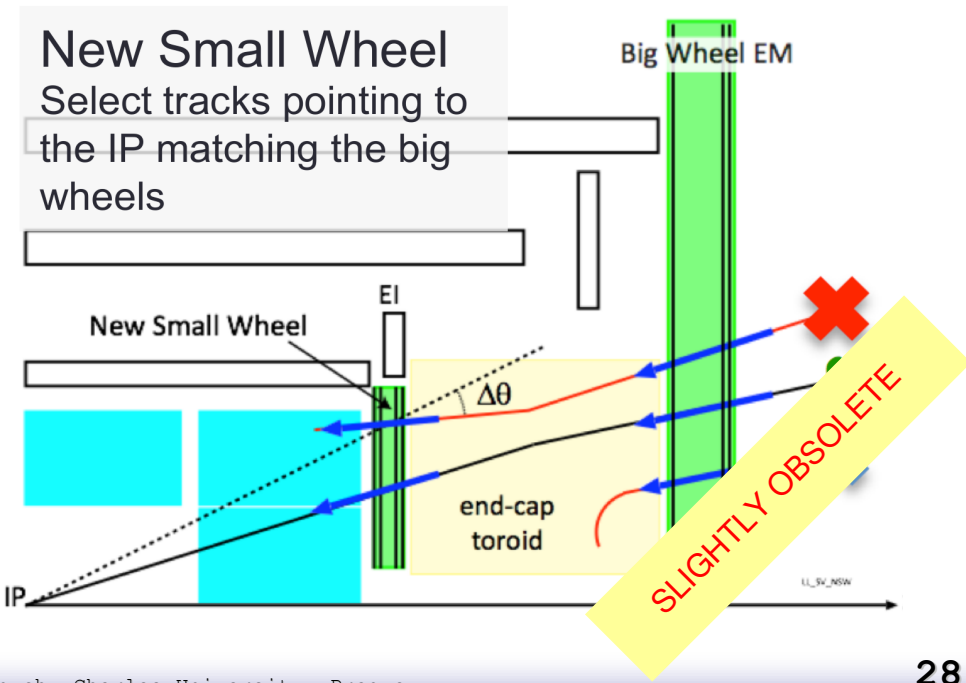

etector & Trigger Upgrades - Phase 2

SLIGHTLY OBSOLETE

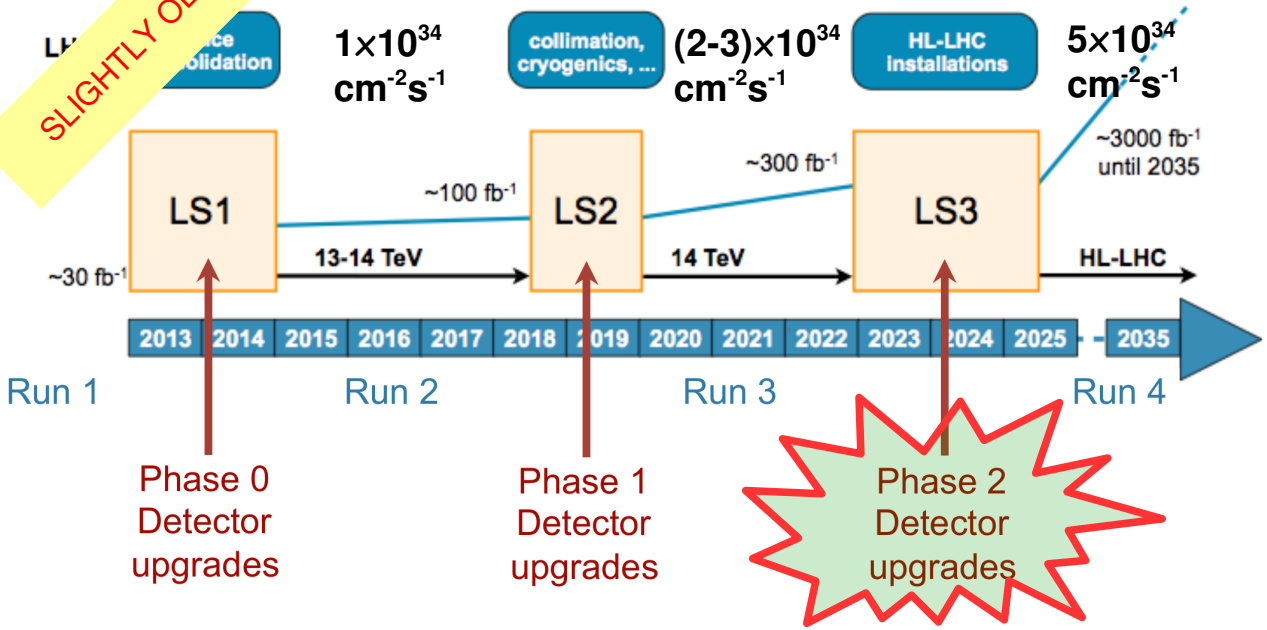

- Goal: maintain/improve performance despite high lumi.
- **Completely new Si based tracking (ITK)**
- New trigger system – possibly will include HW-based L1 track trigger
- Full granularity calorimetry information
- Upgrade part of the muon systems, fast trigger

Phase 2 Inner Tracker: current ID will become inefficient due to radiation damage; too high occupancy in TRT; high granularity (~4x better) required to cope with high pileup (~up to 200)

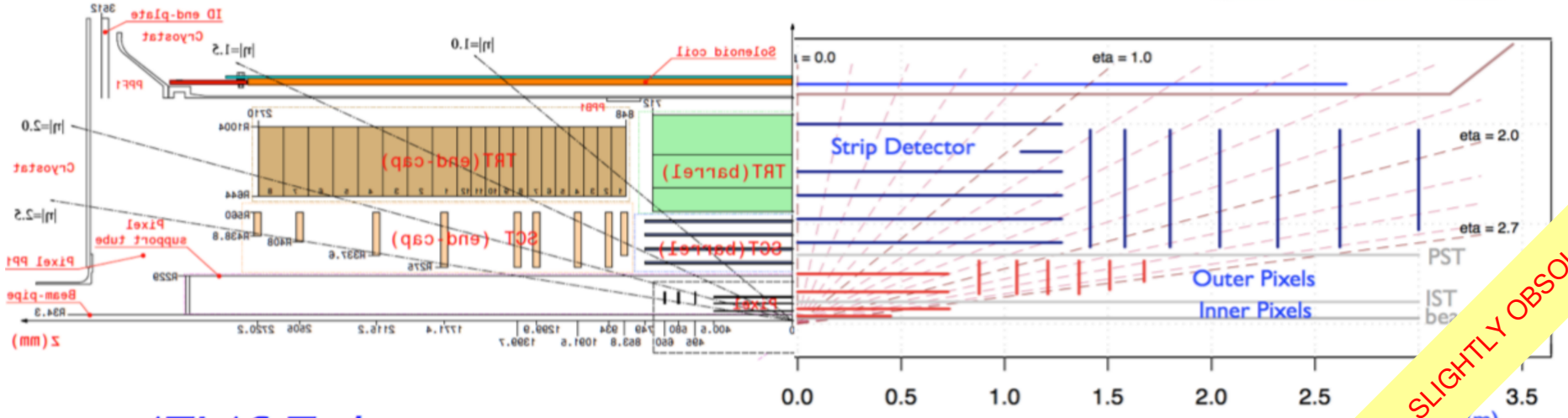

SLIGHTLY OBSOLETE